VOLUME XX, 2026

UNIVERSITY OF CALIFORNIA, RIVERSIDE

UNDERGRADUATE RESEARCH JOURNAL

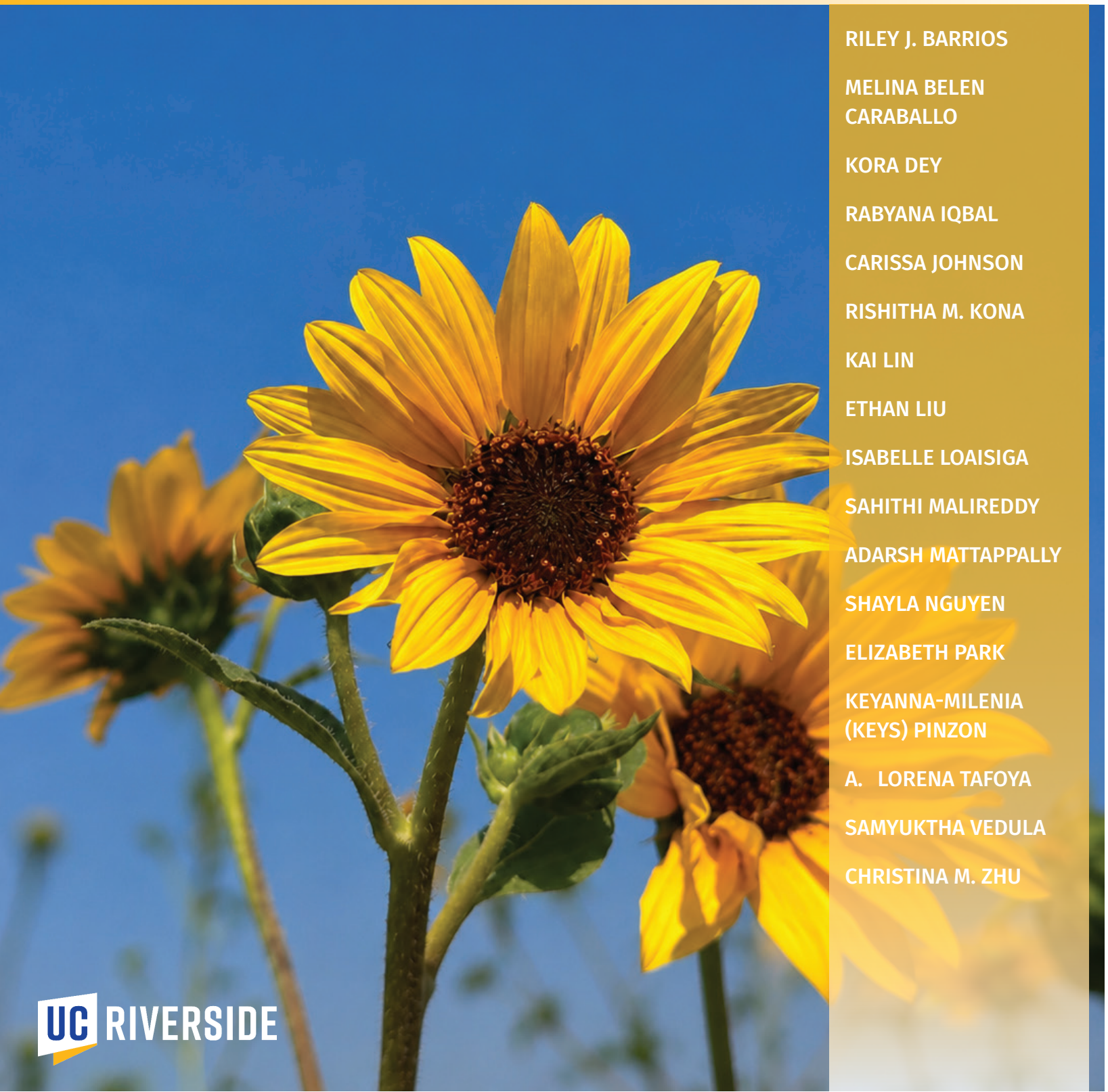

RILEY J. BARRIOS

MELINA BELEN CARABALLO

KORA DEY

RABYANA IQBAL

CARISSA JOHNSON

RISHITHA M. KONA

KAI LIN

ETHAN LIU

ISABELLE LOAISIGA

SAHITHI MALIREDDY

ADARSH MATTAPPALLY

SHAYLA NGUYEN

ELIZABETH PARK

KEYANNA-MILENIA (KEYS) PINZON

A. LORENA TAFOYA

SAMYUKTHA VEDULA

CHRISTINA M. ZHU

UC RIVERSIDE

UNIVERSITY OF CALIFORNIA, RIVERSIDE

UNDERGRADUATE RESEARCH JOURNAL

TABLE OF CONTENTS

UNIVERSITY OF CALIFORNIA, RIVERSIDE

UNDERGRADUATE RESEARCH JOURNAL

TABLE OF CONTENTS (CONT'D)

The *Journal*'s Leadership Team would like to extend our heartfelt gratitude to the following people who made this edition possible:

Laksh Athappan and Flicks UCR for capturing the portraits of our Student Editorial Board members and authors,
Katherine Morrissette for assisting with last-minute proofreading,
Liz Teng for finding and contacting 20 years of *Journal* alumni, and
Taylor Petrich for helping troubleshoot InDesign.

We truly would not have been able to do this without you!

Sincerely,
The UGRJ Team

FROM THE CHANCELLOR

At UC Riverside, discovery is a vital part of the university's mission. Faculty research and creative activities deepen understanding, solve complex challenges, and expand possibilities. By advancing treatments for multiple sclerosis, studying planets outside our solar system, developing drought-tolerant plants, or creating artistic works examining AI's impact, UCR researchers are united by a commitment to knowledge in service to the public good.

Mentored by world-class faculty, our students have access to experiential learning opportunities that offer hands-on research and creative scholarship that shape their journey as learners and scholars.

Our research excellence is reflected throughout the pages of the *UCR Undergraduate Research Journal*. In this volume, our students demonstrate the remarkable inquiry taking place at UCR and the promise of a new generation of scholars and leaders prepared to address the challenges of the future. I hope these papers leave you with a sense of optimism for what these students can contribute to our communities and society, both before and after graduation.

Thank you to the faculty mentors who guide and inspire our students, and congratulations to the students whose work is proudly featured in this issue of the *Journal*.

Sincerely,

Dr. S. Jack Hu
Chancellor
UC Riverside

FROM THE VICE PROVOST AND DEAN

Two decades ago, the *UCR Undergraduate Research Journal* was established to celebrate the very best faculty-mentored undergraduate research and scholarship at UCR. In that first issue, the Vice Provost of Undergraduate Education, Andrew J. Grosovsky, hoped that "the launch of the *Journal* will help grow what is already a very vibrant undergraduate research environment on our campus, and provide a means to disseminate some of the most exemplary work from our undergraduate students." Today, as we celebrate 20 years of the *Journal*, it continues to stand as a testament to the enduring spirit of scholarly inquiry that defines the University of California, Riverside.

The students published in the *Journal* have spent countless hours in labs, community settings, archives, and field sites, navigating the complexities of the research process—from the initial spark of a hypothesis to the rigorous demands of peer review.

Reflecting on 20 Years of Impact:

A Culture of Mentorship: None of this would be possible without our distinguished faculty. Their commitment to guiding the next generation of scholars ensures that UCR remains a powerhouse of transformative undergraduate experiences.

Interdisciplinary Perspectives: True to the mission of our institution, this issue spans a range of disciplines — from the arts and humanities to the physical and social sciences—reminding us that innovation often happens at the intersection of different ideas.

Launching Careers: For many of our alumni featured in previous volumes, the Journal was the starting point for careers in academia, industry, and public service.

As we look forward to the next twenty years, let us continue to champion the pursuit of truth and the bold exploration of the unknown. Under the mentorship of our faculty, our rising student scholars and researchers will continue to embark on new research and creative activities that will solve problems, tell stories, and strengthen our society and world for generations to follow. Thank you to all of the students, staff, and faculty who have supported the Journal during the last 20 years and congratulations on another transformative and illuminating issue!

Sincerely,

Dr. Louie F. Rodriguez
Vice Provost and Dean,
Division of Undergraduate Education
Professor of Education
UC Riverside

UNDERGRADUATE RESEARCH JOURNAL STUDENT EDITORIAL BOARD

Nandini Mannem
Editor-in-Chief
Neuroscience

Sreenidhi Surineni
Editor-in-Chief
Neuroscience

Trusha Bhagwat
Associate Editor-in-Chief
Cell, Molecular, & Developmental Biology

We are proud to present the 20th edition of the *UCR Undergraduate Research Journal*. Two decades of the *Journal* represent more than a number. They represent twenty years of undergraduates choosing to ask difficult questions and contribute original knowledge to their fields. This milestone belongs to every student, editor, and mentor who has shaped the journal into what it is today. This edition carries that legacy forward. The research within these pages spans disciplines and methodologies, but a common thread runs through each article: intellectual courage. These authors did not settle for easy answers. They pursued problems that demanded rigor, creativity, and persistence, and the result is a volume we believe stands among the strongest in the *Journal*'s history.

A publication of this caliber is never the work of authors alone. Our Student Editorial Board and Faculty Advisory Board brought sharp critical eyes and genuine care to every manuscript. Their feedback elevates each piece, and their commitment to the process transforms individual papers into a cohesive scholarly volume. We are deeply grateful for their time and expertise.

As we mark twenty years of the *Journal*, we find ourselves looking ahead as much as looking back. The next twenty years of undergraduate scholarship at UCR will be shaped by students who apply their intellectual curiosity to do meaningful work. If this edition inspires even one reader to pursue a question they cannot let go of, it will have done its job. It has been our privilege to serve as Co-Editors-in-Chief for this milestone edition. We hope it honors the two decades of scholarship that preceded us and encourages even more scholarly success to come.

Sincerely,
Sreenidhi Surineni and Nandini Mannem,
Co-Editors-in-Chief

David Hester
Lead Reviewer
Sociology

Aurchana Manickavasagan
Lead Reviewer
Biochemistry

Dhruv Pathak
Lead Reviewer
Cell, Molecular, & Developmental Biology

Nina Phatak
Lead Reviewer
Biomedical Engineering

Aarushi Saini
Lead Reviewer
Neuroscience

Angela Tran
Lead Reviewer
Psychology

UNDERGRADUATE RESEARCH JOURNAL STUDENT EDITORIAL BOARD

Jacen Lopez
Copy Editor
Neuroscience

Omeid Majd
Copy Editor
Biology

Srinidhi Mallela
Copy Editor
Cell, Molecular, & Developmental Biology

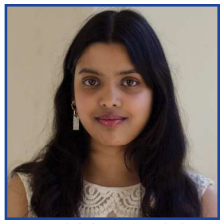

Harshitha Nandula
Copy Editor
Biology

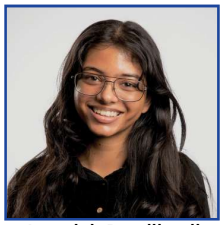

Amariah Peedikayil
Copy Editor
Bioengineering

Varshini Balaji
SEB
Microbiology

Karina Chang
SEB
Neuroscience

Tiffany Chen
SEB
Psychology

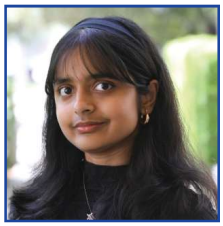

Spoorti Chetty
SEB
Neuroscience

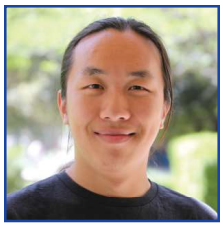

Bryan Deng
SEB
Electrical Engineering

William Dong
SEB
Biology

Annie Hsu
SEB
Biochemistry

Rabyana Iqbal
SEB
Psychology

Raeshal Jha
SEB
Biochemistry

Samuel Jones
SEB
Biochemistry

Nashwaan Khan
SEB
Computer Science

Yuva Krishnapillai
SEB
Neuroscience

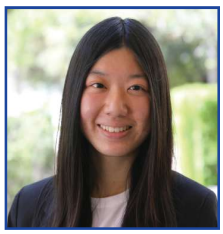

Annabelle Lu
SEB
Cell, Molecular & Developmental Biology

Julia Mathews
SEB
Neuroscience

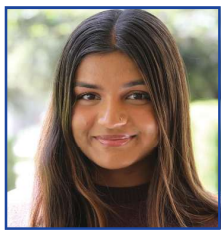

Saachi Raju
SEB
Computer Science

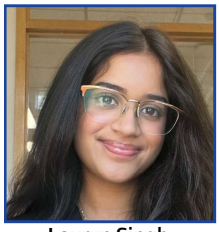

Lauryn Singh
SEB
Cell, Molecular, & Developmental Biology

Antonio Torres
SEB
Public Policy

Natalie Upp
SEB
Psychology

Additional SEB Members
Nisha Ganesan, Neuroscience (SEB)
Elizabeth Teng, Biology (SEB)

FACULTY ADVISORY BOARD

Why do we do research? The obvious answer is that the results of the research have value: research helps us understand the universe and our place in it, learn from the past, and prepare for the future. But there's another benefit of research that's worth considering as we celebrate the 20th issue of the *UCR Undergraduate Research Journal*: the value of research for the researcher. Undergraduate research can be a transformative experience for a student. I'm amazed by how many professors I know who credit their own undergraduate research experience for launching their careers (I'm one of them—thank you Dr. Chambers for welcoming me into your lab at the University of Tennessee 30 years ago!). And even if you go into a career outside of research, the skills that undergraduate research cultivates—how to be observant, analyze data and evidence, draw conclusions, persevere through setbacks, and communicate effectively—are extremely valuable in any field. It's immensely satisfying to read this special issue of the *Journal* and see the incredible things that 20 years' worth of student researchers and editors have accomplished since their time at UCR. You're an inspiration to our current and future students and a reminder of the importance of undergraduate research.

My sincere thanks to the members of the *Journal*'s Student Editorial Board who guided the submitted articles through review and publication, the Faculty Advisory Board members who assisted the students in the peer review process, and Jennifer Kavetsky for the million things she does to make the *Journal* happen each year. We're also grateful for the support of Gladis Herrera-Berkowitz, the CUREL team, and Vice Provost and Dean of Undergraduate Education Dr. Louie Rodriguez. A special thank-you goes to Liz Teng for tracking down and interviewing many of our authors and editors from the last 20 years. And to the undergraduate researchers whose work is featured in this issue, congratulations! We look forward to hearing great things when we check in with you 20 years from now!

Prof. William Grover
Associate Professor of Bioengineering
Chair of the *UCR Undergraduate Research Journal*
Faculty Advisory Board

COLLEGE DEANS

Dr. Christopher Lynch
Dean of the Marlan and Rosemary Bourns College of Engineering

Dr. Daryle Williams
Dean of the College of Humanities, Arts, and Social Sciences

Dr. Peter Atkinson
Dean of the College of Natural and Agricultural Sciences

Dr. Yungzeng Wang
Dean of the School of Business

Dr. Joi Spencer
Dean of the School of Education

Dr. Deborah Deas
Dean of the School of Medicine

Dr. Mark C. Long
Dean of the School of Public Policy

Dr. Mihoko Hosoi
University Librarian

EDITORIAL TEAM

Sreenidhi Surineni
Co-Editor-In-Chief

Nandini Mannem
Co-Editor-In-Chief

Jennifer Kavetsky
Coordinator, CUREL

Gladis Herrera-Berkowitz
Director, CUREL

FACULTY ADVISORY BOARD

Dr. Monia Carson
Biomedical Sciences

Dr. José Del Real Viramontes
Education

Dr. Andrea Denny-Brown
English

Dr. Alejandra Dubcovsky
History

Dr. Jonathan Eacott
History

Dr. William Grover
Bioengineering

Dr. Erica C. Heinrich
Biomedical Sciences

Dr. Xiaoping Hu
Bioengineering

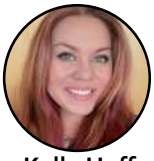

Dr. Kelly Huffman
Psychology

Dr. Brent Hughes
Psychology

Dr. Matthew King
Religious Studies

Dr. Chung-Hao Lee
Bioengineering

Dr. Ye Li
Management

Dr. Hsuan-Ying Liu
Comparative Literature and Languages

Dr. Josh Morgan
Bioengineering

Dr. Leonard Mueller
Chemistry

Dr. Sarah Radi
Biochemistry

Dr. Deepa Ramamurthy
Psychology

Dr. Wendy Saltzman
Evolution, Ecology & Organismal Biology

Dr. Wesley Sims
Education

Dr. Rakesh Singh
Biomedical Sciences

Dr. James Tobias
English

Dr. Emma Wilson
Biomedical Sciences

ABOUT THE COVER

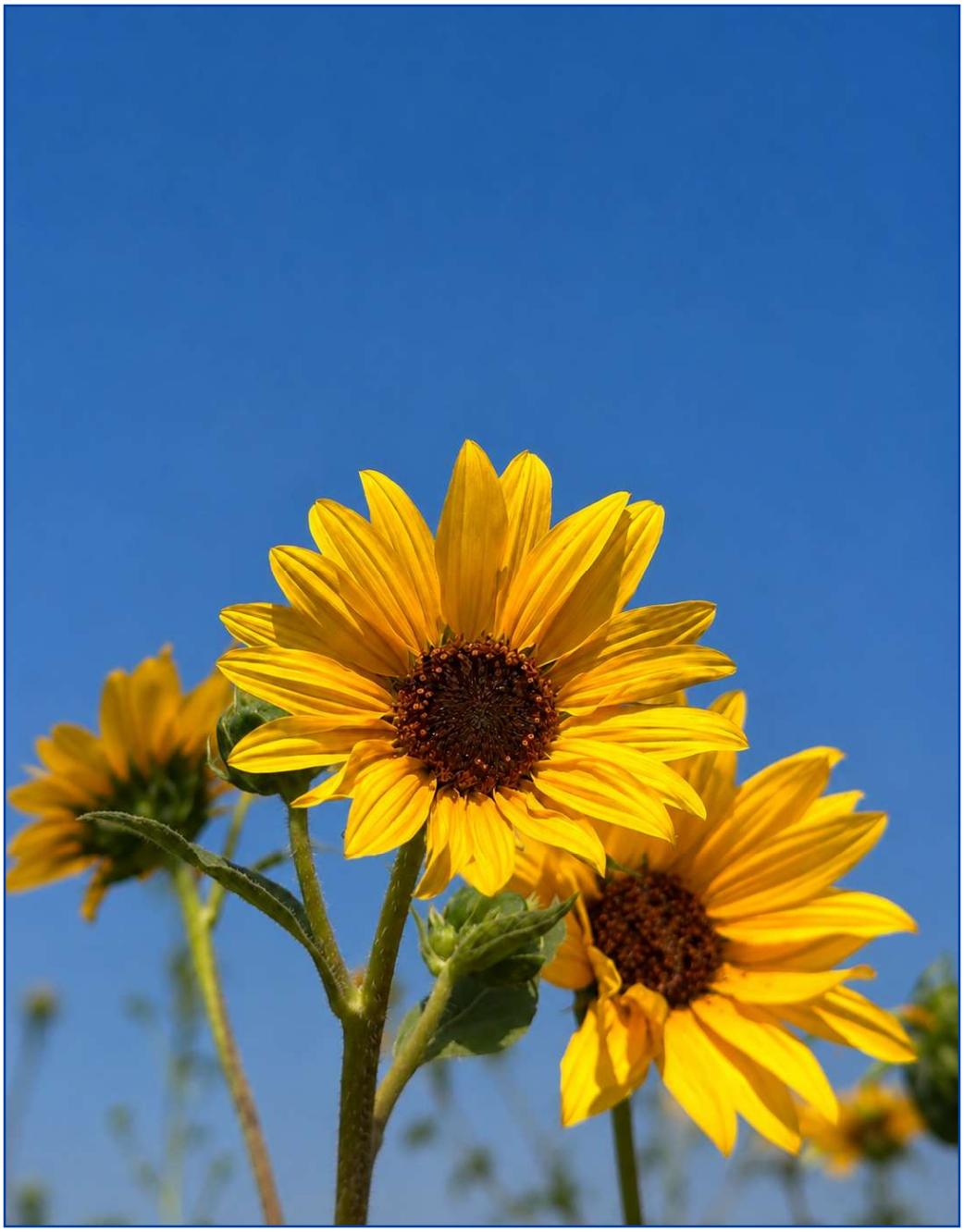

This photograph was taken at UC Riverside Agricultural Operations Center as part of my work with Dr. Ostevik. Our work examines phenotypic and genotypic variation across diverse sunflower populations, with a particular focus on traits associated with drought resilience and local adaptation. One of our recent projects examined drought stress and sunflower moth herbivory across multiple wild sunflower populations to better understand how environmental stress and insect interactions vary among populations.

Omeid Majd

Omeid Majd conducts research in the Ostevik Lab, investigating drought adaptation and insect herbivory in *Helianthus annuus*. He also serves as a copy editor for the *UCR Undergraduate Research Journal* and as a Pre-Health Ambassador with the Pre-Professional Advising Center (PPAC). He is a scholar in the California Alliance for Maximizing Potential (CAMP), an NSF-funded program, and his Honors capstone research examines the impact of interdisciplinary experiences on STEM student development. After graduation, he will pursue a Master of Science in Biomedical Sciences at the UCR School of Medicine before applying to M.D.-Ph.D. programs.

The Effects of *N*-acetyl Cysteine, Gentamicin, and Ciprofloxacin on Bacterial Biofilm *in vitro* in the Presence or Absence of High Oxidative Stress and High Glucose Levels

Samyuktha Vedula; Molecular, Cell and Systems Biology
Shayla Nguyen; Molecular, Cell and Systems Biology
Manuela Martins-Green, Ph.D.; Department of Molecular, Cell and Systems Biology

ABSTRACT

The purpose of this study was to determine if *Enterobacter cloacae*, *Pseudomonas aeruginosa*, and *Staphylococcus xylosus* can form biofilm *in vitro*, and the effects of *N*-acetyl cysteine, ciprofloxacin, and gentamicin on biofilm growth in the presence or absence of oxidative stress and/or high glucose levels. These three bacterial strains were used as they are most commonly found in human chronic wounds. The goal of this study was to determine if *N*-acetyl cysteine can be used as a treatment for chronic wounds. The bacteria were cultured *in vitro* and formed biofilm within 24 hours. Treatments included *N*-acetyl cysteine, gentamicin, and ciprofloxacin, which were added to the cultured biofilm. For the oxidative stress condition, H_2O_2 was used, and for the high glucose levels, d(+)-Glucose was used, both of which were administered in a similar manner to the treatments. When used alone, *N*-acetyl cysteine was able to significantly dismantle the biofilm, even when the bacteria were combined. However, in the presence of oxidative stress or high glucose levels, *N*-acetyl cysteine was less effective at dismantling the biofilm, especially when the bacterial strains were combined. In conclusion, H_2O_2 and glucose diminish the efficacy of our treatments, which have a significantly detrimental effect on biofilm. While *N*-acetyl cysteine is not as effective at dismantling biofilm under conditions of high oxidative stress and high glucose levels, the addition of antibiotics becomes more helpful in these cases, making the treatment viable overall.

KEYWORDS: *Pseudomonas aeruginosa*, *Enterobacter cloacae*, *Staphylococcus xylosus*, Hyperglycemia, Microbial aggregates, Hydrogen peroxide

FACULTY MENTOR - Dr. Manuela Martins-Green, Department of Molecular, Cell and Systems Biology

Dr. Martins-Green is a Professor of Cell Biology at UCR. Originally from Portugal, she came to the U.S. on a Fulbright Fellowship and earned her Ph.D. from UC Davis. She has been on the UC Riverside faculty since 1993. She is a fellow of AAAS and founding Fellow of the Wound Healing Society (WHS). Her research focuses on the initiation and progression of chronic wounds, and she has won the 2026 Lifetime Achievement Award from WHS.

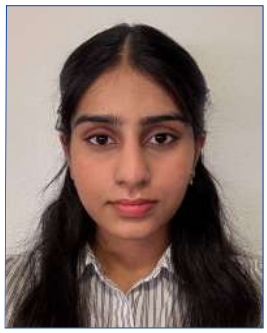

SAMYUKTHA VEDULA

Samyuktha is a researcher in Dr. Martins-Green's chronic wound laboratory. Samyuktha's research focuses on *in vitro* treatments for bacterial biofilms. She has presented at the 2024 Symposium on Advanced Wound Care, held in collaboration with the Wound Healing Society. Samyuktha graduated Summa Cum Laude with a B.S. in Biology and plans to apply to medical school.

SHAYLA NGUYEN

Shayla Nguyen is a fourth-year Biology major and researcher in Dr. Martins-Green's chronic wound laboratory, studying treatments of bacterial biofilms under hyperglycemic and oxidative stress conditions. She presented at the 2024 Symposium on Advanced Wound Care. Shayla received the Dr. Manuela & Mr. Randy Sosa Scholarship Award for her commitment to serving the Inland Empire. She will pursue an M.D. at the UCR School of Medicine.

The Effects of *N*-acetyl Cysteine, Gentamicin, and Ciprofloxacin on Bacterial Biofilm *in vitro* in the Presence or Absence of High Oxidative Stress and High Glucose Levels

INTRODUCTION

Chronic wounds are associated with a significant impact on human health globally. Nearly 8.2 million Americans suffer from chronic wounds, with Medicare costs for treatment ranging from $28.1 billion to $96.8 billion [1]. Chronic wounds are a financial, clinical, and social burden on the healthcare system and on the individuals suffering from them. Chronic wounds cause pain, infection, and may even lead to amputation if the chronicity of the wounds is prolonged. Between 40.4% and 70% of lower extremity amputations result in death within five years post-amputation [2]. Several comorbidities, such as chronic disease, vascular insufficiency, diabetes, malnutrition, and age, can impact wound healing in these patients [3].

Acute wound healing is characterized by four stages: hemostasis, inflammation, proliferation, and remodeling [4,5]. However, chronic wounds do not follow the normal healing process. In these wounds, the healing and repair process is altered, resulting in chronic inflammation, excessive levels of reactive oxygen species (ROS), elevated levels of matrix proteases, and lack of angiogenesis [6,7]. Chronic wounds are colonized by pathogens, primarily bacteria from the skin microbiome. These pathogens result in infections that, in the presence of ROS, lead to development of biofilm [8]. The prevalence of biofilm-forming pathogens in chronic wounds is a key contributing factor to wound chronicity and impaired wound healing [4]. Current treatments with antibiotics are generally ineffective at killing biofilm-forming bacteria because the bacteria are embedded in extracellular polymeric substances (EPS), which provide protection from antibiotics. Furthermore, a "dormant" state is exhibited by these bacteria; therefore, the antibiotics, which affect protein synthesis, become ineffective [9,10].

We have previously shown, in a diabetic mouse model of chronic wounds, that wound healing was significantly improved and chronicity was reversed by *N*-acetyl cysteine (NAC) through the disappearance of the bacteria from the wound, resulting in the breakdown of the EPS [11,12]. EPS are composed of carbohydrates, proteins, extracellular DNA, and lipids, all of which establish biofilm structure [13]. Using an *in vitro* system, we showed that NAC dismantled Pseudomonas aeruginosa-made biofilm by killing the bacteria. At a pH below the pKa, NAC was able to penetrate bacteria and halt protein synthesis, leading to bacterial cell death [12].

Here, we further these studies by identifying the effects of NAC and the antibiotics Gentamicin (G) and Ciprofloxacin (C) on the biofilm formed by three bacterial strains, individually and in combination. *Enterobacter Cloacae (Ec), Staphylococcus Xylosus (Sx),* and *Pseudomonas Aeruginosa (Pa)* were used, as they are commonly found in human chronic wounds. We examined the amount of biofilm that formed *in vitro* after 24 hours of growth, and were able to show that all strains and combinations of bacteria formed biofilm after 24 hours of incubation, and all possessed unique morphologies. Significant dismantling of the established biofilm was observed following treatment with NAC, gentamicin, and ciprofloxacin (NAC+G+C). The addition of high oxidative stress, in the form of hydrogen peroxide, and high glucose levels to mimic hyperglycemia, diminished the effectiveness of our treatments, but they were still able to significantly reduce the amount of biofilm *in vitro.*

MATERIALS AND METHODS

Culturing bacteria *in vitro* to form biofilm: The three bacterial strains were cultured in sterile LB at 37°C for 16-18 h and then diluted to $1x10^6$ CFU/200 µL. 200 µL of the diluted solution was then pipetted into each well of a 96-well plate and incubated for 24 hours. Images were captured from an overhead view every 24 hours over the course of 72 hours.

Staining for biofilm: The contents of each well were transferred to an Eppendorf tube. The well was washed with 200 µL of double distilled water and transferred to the same microcentrifuge tube. The tubes were centrifuged at 21300 rpm for 5 minutes. The supernatants were discarded and the pellets were stained with 50 µL of 0.1% crystal violet stain for 5 minutes. The excess staining solution was then washed with 1000 µL of double-distilled water twice. The samples were then dried overnight or until completely dry.

Destaining of the biofilm: The dried samples were destained using 95% ethanol. 300 µL of 95% ethanol

The Effects of *N*-acetyl Cysteine, Gentamicin, and Ciprofloxacin on Bacterial Biofilm *in vitro* in the Presence or Absence of High Oxidative Stress and High Glucose Levels

was added to each sample to destain the biofilm for 50 minutes. The samples were then centrifuged at 21300 rpm for 5 minutes. 200 µL of the supernatant was removed and analyzed using a spectrophotometer at OD590nm to determine the amount of biofilm present.

Treatment with NAC: *Pa, Ec,* and *Sx* were cultured, diluted, and plated using the method described above to form biofilm. The bacterial cultures were pipetted individually or in combination into the wells of a 96-well plate and incubated for 24 hours. NAC was dissolved in LB broth at 40-50°C. 20 µL of NAC at a concentration of 220 mg/mL was pipetted into each well, to ensure that the final concentration of NAC was 20 mg/mL per well. At the final concentration, the pH of NAC was 2.74. The plates were then incubated for 24 hours before biofilm quantification.

Other Treatments: The methods for all other treatments are the same as the general method described for NAC. Gentamicin, an antibiotic, was at a final concentration of 0.1 mg/ml, ciprofloxacin, another antibiotic, was at a final concentration of 0.2 mg/ml, hydrogen peroxide was at a final concentration of 500 µM, and d(+)-glucose was at a final concentration of 300 mg/dL.

Statistical Analysis: Statistical analysis was conducted using a student's t-test to determine the significance of the differences between the two samples of data. This form of statistical analysis was chosen for its efficiency and relative ease of implementation.

RESULTS

Distinct morphologies of biofilms developed by *Ec*, *Pa*, and *Sx* alone and in combination

To assess the biofilm-forming capabilities of the bacterial strains *Ec, Pa,* and *Sx*, the individual bacteria were cultured for 24 hours to form biofilm. Distinct morphologies were observed for all strains. The biofilm produced by *Ec* was characterized by growth primarily at the bottom of the well that was opaque and smooth. It remained relatively unchanged after culturing for 48 or 72 hours (**Fig. 1A**). The biofilm produced by *Sx* was characterized by growth at the bottom and sides of the well, and it was opaque and smooth. As time progressed, the biofilm increased in opacity and remained smooth (**Fig. 1A**). The biofilm produced by *Pa* formed at the top of the well, having a less smooth appearance than biofilm produced by *Ec* or

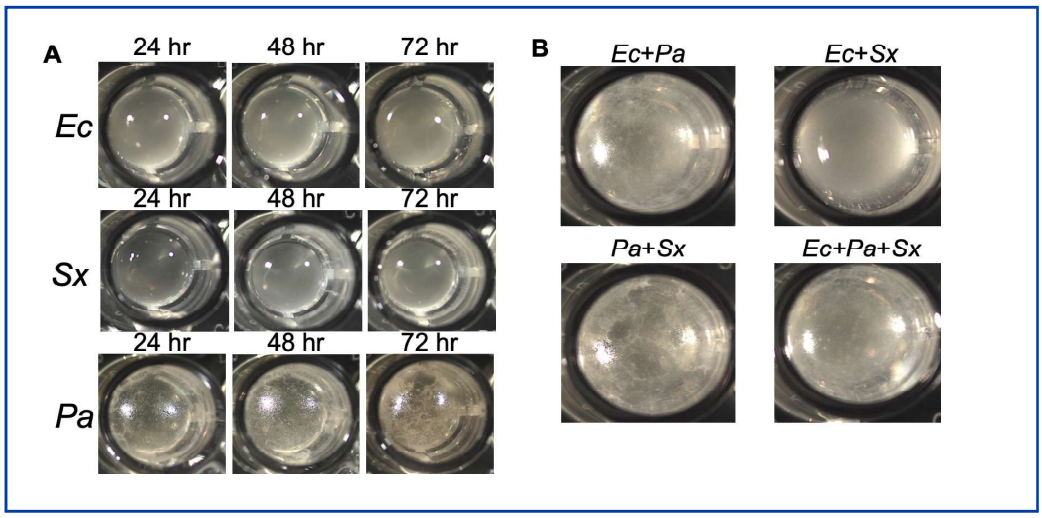

Figure 1. Visual representation of biofilm formation
Each well contained 200 µL of LB with the various cultures of bacteria. They were photographed from overhead. *Ec* is *Enterobacter cloacae*, *Pa* is *Pseudomonas aeruginosa*, and *Sx* is *Staphylococcus xylosus*. **(A)** Biofilms of the individual bacteria were photographed at 24 hour increments. **(B)** Biofilms of the various combinations of bacteria.

The Effects of *N*-acetyl Cysteine, Gentamicin, and Ciprofloxacin on Bacterial Biofilm *in vitro* in the Presence or Absence of High Oxidative Stress and High Glucose Levels

Sx. After 72 hours of incubation, the biofilm took on an orangish hue, as opposed to its initial off-white color (**Fig. 1A**). The combinations of bacteria maintained the unique morphologies observed in the single strains of bacteria and were all able to produce biofilm within 24 hours post-incubation. The combination *Ec*+*Pa* had biofilm at both the top and the bottom of the well, with the biofilm at the top being less smooth than the biofilm at the bottom, which was also more opaque (**Fig. 1B**). The combination *Ec*+*Sx* had biofilm at the bottom and sides of the well, with the biofilm being more opaque at the bottom than at the sides (**Fig. 1B**). The combination *Pa*+*Sx* had biofilm at both the top, bottom, and sides of the well, with the biofilm at the top being less smooth than the biofilm at the bottom and sides, which was more opaque (**Fig. 1B**). The combination *Ec*+*Pa*+*Sx* had biofilm at both the top, bottom, and sides of the well, with the biofilm at the top being less smooth than the biofilm at the bottom and sides (**Fig. 1B**).

The effects of NAC, Gentamicin, Ciprofloxacin, and their combinations on established biofilm

Ec, Pa, Sx, and their combinations, were cultured for 24 hours to develop biofilm. These biofilms were then treated with NAC, NAC+G, NAC+C, and NAC+G+C. They were incubated for another 24 hours before being stained with 0.1% crystal violet and destained with 95% ethanol. The supernatants were analyzed by measuring OD590 nm. For *Ec*, all four treatments had a statistically significant impact on dismantling the established biofilm ($p<0.001$ for NAC, NAC+G, NAC+G+C; $p<0.01$ for NAC+C). The effects of NAC alone or NAC+C were indistinguishable and were significantly better than NAC+G or NAC+G+C. G seems to significantly decrease the effects of NAC, while C does not seem to have a drastic impact on the effectiveness of NAC. The effects of NAC+G+C are like NAC+G, with the addition of C not having a drastic impact on G's inhibitory effect on NAC (**Fig. 2A**). For *Pa*, all four treatments had a statistically significant impact on dismantling the established biofilm ($p<0.001$ for NAC, NAC+G, NAC+G+C; $p<0.01$ for NAC+C). The effect of NAC alone was better than NAC in combination with G and with both antibiotics combined. However, C was highly effective in reversing the effectiveness of NAC alone. (**Fig. 2B**). For *Sx*, NAC was able to significantly dismantle the established biofilm, performing better alone than in combination with the antibiotics ($p<0.001$). The addition of C to NAC did not have a major impact on NAC's effects. However, when G was added to NAC, the effects of NAC on dismantling biofilm were reversed (n.s.). When both antibiotics are combined with NAC, the addition of C appears to combat G's inhibitory effect on NAC (**Fig. 2C**). Overall, NAC alone can significantly dismantle the established biofilm in all three

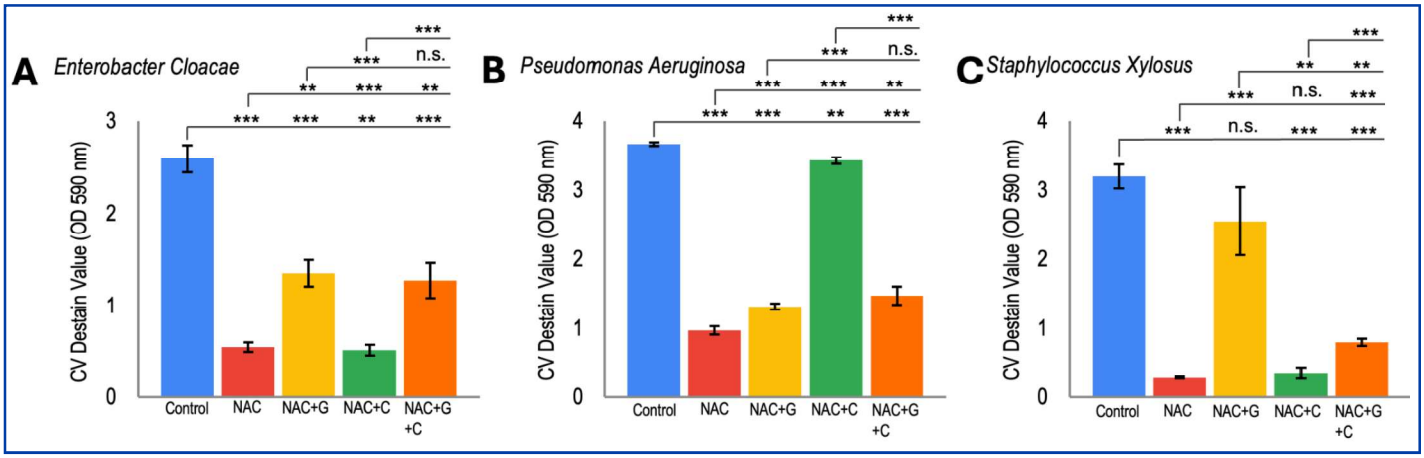

Figure 2. The effects of N-acetyl cysteine (NAC), N-acetyl cysteine+Gentamicin (NAC+G), and N-acetyl cysteine+Ciprofloxacin (NAC+C), and N-acetyl cysteine+Gentamicin+Ciprofloxacin (NAC+G+C) on individual strains of bacteria.

The graphs show the amount of biofilm formed 24 hours post-treatment, stained with crystal violet and quantified at OD590 nm.

The Effects of *N*-acetyl Cysteine, Gentamicin, and Ciprofloxacin on Bacterial Biofilm *in vitro* in the Presence or Absence of High Oxidative Stress and High Glucose Levels

individual strains of bacteria. The effects of NAC by itself were almost always better than NAC in combination with the antibiotics. (**Fig. 2**).

When the bacteria were combined, the established biofilm was dismantled by all of the treatments, but in general, no significant differences were observed between the treatments (**Fig. 3**). For the combination *Ec*+*Pa*, all treatments had a statistically significant impact on the established biofilm, dismantling it significantly ($p<0.001$ for NAC, NAC+C, NAC+G+C; $p<0.01$ for NAC+G). There was no significant difference between the effects of NAC alone and NAC with one or more of the antibiotics (**Fig. 3A**). For the combination *Ec*+*Sx*, a similar pattern was observed. All treatments resulted in a significant dismantling of the established biofilm with no statistically significant difference NAC and NAC plus the antibiotics ($p<0.001$ for NAC+G and NAC+G+C; $p<0.01$ for NAC and NAC+C) (**Fig. 3B**). For the combination of *Pa*+*Sx*, all treatments were similar in that they dismantled the established biofilm even though no statistically significant difference between the effects of NAC and NAC plus the antibiotics were observed ($p<0.001$ for NAC, NAC+C, NAC+G+C; $p<0.05$ for NAC+G) (**Fig. 3C**). For the combination *Ec*+*Pa*+*Sx*, all treatments were effective at dismantling biofilm ($p<0.001$). The combinations of NAC+G and NAC+G+C are significantly better at dismantling established biofilm than NAC alone, although the magnitude of this difference is not dramatic. The addition of G seems to improve NAC's effectiveness, whereas the addition of C does not have a drastic impact (**Fig. 3D**). Overall, the biofilms established by the combined bacteria were all effectively dismantled by all treatments. NAC alone was usually as effective as NAC in combination with the antibiotics (**Fig. 3**). The primary result was that NAC, by itself, was usually almost as good, if not better, than NAC with the antibiotics (**Fig. 2, 3**).

The effects of oxidative stress on the efficacy of NAC and NAC with Gentamicin and Ciprofloxacin in dismantling established biofilm

The bacterial strains *Ec, Pa, Sx,* and their combinations were cultured for 24 hours to form biofilm. To analyze how oxidative stress impacts the efficacy of NAC and NAC plus antibiotics, hydrogen peroxide (H_2O_2) was added to the treatments as a source of oxidative stress. In a dose-dependent experiment, no relevant difference in biofilm development was found when comparing the effects of

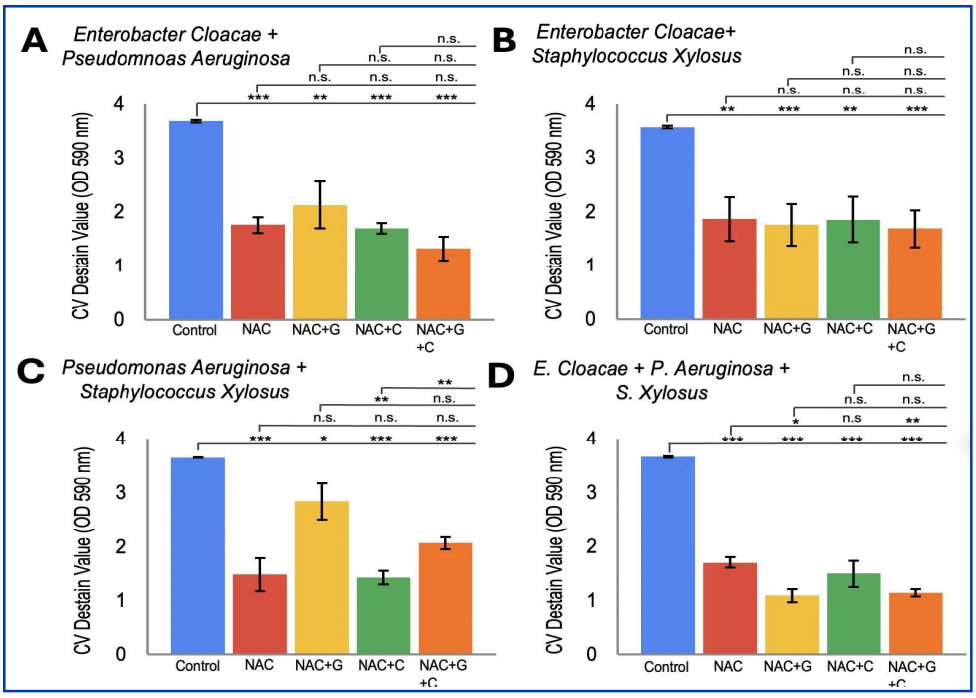

Figure 3. The effects of *N*-acetyl cysteine (NAC), *N*-acetyl cysteine+Gentamicin (NAC+G), and *N*-acetyl cysteine+Ciprofloxacin (NAC+C), and *N*-acetyl ysteine+Gentamicin+Ciprofloxacin (NAC+G+C) on the combined strains of bacteria.

The graphs show the amount of biofilm formed 24 hours post-treatment, stained with crystal violet and quantified at OD590 nm.

The Effects of *N*-acetyl Cysteine, Gentamicin, and Ciprofloxacin on Bacterial Biofilm *in vitro* in the Presence or Absence of High Oxidative Stress and High Glucose Levels

250 μM and 500 μM of H_2O_2 (not shown). Therefore, 500 μM was used. For all three bacteria, the addition of H_2O_2 to increase oxidative stress had no significant impact on the established biofilm (**Fig. 4**). For *Ec*, the addition of H_2O_2 significantly decreased the efficacy of both NAC and NAC+G+C. However, under oxidative stress conditions, NAC and NAC+G+C were still able to significantly dismantle the established biofilm, with no significant difference between their effects ($p<0.001$ for NAC+H_2O_2; $p<0.01$ for NAC+G+C+H_2O_2) (**Fig. 4A**). For *Pa*, the addition of H_2O_2 significantly decreased the efficacy of both NAC and NAC+G+C. While NAC+H_2O_2 became ineffective at dismantling the established biofilm (n.s), NAC+G+C+H_2O_2 was still able to significantly dismantle the established biofilm ($p<0.001$) (**Fig. 4B**). For *Sx*, oxidative stress significantly diminished the effectiveness of both NAC and NAC+G+C. NAC and NAC+G+C, under oxidative stress conditions, were still able to significantly dismantle the established biofilm ($p<0.001$ for NAC+H_2O_2; $p<0.01$ for NAC+G+C+H_2O_2), with no significant difference between the two treatments (**Fig. 4C**).

When we combined the bacteria, the effects of H_2O_2 alone on established biofilms were minimal (**Fig. 5**). For the combination of *Ec*+*Pa*, the ability of NAC to dismantle the biofilm was significantly diminished upon the addition of H_2O_2, but it was still significant when compared to the control with no treatment ($p<0.05$), but not the H_2O_2 treatment (n.s.). The effects of NAC+G+C on biofilm dismantling are similarly diminished upon the addition of H_2O_2, but they were still a significantly effective treatment ($p<0.001$) (**Fig. 5A**). For *Ec*+*Sx*, the effects of NAC were not significantly impacted by the addition of H_2O_2, as the difference between the effects of NAC alone and NAC+H_2O_2 was not significant, and therefore it remains an effective treatment to dismantle the established biofilm ($p<0.001$). The effects of NAC+G+C ($p<0.001$) were also not significantly impacted by the addition of H_2O_2, as the difference between the effects of NAC+G+C alone and NAC+G+C+H_2O_2 is not significant (**Fig. 5B**). With *Pa*+*Sx*, the ability of NAC to dismantle the biofilm was significantly diminished upon the addition of H_2O_2. The effects of NAC+G+C were similarly diminished upon the addition of H_2O_2, but it was still effective at dismantling the biofilm (**Fig. 5C**). For *Ec*+*Pa*+*Sx*, the effects of NAC are significantly diminished upon the addition of H_2O_2. However, it remains an effective treatment for dismantling

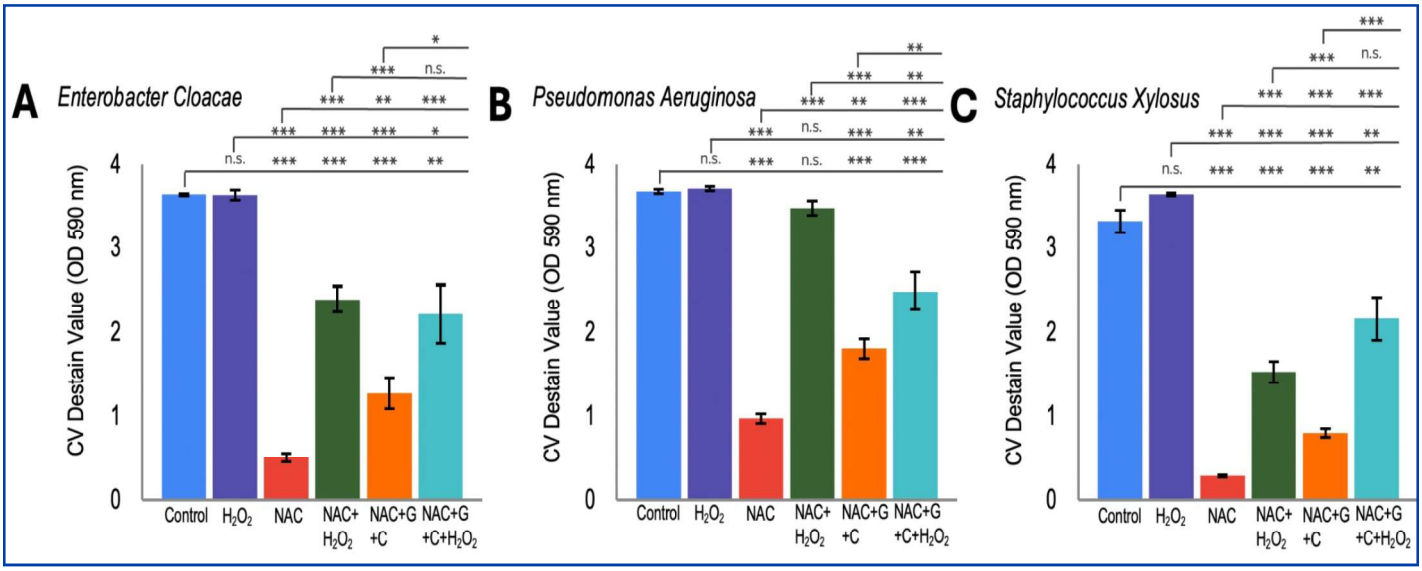

Figure 4. The effects of N-acetyl cysteine (NAC), Gentamicin (G), and Ciprofloxacin (C) on individual bacteria in the presence or absence of oxidative stress.

Hydrogen peroxide was used as a source of oxidative stress. The graphs show the amount of biofilm formed 24 hours post-treatment, stained with crystal violet and quantified at OD590 nm.

The Effects of *N*-acetyl Cysteine, Gentamicin, and Ciprofloxacin on Bacterial Biofilm *in vitro* in the Presence or Absence of High Oxidative Stress and High Glucose Levels

established biofilm. The effects of NAC+G+C are similarly diminished upon the addition of H_2O_2, though it, too, remains a significantly effective treatment against the established biofilm (**Fig. 5D**).

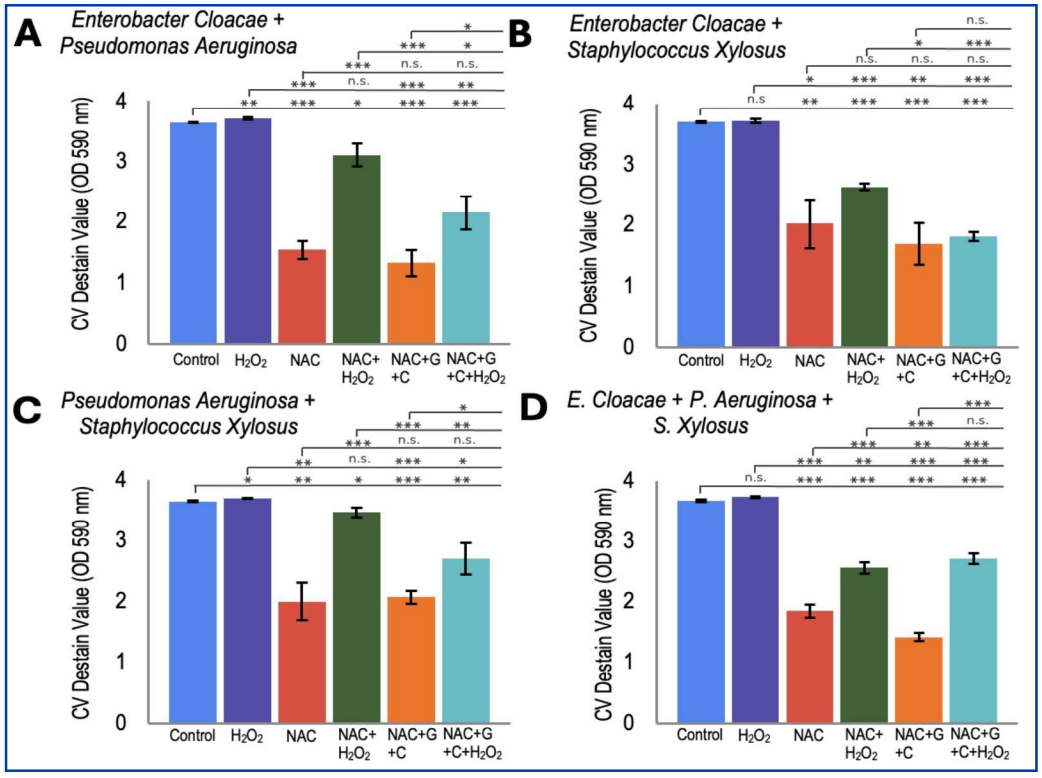

Figure 5. The effects of N-acetyl cysteine (NAC), Gentamicin (G), and Ciprofloxacin (C) on combinations of bacteria in the presence or absence of oxidative stress.

Hydrogen peroxide was used as a source of oxidative stress. The graphs show the amount of biofilm formed 24 hours post-treatment, stained with crystal violet and quantified at OD590 nm.

The effects of D(+)-Glucose on the efficacy of NAC and NAC with Gentamicin and Ciprofloxacin

The bacterial strains *Ec, Pa, Sx,* and their combinations were cultured for 24 hours to form biofilm. This study used d(+)-glucose to emulate the heightened blood glucose levels of a diabetic patient, as chronic wounds are prevalent in people with Type II diabetes. To analyze how high glucose levels impact the efficacy of NAC and NAC+G+C, d(+)-glucose was added to the culture media. In a dose-dependent experiment, we found that there was no relevant difference in biofilm development when comparing the effects of 150, 200, 250, and 300 mg/dL of d(+)-glucose (not shown). Therefore, 300 mg/dL of glucose was used. Specifically, 300 mg/dL is the blood glucose concentration of an untreated diabetic patient. For all three bacteria, the established biofilm was not significantly impacted by the addition of glucose to mimic hyperglycemia (**Fig. 6**). For *Ec*, the efficacy of NAC was significantly diminished upon the addition of glucose. However, it remains a significantly effective treatment at dismantling established biofilm ($p<0.001$). The effects of NAC+G+C were not significantly impacted by the addition of glucose, as there was no significant difference between NAC+G+C and NAC+G+C+Glucose; the established biofilm was effectively dismantled by both treatments ($p<0.001$) (**Fig. 6A**). For *Pa*, the addition of glucose significantly diminishes the effectiveness of NAC ($p<0.05$). The addition of glucose also significantly diminished the effectiveness of NAC+G+C ($p<0.01$). However, in this case, it remains a significantly effective treatment at dismantling established biofilm (Fig. 6B). For *Sx*, the addition of glucose significantly diminishes the effectiveness of NAC. However, its effects remain significant at dismantling the established biofilm ($p<0.001$). The effects of NAC+G+C were also significantly inhibited by the addition of glucose. Nevertheless, it also remains an effective treatment at dismantling the established biofilm ($p<0.001$) (**Fig. 6C**).

The Effects of *N*-acetyl Cysteine, Gentamicin, and Ciprofloxacin on Bacterial Biofilm *in vitro* in the Presence or Absence of High Oxidative Stress and High Glucose Levels

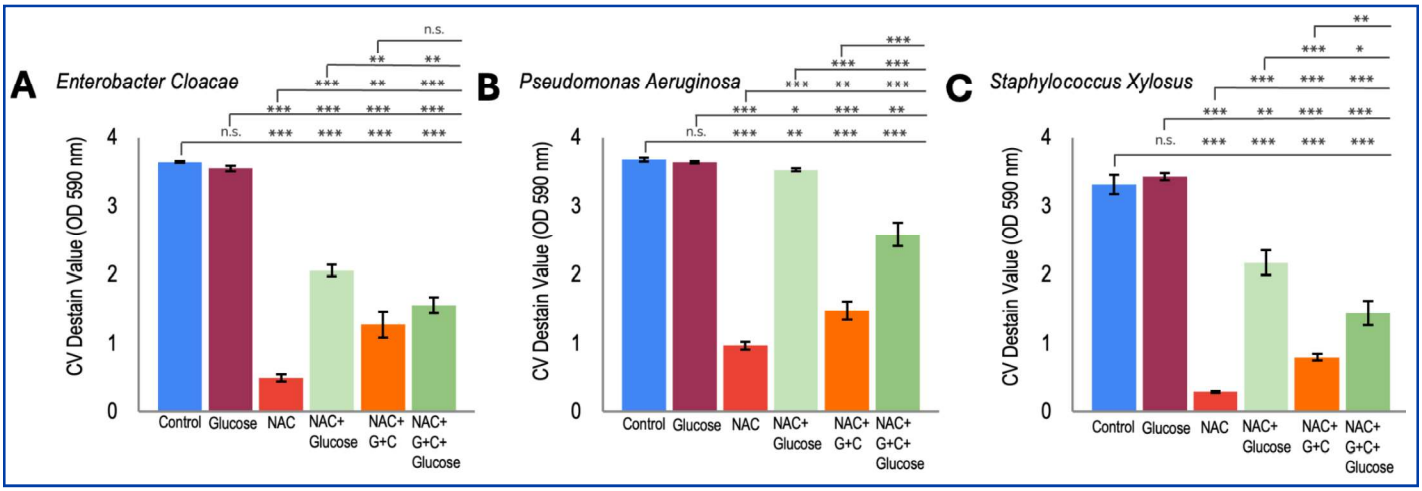

Figure 6. The effects of N-acetyl cysteine (NAC), Gentamicin (G), and Ciprofloxacin (C) on singular strains of bacteria in the presence or absence of heightened glucose levels.

D(+)-glucose was used to emulate heightened glucose levels characteristic of diabetes. The graphs show the amount of biofilm formed 24 hours post-treatment, stained with crystal violet and quantified at OD590 nm.

For all bacteria combinations, the addition of glucose to emulate hyperglycemia had no significant impact on the established biofilm (**Fig. 7**). For *Ec*+*Pa*, the addition of glucose significantly diminished the effectiveness of NAC (n.s.) at dismantling the biofilm. The same is true for the effects of NAC+G+C on biofilm (n.s.); they too are significantly decreased by the addition of glucose. There is no significant difference between the effects of NAC and NAC+G+C when glucose is added (**Fig. 7A**). For *Ec*+*Sx*, the effects of NAC were not significantly impacted by the addition of glucose ($p<0.01$); there was no significant difference between the effects of NAC alone and NAC+Glucose. The effects of NAC+G+C were also not significantly impacted by the addition of glucose ($p<0.001$) as the difference between the effects of NAC+G+C alone and NAC+G+C+Glucose were also not significant. It, too, remains an effective treatment for dismantling the established biofilm (**Fig. 7B**). For *Pa*+*Sx*, the addition of glucose significantly diminished the effectiveness of NAC at dismantling the biofilm. Although its effects remain significant when compared to the non-treated control, it becomes insignificant when compared to the biofilm solely treated with glucose. The effects of NAC+G+C are also significantly inhibited by the addition of glucose (n.s.). There is no significant difference between the effects of NAC and NAC+G+C when glucose is added (**Fig. 7C**). For *Ec*+*Pa*+*Sx,* the effects of NAC are significantly diminished upon the addition of glucose. The effects of NAC+G+C are similarly diminished upon the addition of glucose, though it, too, remains a significantly effective treatment against the established biofilm. While both are effective ($p<0.05$ for NAC; $p<0.001$ for NAC+G+C), NAC+G+C is a significantly better treatment than NAC alone when glucose is added (**Fig. 7D**).

The Effects of *N*-acetyl Cysteine, Gentamicin, and Ciprofloxacin on Bacterial Biofilm *in vitro* in the Presence or Absence of High Oxidative Stress and High Glucose Levels

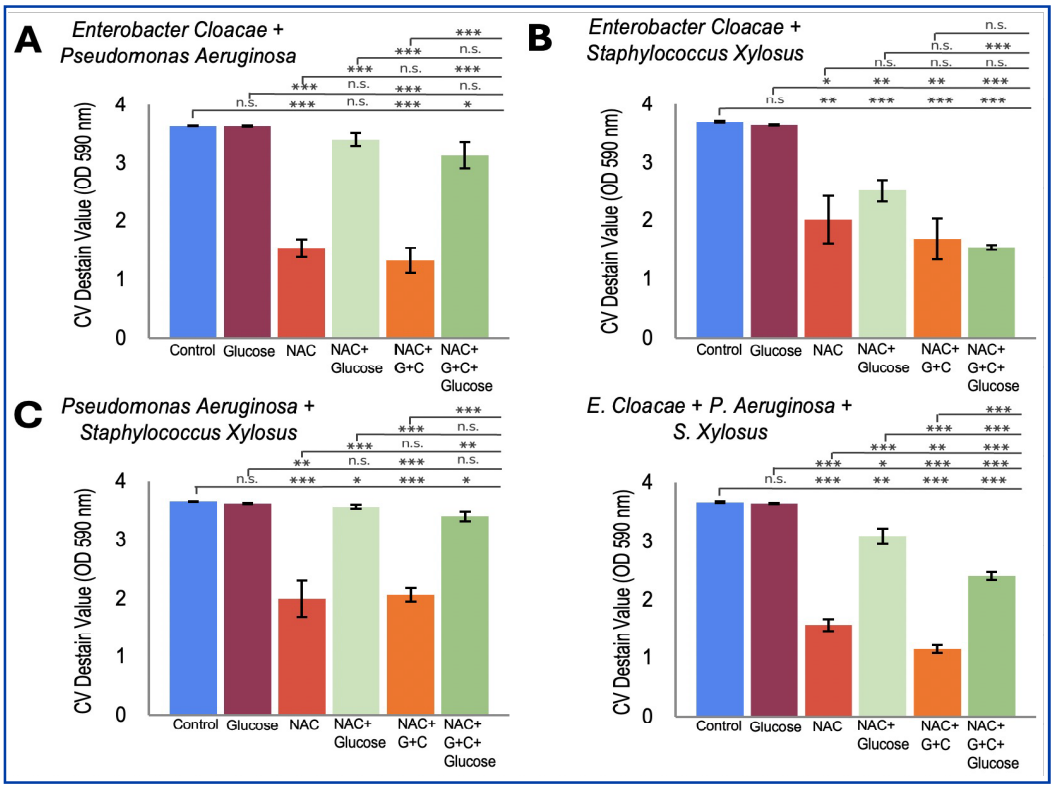

Figure 7. The effects of *N*-acetyl cysteine (NAC), Gentamicin (G), and Ciprofloxacin (C) on combinations of bacteria in the presence or absence of heightened glucose levels.

D(+)-glucose was used to emulate heightened glucose levels characteristic of diabetes. The graphs show the amount of biofilm formed 24 hours post-treatment, stained with crystal violet and quantified at OD590 nm.

DISCUSSION

In this study, *in vitro* biofilm formation by the bacterial strains *Ec, Pa,* and *Sx* was shown within 24 hours of incubation, individually and in combination. The treatments, under varying conditions, significantly dismantled the established biofilm. Specifically, NAC was generally very effective at dismantling established biofilms. However, under conditions of high oxidative stress and hyperglycemia, NAC's efficacy was decreased, as was the efficacy of the other treatments for nearly all the bacteria, though they are not rendered ineffectual. Overall, the treatments remain effective at dismantling biofilm.

Macroscopic visualization of the biofilms showed that the bacteria can develop unique biofilms. The integrity of the EPS, which surrounds microbial communities, and the three-dimensional structure of the matrix determine biofilm morphology. Furthermore, biofilm formation is influenced by many factors, such as bacterial motility and intercellular communication [9]. Each of the three bacterial strains displayed unique morphological characteristics that were retained even when cultured together. This could be attributed to the unique properties of each bacterial strain, such as bacterial motility, cellular communication, and EPS composition, which influence and direct the emergence of biofilm. This could also lead to varying responses to the treatments.

NAC was shown to be an effective treatment for dismantling the biofilms from *Ec, Pa,* and *Sx*, individually or in combination. Specifically, the effect of NAC alone was statistically significant for all three bacteria. Moreover, when considering the individual bacteria, the effect of NAC alone was better than in combination with the antibiotics. We have previously shown that application of NAC to chronic wounds in the diabetic db/db mice, a model that we have developed, leads to the breakdown of biofilm, resulting in the healing of the chronic wounds [11].

The combination of NAC with antibiotics demonstrated variable effects on treatment efficacy in dismantling the biofilms of individual bacteria. Gentamicin (G), for instance, abrogated the efficacy of NAC for *Ec* and *Sx*,

The Effects of *N*-acetyl Cysteine, Gentamicin, and Ciprofloxacin on Bacterial Biofilm *in vitro* in the Presence or Absence of High Oxidative Stress and High Glucose Levels

whereas Ciprofloxacin (C) inhibited the efficacy of NAC for *Pa* biofilms. A study that used EBV-transformed lymphoblastoid cells showed that G was able to catalyze the production of ROS in the presence of iron and/or arachidonic acid [14]. Furthermore, another study that used human fibroblasts showed that C induced lipid peroxidation and decreased intracellular glutathione concentration in a dose-dependent manner. Both measurements indicate an increase in ROS [15]. As NAC is an antioxidant, the variation in its efficacy could be explained by the differing levels of ROS induced by the antibiotics. As stated previously, these inhibitory effects are not consistent across all three individual strains of bacteria, as G inhibits NAC's effectiveness in *Ec* and *Sx*, but not *Pa*. Conversely, the efficacy of NAC was decreased by the presence of C in *Pa* biofilms.

A significant reduction in the efficacy of the treatments was observed in the presence of oxidative stress, *Ec*+*Sx* being an exception. However, the treatments, especially NAC+G+C, remained generally effective at dismantling the established biofilm. A study testing the antioxidant capabilities of NAC found that, although NAC reacts with H_2O_2, it does so at a slow rate [16]. Therefore, the suppression of the efficacy of NAC to dismantle biofilm in the presence of H_2O_2 may be attributed more to temporal limitations than to its capability as an antioxidant. In addition, it is noteworthy that in conditions with added oxidative stress, in biofilms where *Pa* may make up a larger proportion of the biofilm, such as in the cases of *Ec*+*Pa* and *Pa*+*Sx*, the effects of NAC were diminished greatly. In contrast, this effect was not observed when all three bacterial strains were in combination, potentially due to an increase in the proportion of *Ec* and *Sx*.

Gram-negative bacteria possess an outer membrane that acts as an additional permeability barrier, which gram-positive bacteria do not have [17]. Because *Pa* is a gram-negative bacterium, its resistance to NAC, when compared with *Sx*, may be explained by the presence of this additional outer membrane, which decreases permeability to NAC. In addition, unlike Enterobacteria, Pseudomonads lack general diffusion porins in their outer membranes, resulting in lower outer membrane permeability [18]. Although both *Ec* and *Pa* are gram-negative bacteria, lower permeability to NAC may be exhibited by *Pa*, which could explain why *Pa* has greater resilience to NAC's inhibitory effects. Regarding the treatment and its decreased efficacy in the presence of *Pa*, *in vivo*, the biofilms that form on chronic wounds will likely involve a plethora of different strains. Therefore, it is likely that the treatment of NAC will be effective in dismantling established biofilms due to the lower likelihood of *Pa* dominating the biofilms and the competition the bacteria face with each other.

Diabetes has been associated with delayed wound healing, often correlating with the onset of wound chronicity [19]. Because a characteristic condition of diabetes is hyperglycemia, d(+)-glucose was added to the established biofilms. The addition of glucose, much like the addition of H_2O_2, attenuated the ability of our treatments to dismantle established biofilm. Although both NAC and NAC+G+C have their effects abrogated by the addition of glucose, the inhibitory effects of NAC are bolstered by the addition of the antibiotics, as NAC+G+C is a significantly better treatment than NAC alone. Under hyperglycemic conditions, the treatments remained generally effective at dismantling biofilm, with the exceptions of *Ec*+*Pa* and *Pa*+*Sx*, where the effects of both NAC and NAC+G+C were statistically insignificant. Even with *Pa* alone, although both our treatments remain significantly effective, the impact of NAC alone is minor. As observed with the addition of H_2O_2, in biofilms where *Pa* might make up a larger proportion of the bacteria, the efficacy of our treatments is decreased drastically, possibly due to the reduced permeability of *Pa* in comparison to the other bacteria. However, as stated previously, biofilms *in vivo* are composed of multiple strains of bacteria, which makes it more likely for our treatments to remain effective at dismantling established biofilms. In addition, the inhibitory effects of the added glucose might be two-pronged. Glucose is an energy source for the bacteria, which could aid in their growth. In addition, a study that researched the glycosylation of low-molecular-weight thiols found a possible mechanism for such a process in Lincomycin A Biosynthesis, which occurs in the bacterium *Streptomyces lincolnensis* [20]. The glycosylation of thiol groups is possible through both enzymatic and chemical means. Direct reactions between glucose and the thiol group of NAC may result in inactivation of NAC, thereby reducing its efficacy. However, our treatments are still broadly effective, especially when all three bacteria are combined

The Effects of *N*-acetyl Cysteine, Gentamicin, and Ciprofloxacin on Bacterial Biofilm *in vitro* in the Presence or Absence of High Oxidative Stress and High Glucose Levels

Therefore, NAC could prove to be an effective treatment to dismantle established biofilms. As biofilms contribute to wound chronicity, a treatment that abrogates their impact could serve as a treatment for chronic wounds, which would decrease the impact chronic wounds have on the global healthcare system.

CONCLUSIONS

N-acetyl cysteine, particularly with the aid of Gentamicin and Ciprofloxacin, was shown to significantly dismantle *in vitro* established biofilm, with or without oxidative stress and elevated glucose levels. Although the addition of the latter two diminished its effects, the effects of NAC remained statistically significant. Because NAC was consistently effective in dismantling the biofilms formed by *Ec+Pa+Sx*, it could prove to be an effective treatment *in vivo* against biofilm. This is significant because biofilms contribute to wound chronicity, a widespread global health concern. Therefore, NAC has the potential to effectively treat chronic wounds, although it is important to note that, as this study was conducted *in vitro*, it may not fully mimic the situation *in vivo*. In future experiments, we will perform molecular studies after treatment with NAC, to determine the impact of NAC on a more molecular level. We will also perform experiments to determine the impact of NAC on bacteria grown in media that more closely resemble the chronic wound environment to further investigate the therapeutic potential of NAC.

ACKNOWLEDGMENTS

The authors would like to thank Mr. Terrence Lin for his assistance with the project and with gathering data, and Dr. Proma Basu for her aid with general lab techniques.

REFERENCES

1. Sen CK. Human wounds and its burden: an updated compendium of estimates. Advances in wound care. 2019 Feb 1;8(2):39-48.

2. Beeson SA, Neubauer D, Calvo R, et al. Analysis of 5-year mortality following lower extremity amputation due to vascular disease. Plast Reconstr Surg Glob Open. 2023;11(1):e4727. doi:10.1097/GOX.0000000000004727

3. Zhao R, Liang H, Clarke E, Jackson C, Xue M. Inflammation in chronic wounds. International journal of molecular sciences. 2016 Dec 11;17(12):2085.

4. Schultz GS, Chin GA, Moldawer L, Diegelmann RF. Principles of wound healing. Mechanisms of vascular disease: A reference book for vascular specialists [Internet]. 2011; 23.

5. Kim JH, Yang B, Tedesco A, Lebig EG, Ruegger PM, Xu K, Borneman J, Martins-Green M. High levels of oxidative stress and skin microbiome are critical for initiation and development of chronic wounds in diabetic mice. Scientific reports. 2019 Dec 17;9(1):19318.

6. Diegelmann RF, Evans MC. Wound healing: an overview of acute, fibrotic and delayed healing. Front Biosci. 2004 Jan 1;9:283-9.

7. Wlaschek M, Scharffetter-Kochanek K. Oxidative stress in chronic venous leg ulcers. Wound Repair and Regeneration. 2005 Sep;13(5):452-61.

8. Bowler PG, Duerden BI, Armstrong DG. Wound microbiology and associated approaches to wound management. *Clin Microbiol Rev* 2001;14:244–269.

9. Flemming HC, Wingender J. The biofilm matrix. Nature reviews microbiology. 2010 Sep; 8(9):623-33.

10. Petreaca ML, Do D, Dhall S, McLelland D, Serafino A, Lyubovitsky J, Schiller N, Martins-Green MM. Deletion of a tumor necrosis superfamily gene in mice leads to impaired healing that mimics chronic wounds in humans. Wound repair and regeneration. 2012 May;20(3):353-66.

11. Dhall S, Do DC, Garcia M, Kim J, Mirebrahim SH, Lyubovitsky J, Lonardi S, Nothnagel EA, Schiller N, Martins-Green M. Generating and reversing chronic wounds in diabetic mice by manipulating wound redox parameters. Journal of diabetes research. 2014;2014(1):562625.

12. Li X, Kim J, Wu J, Ahamed AI, Wang Y, Martins-Green M. N-Acetyl-cysteine and Mechanisms Involved in Resolution of Chronic Wound Biofilm. Journal of Diabetes Research. 2020;2020(1):9589507.

13. More TT, Yadav JS, Yan S, Tyagi RD, Surampalli RY. Extracellular polymeric substances of bacteria and their potential environmental applications. Journal of environmental management. 2014 Nov 1;144:1-25.

14. Sha SH, Schacht J. Formation of reactive oxygen species following bioactivation of gentamicin. Free Radic Biol Med. 1999;26(3-4):341-347. doi:10.1016/s0891-5849(98)00207-x.

15. Hincal F, Gürbay A, Favier A. Biphasic Response of Ciprofloxacin in Human Fibroblast Cell Cultures. Nonlinearity in Biology, Toxicology, Medicine. 2003;1(4). doi:10.1080/15401420390271083.

15. Aruoma OI, Halliwell B, Hoey BM, Butler J. The antioxidant action of N-acetylcysteine: its reaction with hydrogen peroxide, hydroxyl radical, superoxide, and hypochlorous acid. Free Radic Biol Med. 1989;6(6):593-597. doi:10.1016/0891-5849(89)90066-X

16. Saxena D, Maitra R, Bormon R, et al. Tackling the outer membrane: facilitating compound entry into Gram-negative bacterial pathogens. npj Antimicrob Resist. 2023;1:17. doi:10.1038/s44259-023-00016-1.

17. Chevalier S, Bouffartigues E, Bodilis J, et al. Structure, function and regulation of Pseudomonas aeruginosa porins. FEMS Microbiol Rev. 2017;41(5):698-722. doi:10.1093/femsre/fux020.

18. Blakytny R, Jude E. The molecular biology of chronic wounds and delayed healing in diabetes. Diabetic Medicine. 2006 Jun;23(6):594-608.

19. Dai Y, Cheng Y, Ding W, et al. Structural Basis of Low-Molecular-Weight Thiol Glycosylation in Lincomycin

20. A Biosynthesis. ACS Chem Biol. 2023;18(6):1271-1277. doi:10.1021/acschembio.3c00185.

Does Locus Coeruleus Structure Relate to Associative Memory Related-Activity in Older Adults?

Riley Barrios, Department of Neuroscience
Ilana Bennett, Ph.D.; Department of Psychology

ABSTRACT

Older adults show well-documented declines in memory for relationships among items, especially as the number of items being bound together increases. Less is known about the neural mechanisms that support this type of associative memory, particularly the role of the hippocampus and its neuromodulatory input from the locus coeruleus (LC). In the current study, cognitively healthy older adults completed the QuadMax associative memory task during fMRI scanning to assess hippocampal activity. They studied word pairs, triplets, and quadruplets and were subsequently tested on their memory for repeated, recombined, and novel word sets. Diffusion-weighted MRI was collected to assess LC microstructural integrity. Results revealed that associative memory, recognition, and hit rates declined significantly as associative load increased from pairs to triplets to quadruplets, but these effects were no longer significant when controlled for age and sex. Associative memory encoding led to greater hippocampal BOLD activity for pairs relative to quadruplets in the left hippocampus, with a similar trend in the right hippocampus, and this activity was significantly associated with worse associative memory and recognition performance for quadruplets. Finally, LC mean diffusivity was significantly associated with poorer recognition performance for pairs, but not with hippocampal associative memory-related activity. These findings suggest that age-related variability in hippocampal engagement, not LC integrity, contributes to individual differences in associative memory performance in older adults. Our study highlights the importance of examining both neural activity and neuromodulatory structure to better understand the neural mechanisms that support associative memory in aging.

KEYWORDS: Locus Coeruleus, Associatve Memory, Cognitive Decline, Aging

FACULTY MENTOR - Dr. Ilana Bennett, Department of Psychology

Dr. Bennett earned her doctorate in lifespan cognitive neuroscience from Georgetown University. Her research seeks to advance our understanding of neurocognitive aging by examining age-related differences in the way we acquire, retain, and retrieve information and identifying the neural substrates that underlie these learning and memory processes. Her work has attracted funding from the National Institute on Aging.

Riley J. Barrios

Riley Barrios is a neuroscience major in the University Honors Program at the University of California, Riverside with a strong interest in Alzheimer's disease, cognition, and disparities in brain aging across different populations. As a researcher in the Lani Lab, Riley has studied glial cell activity in younger and older participants and has led the lab's Glia Project while presenting individual research related to neurodegeneration and aging in the Locus Coeruleus. Outside the lab, Riley is passionate about bridging medicine and advocacy through culturally informed research and healthcare.

Does Locus Coeruleus Structure Relate to Associative Memory Related-Activity in Older Adults?

INTRODUCTION

A key component of our memory in daily life is inherently associative (Mayes, Montaldi, & Migo, 2007; Tulving, 1983). When we remember a past event (e.g., meeting a friend for coffee), we retrieve not only isolated items (e.g., a mug or café table), but we also retrieve the relationships among items (e.g., who sat where or who drank what), their features (e.g., the size or color of the mug), and the environment in which they occurred (e.g., the café's background noises). Relative to memory for isolated items, memory for associative relationships among items shows a pronounced age-related decline in accuracy (Franco et al., 2022). Functional magnetic resonance imaging (fMRI) has shown that the hippocampus is active during associative memory performance (Chen & Chang, 2016), indicating that it has a central role in constructing associative memory traces and that associative memory-related activity in the hippocampus varies with age. The hippocampal memory network is thought to be shaped by neuromodulatory input from the locus coeruleus (LC), which is the brain's primary source of noradrenaline, including projections to the hippocampus (Khakpour-Taleghani et al., 2021). However, no studies have examined if LC microstructure relates to hippocampal associative memory-related activity in older adults. The focus of the current study is to better understand how hippocampal and LC systems support associative memory.

Decades of work have shown that older adults exhibit disproportionate impairments in associative memory relative to the memory of items alone (Naveh-Benjamin et al., 2004). For example, in typical paired-associative tasks, participants study pairs of items (e.g., word-word pairs) and are later tested on their ability to distinguish intact pairs from recombined pairs containing previously studied items presented in new combinations (Gold et al., 2006). In these tasks, associative memory is measured by how well participants can recognize intact pairs relative to recombined sets of previously studied items. Using these tasks, older adults reliably show lower associative memory (Naveh-Benjamin et al., 2004), despite preserved recognition of individual items. This pattern supports the idea that aging selectively disrupts associative binding, although these studies have been limited to associations between pairs of items.

Our group used the QuadMax task to extend this literature by parametrically increasing associative load. Participants studied sets of two, three, or four unrelated words and were later tested on their ability to distinguish intact (repeated) from recombined word sets. Prior work using this task showed that associative memory (hit rate minus recombined false alarms) and recognition (hit rate minus novel false alarms) declined significantly with increasing set size, with larger associative memory declines in older adults (Franco et al., 2022). These findings indicate that increasing associative load places greater demands on the memory processes that help link multiple elements into a single episodic representation and that these processes are impaired during aging.

Previous neuroimaging studies using paired-associative paradigms have consistently shown strong hippocampal engagement during associative encoding, with greater activity for conditions that require binding relations between items compared with conditions that emphasize single-item processing (Davachi, 2006). These findings support the idea that the hippocampus plays a central role in linking multiple elements of an experience into a unified memory representation, at least when examining associations between pairs of items.

The locus coeruleus (LC), the brain's primary source of noradrenergic input to the hippocampus, plays an important role in modulating hippocampal memory function. Noradrenergic input from the LC enhances synaptic plasticity and supports memory encoding, consolidation, and retrieval processes that are critical for episodic memory (Uematsu et al., 2015). The LC's microstructure has been shown to measurably decline with age (Bennett et al., 2024) and to be linked to episodic memory performance in older adults (Fukabori et al., 2020), albeit not to associative memory performance in humans. This suggests that LC structural variability may influence hippocampal recruitment and ultimately to associative memory success. Studies using associative memory tasks have found activity in the hippocampus, but none have examined if this activity is modulated by LC structure.

The current study aims to test if LC microstructural integrity is related to hippocampal activity during associative

Does Locus Coeruleus Structure Relate to Associative Memory Related-Activity in Older Adults?

memory encoding in older adults. The older adults completed the QuadMax associative memory task during fMRI scanning along with diffusion-weighted imaging to assess LC microstructure. We predicted that older adults would show worse associative memory performance as associative load increased and would show measurable hippocampal engagement during study. We also predicted individual differences in LC integrity would relate to the level of hippocampal activity observed during associative memory processing, supporting the LC's role in moderating hippocampal function during demanding memory tasks.

METHODS

Participants

Forty-four older adults (>65 years old) were recruited from communities surrounding the University of California, Riverside. Prior to study enrollment, potential participants were screened over the phone for: (1) normal global cognition (>17 score on the Montreal Cognitive Assessment [MoCA] adapted for phone screening; [Pendlebury et al., 2013]); (2) hearing or vision loss, (3) history of neurological conditions or psychiatric disorders that could influence performance (e.g. depression, schizophrenia), (4) recent medications that could influence image quality (e.g. mood stabilizers, benzodiazepines, psychotropics), (5) major health conditions (e.g. diabetes), (6) MRI contraindications (e.g. pregnancy, claustrophobia), and (7) comfort using keyboard buttons. After enrollment, participants were excluded from final analyses due to issues with data collection (n = 4; e.g., not recording all responses, running the same condition twice, coughing fit during fMRI scans) or for failing to respond to more than 30% of the trials (n = 1). The final sample consisted of 39 older adults (mean age = 68.9 years; 71.8% female). All participants gave informed consent and received monetary compensation for participation.

General Procedure

After informed consent was provided, participants completed two MRI sessions as part of two separate studies using a 3.0 Tesla MRI system (Siemens Magnetom Trio) with a standard 32-channel head coil at the Center for Advanced Neuroimaging at the University of California, Riverside. Structural MRI sequences in Session 1 were used to assess locus coeruleus structure and an associative memory task was completed during functional MRI acquisition in Session 2.

Associative Memory Task

Participants completed two versions of the QuadMax task (Figure 1) in the MRI scanner. In the study phase, participants viewed 60 word sets of two (pairs), three (triplets), and four (quadruplets) semantically unrelated words (20 per set size) and indicated if they could "imagine the words doing something together" or not using button presses.

In the test phase, participants viewed 90 word sets: 30 identical to studied sets (repeated; 10 per set size), 30 recombinations of studied sets (recombined; 10 per set size), and 30 comprised of new words (novel; 10 per set size). Participants indicated if they had seen the exact word set in the study phase ("old") or if they had not ("new") using button presses.

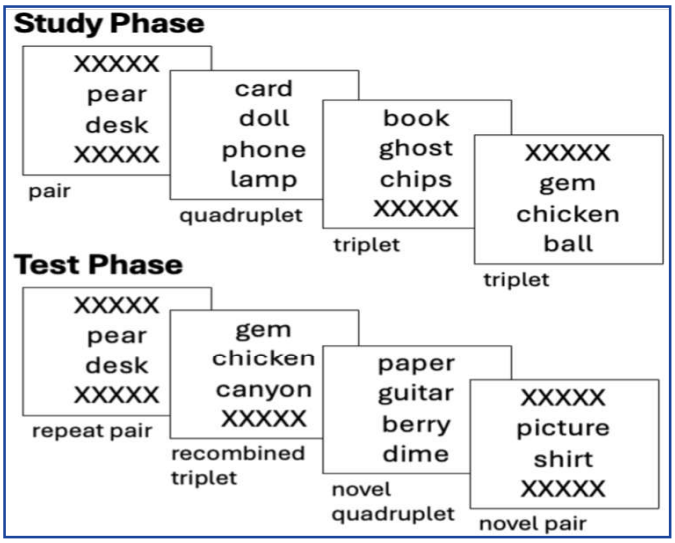

Figure 1: Example trials from the study phase (top) and test phase (bottom) of the QuadMax task show the set size (pairs, triplets, quadruplets) and trial type (repeated, recombined, novel) conditions.

Does Locus Coeruleus Structure Relate to Associative Memory Related-Activity in Older Adults?

Metrics

For each participant and each set size, the proportion of correct "old" responses to repeated (hit rate), incorrect "old" responses to recombined (recombined false alarm [FA] rate), and incorrect "old" responses to novel (novel FA rate) sets were calculated. Associative memory was calculated as hit rate minus recombined FA rate. Recognition was calculated as hit rate minus novel FA rate. Average scores across set sizes and task versions were also calculated.

Structural Imaging Data

We acquired T1-weighted MP-RAGE (echo time (TE)/ repetition time (TR)/inversion time = 3.02/2600/800 ms, GRAPPA acceleration = 2, flip angle = 8°, voxel size = 0.8 mm^3), magnetization transfer-prepared gradient echo (MT-GRE; TE/TR = 3.21/385 ms, flip angle = 40°, field of view (FOV) = 220 × 186 mm^2, slice thickness = 3 mm), and diffusion-weighted single-shot spin-echo, echo planar (TE/ TR = 75/4100 ms, voxel size = 1.15 × 1.15 × 2.5 mm^3, 30 directions with gradient strengths of b = 500 s/mm^2 and 2000s/mm^2) images.

Locus coeruleus region of interest. A standardized atlas of bilateral locus coeruleus (LC) (Langley et al., 2020) was aligned to each participant's MT-GRE and diffusion-weighted spaces using registration tools in the FMRIB Software Library (FSL) (Jenkinson et al., 2002).

MTC metrics. For each participant, raw MT-GRE acquisitions were corrected for motion and averaged. A maximum MT contrast (MTC) metric was calculated as the peak MTC value relative to the pontine reference region within the MT-GRE-aligned LC region of interest. Values exceeding four standard deviations from the sample mean were excluded (n = 2 older adults).

Diffusion metrics. For each participant, raw diffusion-weighted data were corrected for motion, susceptibility distortions, and eddy currents using FSL's TOPUP and EDDY (Andersson, Skare, & Ashburner, 2003; Andersson & Sotiropoulos, 2016). Mean diffusivity (MD) was estimated using the b = 0 and 500 data with FSL's DTIFIT. Mean MD in the LC was calculated by averaging values within the diffusion-aligned region of interest.

Functional Imaging Data

Acquisition. Separate echo-planar imaging (EPI) pulse sequences were acquired during performance of the study and test phases of each version (C, D) of the QuadMax task (TR/TE = 1750/32 ms, field of view = 221 × 190.4 mm, flip angle = 77 degrees, spatial resolution = 1.7 mm^3, 72 slices with no gap, AP phase encoding direction, GRAPPA acceleration factor = 2, and multiband factor = 3). Additional spin echo EPI images with opposite phase-encoding directions were acquired to correct for susceptibility distortions (identical except TR/TE = 7700/58 ms). Only the study phase data are reported here.

Preprocessing. Raw fMRI data were corrected for susceptibility-induced distortions (TOPUP; Andersson et al., 2003) and then preprocessed using FEAT (FMRI Expert Analysis Tool), which included motion correction, brain extraction, spatial smoothing (5 mm FWHM Gaussian kernel), and high-pass filtering (100 s). Preprocessed data were registered to the participant's T1-weighted image using FLIRT (Jenkinson et al., 2002), and then to a standard Montreal Neurological Institute (MNI) 152 template that was resampled to 1.7 mm^3 resolution using a combination of FLIRT with BBR and FNIRT (Andersson et al., 2007).

Lower-level analysis. Separate lower-level analyses were conducted for each participant and each task version (C, D) from the study phase, using FILM with local autocorrelation correction (Woolrich et al., 2001). Analyses modeled each set size (pairs, triplets, quadruplets) and these three explanatory variables were convolved with a gamma-variate hemodynamic response function (standard deviation = 3 s, mean lag = 6 s). Two contrasts captured associative memory-related activity by contrasting pairs and quadruplets (pairs > quadruplets, quadruplets > pairs).

Higher-level analyses. A mid-level analysis was conducted to capture variance across task versions within each participant using fixed effects. One explanatory variable modeled activity from the lower-level analyses for each participant and one contrast captured average activity for each participant across task versions.

Higher-level analyses were conducted across participants on outputs of the mid-level analyses using FSL's Local Analysis of Mixed Effects (FLAME) stage 1. One explanatory

Does Locus Coeruleus Structure Relate to Associative Memory Related-Activity in Older Adults?

variable modeled activity from the mid-level analyses and one contrast captured within-group mean effects by average activity across participants. We applied the default nonparametric statistical threshold using clusters determined by $Z > 3.1$ and a (corrected) cluster significance threshold of $P = 0.05$ (Worsley 2001). FSL's Featquery was used to extract parameter estimates for each contrast for each participant from the left and right hippocampus.

RESULTS

Associative Memory Performance

Separate repeated-measures ANOVAs were conducted for each outcome metric (associative memory, recognition, hits, recombined FA, novel FA) using Set Size (pairs, triplets, quadruplets) as the within-subjects variable (Figure 2). For associative memory, there was a significant main effect of Set Size, $F(2, 78) = 25.2$, $p < 0.001$. Post hoc pairwise comparisons revealed that associative memory was worse (lower) for each increase in set size from pairs (0.51 ± 0.29) to triplets (0.33 ± 0.17) to quadruplets (0.23 ± 0.24), $ps < 0.022$. For recognition, there was a significant main effect of Set Size, $F(2, 78) = 37.1$, $p < 0.001$, with worse recognition for each increase in set size from pairs (0.82 ± 0.17) to triplets (0.70 ± 0.17) to quadruplets (0.60 ± 0.19), $ps < 0.001$. For hits, there was a significant main effect of Set Size, $F(2, 78) = 38.0$, $p < 0.001$, with lower hits for each increase in set size from pairs (0.90 ± 0.14) to triplets (0.76 ± 0.17) to quadruplets (0.66 ± 0.20), $ps < 0.001$. There was no significant main effect of Set Size for recombined FA, $p = 0.108$, or novel FA, $p = 0.856$.

Effects of age and sex. When controlling for age and sex, main effects of Set Size were no longer significant for any outcome metric, $ps > 0.10$. However, age had a significant effect on associative memory, $F(1, 36) = 5.2$, $p = 0.029$, recognition, $F(1, 36) = 4.3$, $p = 0.044$, and novel FA, $F(1,36) = 4.8$, $p = 0.035$, performance.

Associative Memory-Related Activity

Whole-brain maps showing regions with significant BOLD activation are shown in Figure 3. One sample t-tests determined if there was significant activity in the left and right hippocampus during the study phase of the associative memory task. Results revealed significant activity for the pairs > quadruplets contrast in the left hippocampus (13.0 ± 3.6), $t(38) = 3.55$, $p = 0.001$. Results revealed no significant activity for the quadruplets > pairs contrast in the left hippocampus (2.2 ± 4.2), $p = 0.608$. Results revealed a non-significant trend for activity for the pairs > quadruplets (9.8 ± 5.1), $p = 0.059$, and quadruplets > pairs (6.8 ± 3.7), $p = 0.073$, contrasts in the right hippocampus. Although the right hippocampus only showed a trend-level effect, the results suggest associative memory related activity was higher for pairs compared to quadruplets in both hemispheres.

Effects of age and sex. Note that there were no significant correlations between age and task-related activity in either hippocampal hemisphere, $ps > 0.36$. There were also no significant sex group differences in task-related activity in the hippocampus, $ps > 0.17$.

Figure 2: Increasing set size from pairs to triplets to quadruplets led to lower associative memory, recognition, and hit rates, while recombined and novel false alarms showed no significant differences among set sizes.

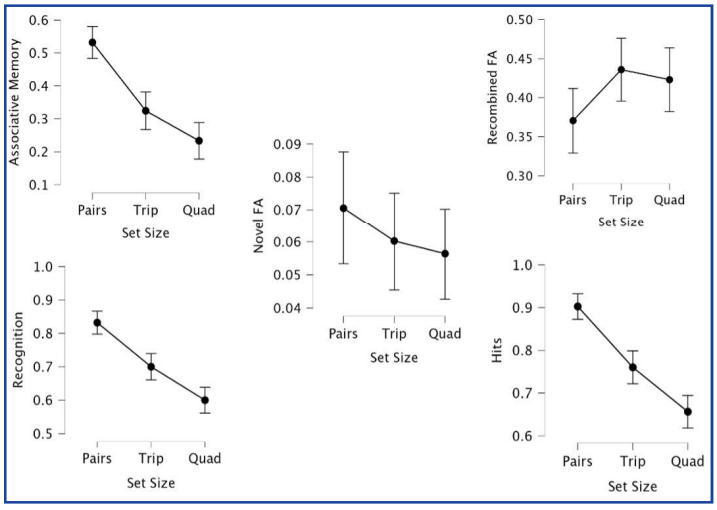

Does Locus Coeruleus Structure Relate to Associative Memory Related-Activity in Older Adults?

Associative Memory Performance Correlates with Associative Memory-Related Activity

Partial correlations examined relationships between associative memory performance (associative memory, recognition) for each set size (pairs, triplets, quadruplet) and associative memory-related activity in the left and right hippocampus, controlling for age and sex. For associative memory, results revealed that greater activity for the pairs > quadruplets contrast in the left, r = -0.38, p = 0.021, and right, r = -0.34, p = 0.040, hippocampus was significantly related to worse associative memory for quadruplets. For recognition, results revealed that greater activity for the pairs > quadruplets contrast in the left, r = -0.43, p = 0.008, and right, r = -0.34, p = 0.037, hippocampus was significantly related to worse recognition for quadruplets.

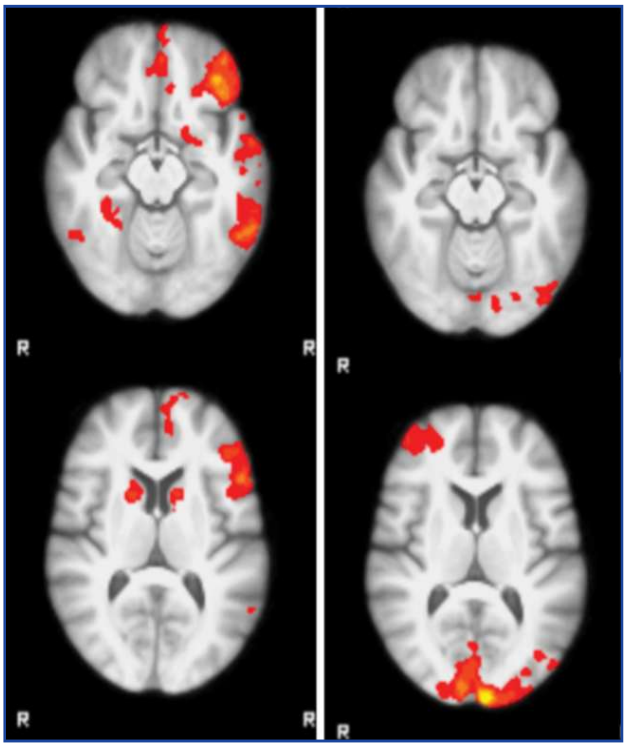

Figure 3: Whole-brain maps showing regions with greater BOLD activation for pairs compared to quadruplets (left) and quadruplets compared to pairs (right) during the study phase.

Locus Coeruleus Structure Correlates with Memory Performance

Partial correlations then examined relationships between memory performance (associative memory, recognition) for each set size (pairs, triplets, quadruplet) and locus coeruleus metrics (MD and Maximum CNR), controlling for age and sex. Results revealed that higher LC MD was significantly associated with worse recognition for pairs, $r = -0.48$, p = 0.029. No other relationships achieved significance, ps > 0.16.

Locus Coeruleus Structure Does Not Correlate with Associative Memory-Related Activity

Partial correlations examined relationships between locus coeruleus structural metrics (MD, Maximum CNR) and task-related hippocampal activity (pairs > quadruplets, quadruplets > pairs) in the left and right hippocampus, controlling for age and sex. Results revealed no significant relationships, ps > 0.14.

DISCUSSION

The current study examined if locus coeruleus (LC) microstructural integrity relates to associative memory performance and hippocampal associative memory-related activity in older adults. Thirty-nine cognitively healthy older adults completed the QuadMax associative memory task during fMRI scanning, along with diffusion-weighted and magnetization transfer imaging to assess LC microstructure. At the behavioral level, associative memory, recognition, and hit rates declined significantly as associative load increased from pairs to triplets to quadruplets, but only before controlling for age or sex. At the level of hippocampal BOLD activity, associative memory encoding elicited significantly greater activity for pairs relative to quadruplets in the left hippocampus, with a similar trend observed in the right hippocampus. Greater hippocampal activity for the pairs > quadruplets contrast was significantly associated with worse associative memory and recognition performance for quadruplets. Finally, LC structure was selectively related to behavior such that higher LC mean diffusivity was associated with worse recognition performance for pairs, but not with hippocampal associative memory-related activity.

Does Locus Coeruleus Structure Relate to Associative Memory Related-Activity in Older Adults?

When not controlling for age or sex, associative memory, recognition, and hit rates were significantly worse for quadruplets than for triplets and for triplets than for pairs. This replicates our prior work in which we found declines in associative memory and related measures as set size increased in older adults (Franco et al. 2022). Interestingly, when controlling for age and sex, these effects were no longer significant, suggesting that age- and sex-related differences were the primary drivers of performance rather than associative load. Recombined and novel false alarm rates did not differ with set size, regardless of if age and sex were controlled. This finding was unexpected given our prior work and may reflect methodological differences among the studies that reduced sensitivity to associative load effects on FA rates, including the use of two task versions with a larger total number of study sets as well as a substantially smaller sample size. This may have increased variability and limited the power to detect load-related differences in false alarms. Nonetheless, these behavioral findings suggest that age and sex are key factors that play a significant role in associative memory performance in older adults.

fMRI data revealed significantly greater hippocampal BOLD activity for pairs relative to quadruplets during the study phase of the associative memory task in the left hippocampus, with a non-significant trend in the right hippocampus. This finding is consistent with prior literature showing that the hippocampus is critical for binding multiple items into a cohesive memory representation (Davachi, 2006). However, our finding that hippocampal activity during encoding was higher for pairs than for triplets or quadruplets (i.e., higher associative loads) is not consistent with prior work, which has instead found that hippocampal activity during encoding was higher for conditions in which two items needed to be associated relative to conditions with one or zero items to be associated (Addis et al., 2006). One interpretation is that the hippocampus may be recruited when binding two items, whereas binding four may exceed the capacity of its binding mechanisms in older adults, resulting in lower activity (Reuter-Lorenz and Cappell, 2008).

Individual differences in hippocampal activity were related to memory performance at higher loads. Greater hippocampal activity for the pairs > quadruplets contrast was associated with worse associative memory and recognition performance for quadruplets. This negative correlation suggests that heightened hippocampal engagement under lower associative loads may reflect inefficient processing rather than more effective memory formation. As associative load increases, the hippocampus may reach a functional limit in its ability to bind multiple elements into a cohesive representation, similar to what has been previously reported in frontal cortex during high working memory load (Reuter-Lorenz and Cappell, 2008). This limit may result in reduced engagement during quadruplet trials in the study phase, impairing encoding of the word sets and ultimately leading to worse memory performance, especially for quadruplets. Together, these findings may suggest that reduced hippocampal engagement at higher associative loads may contribute to poorer associative memory performance in aging adults.

Finally, LC microstructure was selectively related to memory performance, but not to associative memory-related hippocampal activation. Specifically, higher LC mean diffusivity was significantly associated with worse recognition performance for pairs. This finding extends prior work that has similarly shown that LC microstructure relates to episodic memory performance in older adults (Fukabori et al., 2020) and is consistent with the notion that noradrenergic input from the LC enhances synaptic plasticity and processes that are critical for episodic memory (e.g., encoding, consolidation, and retrieval) (Uematsu et al., 2015). However, because LC microstructural measures were not significantly related to hippocampal associative memory-related activity during the study phase, the contribution of LC microstructure to individual differences in recognition accuracy may be independent of mechanisms captured by task-related hippocampal BOLD activation. Thus, our findings did not support the notion that activity in the hippocampal memory network is shaped by neuromodulatory input from the LC.

Several limitations should be considered. Although the QuadMax task isolates associative memory demands by holding item familiarity constant and increasing the number of inter-item relationships, larger set sizes may place greater demands on working memory and strategic organization during study, particularly in older adults. Thus, some of the associative load effects in performance and the BOLD response may reflect both associative binding demands and

age-related differences in maintaining multiple elements in working memory during study. Although hippocampal activity was measured during task performance, fMRI cannot determine if LC-related influences on memory occur through modulation of hippocampal associative binding or broader network-level effects. Future studies using higher-resolution LC imaging, functional connectivity approaches, and larger samples could clarify these mechanisms. Despite these limitations, the present study extends prior work using the QuadMax task by demonstrating that associative load impairs associative memory and recognition memory performance in older adults including at higher set sizes, that greater activity in the hippocampus during study of pairs relative to quadruplets was associated with worse performance (associative memory and recognition for quadruplets), whereas LC microstructural variability was selectively related to recognition performance. Together, these findings suggest that age-related associative memory decline may separately reflect hippocampal engagement and integrity of the neuromodulatory LC system that supports memory. These results return to the broader idea that successful memory for daily events relies on both hippocampal and LC systems that become increasingly vulnerable with aging. Importantly, these findings strengthen models of cognitive aging by identifying hippocampal inefficiency under increasing load as a key mechanism of associative memory decline and suggest that hippocampal function may be a more sensitive target for intervention than LC integrity.

Does Locus Coeruleus Structure Relate to Associative Memory Related-Activity in Older Adults?

REFERENCES

Addis, D. R.; McAndrews, M. P. NeuroImage 2006, 33 (4), 1194–1206.

Andersson, J. L. R.; Skare, S.; Ashburner, J. NeuroImage 2003, 20, 870–888.

Andersson, J. L. R.; Jenkinson, M.; Smith, S.; Andersson, J. FMRIB Technical Report TR07JA2; FMRIB Centre: Oxford, 2007.

Andersson, J. L. R.; Sotiropoulos, S. N. NeuroImage 2016, 125, 1063–1078.

Bennett, I. J.; Langley, J.; Sun, A.; Solis, K.; Seitz, A. R.; Hu, X. P. Sci. Rep. 2024, 14 (1), 15372.

Chen, P.-C.; Chang, Y.-L. Neuropsychologia 2016, 85, 216–225.

Franco, C. Y.; Alcaraz-Torres, A.; Bennett, I. J. Exp. Aging Res. 2022.

Davachi, L. Curr. Opin. Neurobiol. 2006, 16 (6), 693–700.

Fukabori, R.; Iguchi, Y.; Kato, S.; Takahashi, K.; Eifuku, S.; Tsuji, S.; et al. J. Neurosci. 2020, 40 (43), 8367–8385.

Gold, J. J.; Hopkins, R. O.; Squire, L. R. Learn. Mem. 2006, 13 (5), 644–649.

Jenkinson, M.; Bannister, P.; Brady, M.; Smith, S. NeuroImage 2002, 17, 825–841.

Khakpour-Taleghani, B.; Akhoondian, M.; Jafari, A. J. Curr. Biomed. Rep. 2021, 2 (4), 142–149.

Langley, J.; Hussain, S.; Flores, J. J.; Bennett, I. J.; Hu, X. Neurobiol. Aging 2020, 87, 89–97.

Mayes, A.; Montaldi, D.; Migo, E. Trends Cogn. Sci. 2007, 11 (3), 126–135.

Naveh-Benjamin, M.; Guez, J.; Shulman, S. Psychon. Bull. Rev. 2004, 11 (6), 1067–1073.

Pendlebury, S. T.; Welch, S. J.; Cuthbertson, F. C.; Mariz, J.; Mehta, Z.; Rothwell, P. M. Stroke 2013, 44 (1), 227–229.

Reuter-Lorenz, P. A.; Cappell, K. A. Curr. Dir. Psychol. Sci. 2008, 17 (3), 177–182.

Tulving, E. Philos. Trans. R. Soc. London, B 1983, 302 (1110), 361–371.

Uematsu, A.; Tan, B. Z.; Johansen, J. P. Learn. Mem. 2015, 22 (9), 444–451.

Woolrich, M. W.; Ripley, B. D.; Brady, M.; Smith, S. M. NeuroImage 2001, 14 (6), 1370–1386.

Worsley, K. J. In Functional MRI: An Introduction to Methods; Jezzard, P.; Matthews, P. M.; Smith, S. M., Eds.; OUP: Oxford, 2001; Ch. 14.

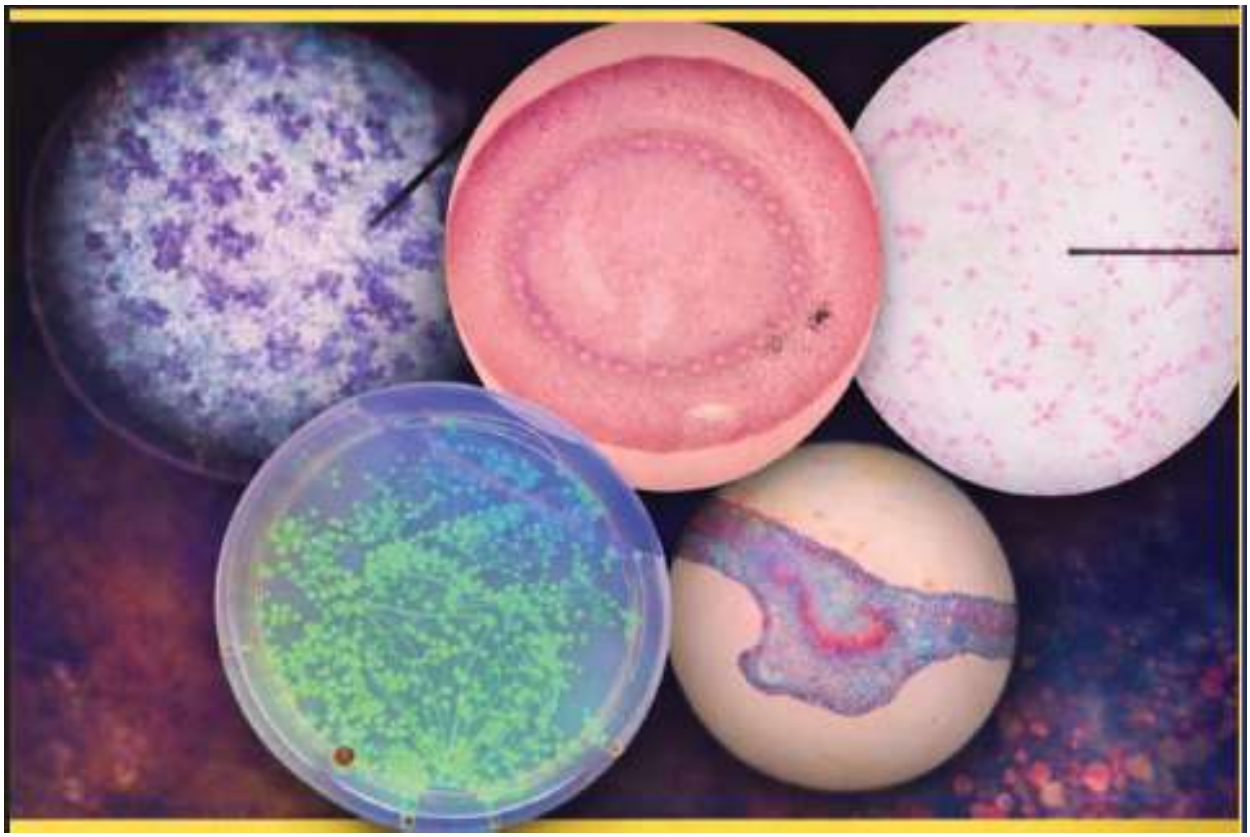

This image was created by Kora Dey. It shows images taken through a microscope and from petri dishes, and reflects the detail and effort behind research.

Adversity and Visual Working Memory: The Role of Lifetime Adversity When Shaping Visual Working Memory in Emotional Recall

Carissa Johnson, Department of Psychology
Rishitha M. Kona, Department of Psychology and Department of Business Administration
Yessella Moreno, Department of Psychology
Jessica Golding, Ph.D Candidate; Department of Psychology
Weiwei Zhang, Ph.D.; Department of Psychology

ABSTRACT

Prior research has suggested that adversity is linked to cognitive impairments, including reduced memory, attention, and decision-making abilities. There has also been evidence of negativity biases in memory, where humans tend to allocate more attention and remember negative information more vividly than other forms of emotional stimuli. Data was collected from students (ages 19-31) at the University of California, Riverside in an upper-division psychology laboratory course through an online Google Form. Participants were split into different sections of which included general demographic information (age/gender); their recall across three trials of positive, negative, and neutral words pulled from the Affective Norms for English Words (ANEW) database; and their responses to the Stress and Adversity Inventory Screener for Adults (STRAIN). No correlation was found between adversity and overall recall performance. There was also no correlation between adversity scores and any of the emotional stimuli separately. An ANOVA found that emotional tone significantly affected recall performance, with a Post-Hoc Analysis revealing specifically that negative word recall was the lowest overall, while neutral was highest. However, there was no significant effect of emotional tone on levels of adversity. In support of the alternative hypotheses, emotional tones did have a significant effect on how frequently a valenced word was recalled. However, there was insufficient evidence to support our main hypothesis and no evidence to reject the null hypothesis, suggesting that there is no relationship between adversity and memory performance.

KEYWORDS: visual working memory, lifetime adversity, emotional valence, negativity bias, recall performance, STRAIN inventory, cognitive processing.

FACULTY MENTOR - Dr. Zhang, Department of Psychology

Dr. Zhang joined UCR's Department of Psychology in 2012. The Zhang Lab uses cognitive neuroscience methods to research perception, attention, memory, and higher cognition in healthy and clinical populations. His work is funded by the National Institute of Mental Health (NIMH) and National Institute on Aging (NIA).

CARISSA JOHNSON

Carissa is a psychology student at UCR and an incoming Psy.D. student at the University of La Verne with research interests in self/social stigma, clinician bias, and cultural competency. She is a Chancellor's Research Fellow and conducts research on how adversity and emotional regulation strategies influence visual working memory. Her long-term goal is to pursue a career in clinical psychology that integrates research, mentorship, and evidence-based mental health care.

RISHITHA KONA

Rishitha is double majoring in Psychology and Business Administration at UCR. She serves as a research assistant in Weiwei Zhang's CONPAM Lab, where she has contributed to research examining facial recognition, handgrip strength's link to leadership qualities, and adversity's relationship with visual working memory. Her academic interests center on cognitive psychology and the intersection of psychology and business. Following graduation, she will continue her education by earning an M.S. in Applied Psychology at the University of Southern California.

Adversity and Visual Working Memory: The Role of Lifetime Adversity When Shaping Visual Working Memory in Emotional Recall

INTRODUCTION

Understanding how perception interacts with cognition remains one of the most intriguing and underexplored areas in cognitive science. Recent research has begun to shed light on these processes, particularly visual working memory (VWM), a sophisticated cognitive system that temporarily stores and manipulates visual information. Landmark work by Luck and Vogel (1997), employing a change detection paradigm, demonstrated that VWM stores integrated objects rather than isolated features, catalyzing a surge of research into the mechanisms and boundaries of VWM. Building on this, Bays and Husain (2008) showed that VWM capacity is flexible, with allocation varying according to task demands, and that attention modulates the precision of memory representations. As El-Hage et al. (2006) note, working memory forms a crucial link between perception and controlled action. However, the specific ways in which life experiences, particularly adversity, shape the dynamics of VWM remain insufficiently understood. The present study is motivated by the need to clarify this relationship: it systematically investigates how lifetime adversity influences the allocation of attention and recall during VWM tasks involving emotionally valenced stimuli. By doing so, the study aims to advance our understanding of how emotional relevance and life experience shape core cognitive processes, with implications for education, occupational performance, and well-being.

The influence of adversity and trauma on memory remains a critical frontier in cognitive science. Levens et al. (2016) found that distant adversity can enhance working memory performance. In contrast, recent adversity tends to impair it, underscoring the complex and dynamic effects of life experiences on cognitive functioning. While these findings illuminate the importance of emotional context, they fall short of clarifying how the degree of adverse experiences shapes future memory processes. Most previous research has focused on the impact of acute emotional states on immediate visual memory, often overlooking critical individual differences, such as cognitive ability and attentional capacity. Studies on adversity typically emphasize long-term memory or focus narrowly on childhood experiences, leaving adult and lifetime adversity underexplored. This study is motivated by the emerging possibility that lifetime adversity plays a more significant and nuanced role in shaping the emotional dynamics of VWM than previously recognized.

The central aim of this study is to determine how lifetime adversity influences the recall of emotionally valenced stimuli during VWM tasks. Gaining a clearer understanding of how adversity shapes cognition has critical implications for educational achievement, occupational performance, and overall well-being. Based on previous literature, two primary hypotheses were formulated: the main hypothesis predicts that individuals with higher lifetime adversity will exhibit a recall bias toward negative words, remembering more negative than positive or neutral words, consistent with the negativity bias framework (Levens et al., 2016). The null hypothesis is that there will be no significant association between adversity scores and recall performance across emotional valences. This study also explores the alternative possibility that higher adversity is associated with poorer recall across all categories, reflecting the inhibitory effects of trauma and stress, as documented by Ji and Wang (2018). Notably, our design improves on past studies by examining differences across valences rather than focusing solely on overall recall or limited emotional categories.

METHODOLOGY

Participants

Participants were undergraduate students at the University of California, Riverside, enrolled in an upper-division psychology laboratory course, ensuring a similar educational background. The sample was very small (N=18; both males and females aged 19 to 31), which limits the generalizability and statistical power of the findings and should be considered when interpreting results. This limitation is acknowledged up front to promote transparency and rigor. Participants voluntarily completed the study in a classroom setting through a digital survey accessed by a link or QR code. All participants provided informed consent before participating and were debriefed afterward, in accordance with ethical guidelines. This classroom-based study was reviewed for ethical compliance and approved by the course instructor, in line with university IRB policies for minimal-risk educational research.

Adversity and Visual Working Memory: The Role of Lifetime Adversity When Shaping Visual Working Memory in Emotional Recall

Materials

A digital form, accessible via link or QR code, was used to collect participant age and sex and to present task instructions. To assess the impact of emotional valence on VWM, participants viewed lists of positive, neutral, and negative words selected from the Affective Norms for English Words (ANEW) database (Bradley et al., 1999). Words were chosen based on valence ratings (1 = unhappy; 9 = happy) to ensure consistent emotional impact: positive ($\geq$ ~7), negative ($\leq$ ~3), and neutral ($\approx$ 5).

The stimuli consisted of three blocks of 12 words (see Appendix A), each containing four words per valence category in randomized order. During the encoding phase, a PowerPoint presentation displayed each word for 1 second, with a 1-second fade. In the retrieval phase, participants had two minutes to recall and report words via the digital form after each block. Recall was scored by counting only correct words that matched the presented list exactly and were written in the correct tense; extraneous or incorrectly recalled words were excluded. Emotional categories were analyzed separately to identify valence-specific effects.

Adversity Assessment

Following the memory tasks, participants were invited to anonymously complete the Stress and Adversity Inventory Screener for Adults (STRAIN) (Slavich, 2022). While the original STRAIN contains 220 items, this study used the 20-item shortened version (see Appendix B) to quantify the total number of lifetime stressors.

Responses were scored dichotomously (1 = "YES," 0 = "NO"), with a "DECLINE TO STATE" (0) option for sensitive questions. Higher total scores indicate greater adversity; individuals with high "Decline" rates were excluded from the final analysis. This screening was administered after the primary memory task to minimize biases toward negative information arising from a priming effect triggered by the survey content. Participants were explicitly informed that this portion was optional and confidential.

Procedures

Prior to starting the experiment, participants provided informed consent and completed a digital demographic form. They were then given specific instructions for the memory task:

> "In this next part, you will be presented with a series of 12 random words, one at a time for one second. After the last word, the screen will tell you to list as many words as you can remember. At this time, you may click 'next' on your form. You will have two minutes to write. When the timer goes off, click next once more. Please do not continue on until prompted to do so."

This process consisted of three trials with identical parameters but different words to ensure data consistency Following the memory tasks, researchers explained the purpose of the STRAIN survey, the full scope of the study, and the reason for the initial omission of the survey details. Participants then completed the STRAIN assessment with renewed assurances of anonymity and the option to decline sensitive questions.

Statistical Analyses

Responses to the STRAIN were aggregated to reflect adversity levels, and the quantity of words recalled (by category and total) was calculated. The selection of these variables and analyses was designed to isolate the impact of lifetime adversity on recall performance across emotional valences and to control for potential confounds, such as overall recall ability. To examine the relationship between lifetime adversity and emotional recall, five variables were included: 1) adversity score (0–20), 2) positive words recalled (0–12), 3) negative words recalled (0–12), 4) neutral words recalled (0–12), and 5) total words recalled (0–36). Recalled words were adjusted to the maximum total correct; words not on the list or in incorrect tenses were excluded. This approach enabled a nuanced analysis of if adversity influences not only total recall but also preferential recall of specific emotional categories.

Correlation Analysis. A Pearson correlation coefficient (r) was used to assess the strength and direction of the relationship between adversity scores and the recall of positive, negative, and neutral words. Pearson's correlation was chosen for its effectiveness in evaluating linear relationships between continuous variables in small samples. Significance was evaluated using a two-tailed test ($\alpha = 0.05$).

Adversity and Visual Working Memory: The Role of Lifetime Adversity When Shaping Visual Working Memory in Emotional Recall

Group Comparisons. To observe differences in word recall and adversity, mean totals were compared using a Repeated Measures ANOVA (two-tailed, $\alpha = 0.05$). A repeated-measures ANOVA was selected because it allows comparisons of recall rates within subjects across emotional valence, increasing statistical power, and controlling for individual differences. To convert adversity from a continuous to a discrete variable, a median split created high (score >5) and low (score ≤5) groups, each containing 9 participants. The first ANOVA measured the main effects of emotional tones on recall; a second iteration included adversity level as a between-subjects factor to determine whether adversity modulated the effect of emotional tone on recall.

RESULTS

Descriptive statistics (Table 1) were conducted to identify trends in recall performance across emotional valences. Table 1 summarizes the mean recall scores for positive, negative, and neutral words, showing that participants recalled more neutral words than either positive or negative words. The descriptive statistics helped contextualize the subsequent inferential analysis of average positive words.

A repeated-measures ANOVA revealed a significant difference in recall rates by emotional tone; neutral words were recalled most (M = 7.06), negative words least (M = 6.56), with negative recall significantly lower than both positive (p = 0.008) and neutral (p = 0.008), and no difference between positive and neutral recall (p > 0.05)

Correlation analyses showed no significant relationship between adversity score and recall of negative (r = -0.38, p = 0.12), positive (r = -0.31, p = 0.22), neutral (r = 0.07, p = 0.79), or total words (r = -0.38, p = 0.12); thus, adversity score was not correlated with recall for any emotional valence (all p > 0.05)

An additional repeated-measures ANOVA including adversity level as a between-subjects factor found no significant interaction between adversity level and recall of positive, negative, or neutral words (F(1,16) = 0.694, p = 0.417)); thus, adversity did not affect the pattern of recall across emotional tones..

Descriptive Statistics ▼

	Valid	Mean	Std. Deviation	Range	Minimum	Maximum
Negative recall	18	5.056	1.798	6.000	2.000	8.000
Positive recall	18	6.556	1.653	6.000	4.000	10.000
Neutral recall	18	7.056	2.313	8.000	3.000	11.000
Total Correct Recall	18	18.611	3.806	13.000	13.000	26.000
Adversity Score	18	6.444	4.342	13.000	2.000	15.000

Table 1

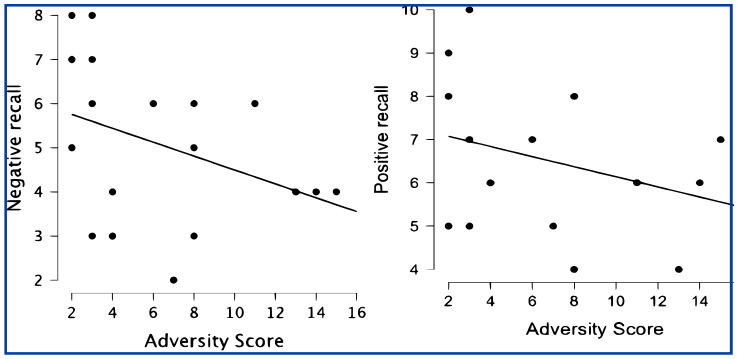

Figure 1. Mean Recall Scores vs Emotional Tone.
(a) scatter plot of data; (b) bar plot of data means. Depictions of a repeated-measures ANOVA showed a statistically significant difference in scores for emotional tones, $F(2, 34) = 6.314$, $p < 0.05$. ($p = 0.005$).

Adversity and Visual Working Memory: The Role of Lifetime Adversity When Shaping Visual Working Memory in Emotional Recall

Post Hoc Comparisons - Emotional Tone ▼

		Mean Difference	SE	t	Cohen's d	p_{holm}
Positive	Neutral	−0.500	0.715	−0.699	−0.257	0.494
	Negative	1.500	0.430	3.491	0.772	0.008**
Neutral	Negative	2.000	0.577	3.464	1.030	0.008**

Table 2. Post-Hoc Differences between Stimuli Recall. Post Hoc comparisons revealed that negative stimuli were recalled significantly less than positive (M = 6.556, p = 0.008) and neutral (M = 7.056, p = 0.008).

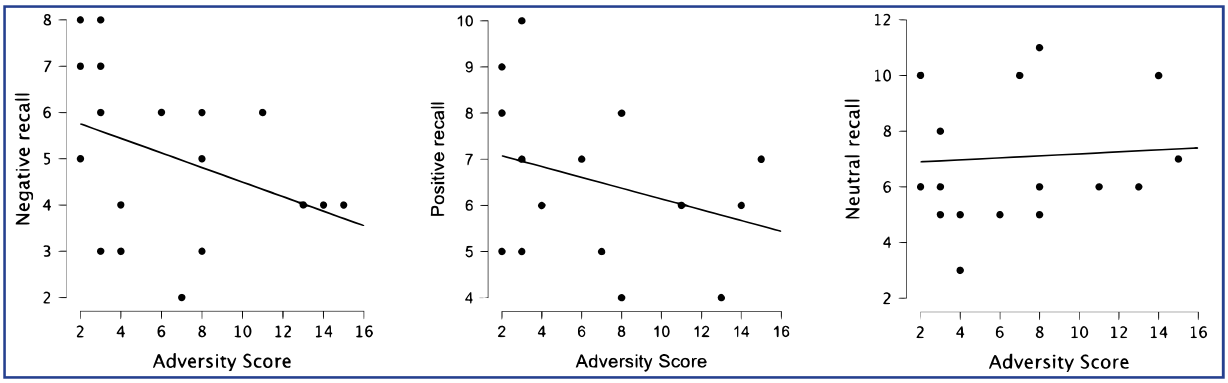

Figure 2. Correlation between STRAIN Scores and Recall of Each Stimulus. (a) STRAIN scores and negative word recall: Pearson's r = -0.38, p = 0.12 (weak, non-significant negative trend). (b) STRAIN scores and positive word recall: r = -0.31, p = 0.22 (weak, non-significant negative trend). (c) STRAIN scores and neutral word recall: r = 0.07, p = 0.79 (weak, non-significant positive trend).

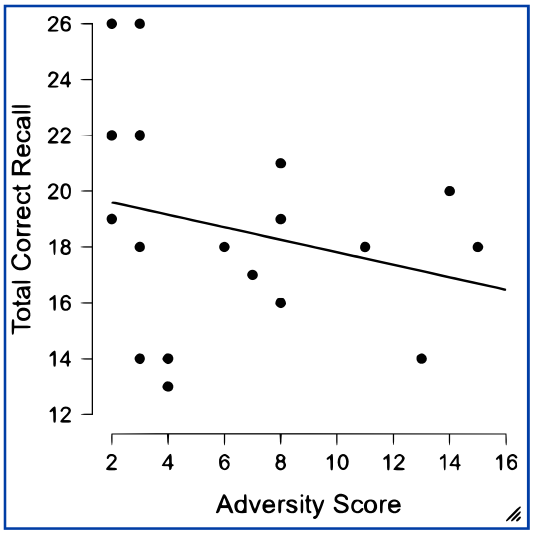

Figure 3. Correlation between STRAIN Scores and Total Correct Words Recalled. Relationship between the scores on the STRAIN and Total words correctly recalled. Pearson's r indicates a weak, non-significant negative trend, r = -0.380, p = 0.120.

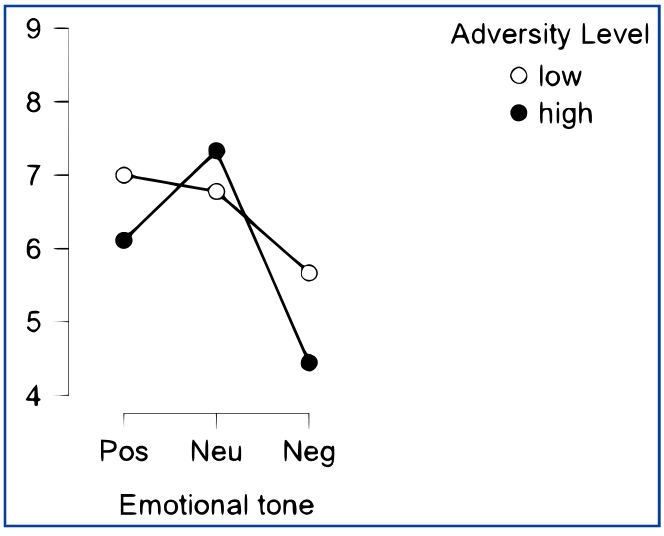

Figure 4. Main Effects of Emotional Tones and Interaction of Adversity Level. Repeated Measures ANOVA observing the effect of Adversity Level. No significant difference, $F(1,16)$ = 0.694, p > 0.05.

Adversity and Visual Working Memory: The Role of Lifetime Adversity When Shaping Visual Working Memory in Emotional Recall

DISCUSSION

The main hypothesis, that individuals with higher adversity scores would recall more negative words, was not supported in this sample. Instead, the data best fit the null hypothesis, with no significant correlation between adversity and recall of emotionally valenced stimuli. However, recall performance did differ by emotional tone: neutral words were recalled most, and negative words least. One issue that complicates the interpretation of these findings is the small sample size, which reduced statistical power and may have masked subtle group differences. Additionally, the analytic decision to employ a median split for adversity, while facilitating categorical comparisons, may have limited the sensitivity to detect more nuanced, linear effects. Future studies should either treat adversity as a continuous variable or employ more advanced analytic models.

The connection between these results and the study hypotheses is clear: the lack of a relationship between adversity and recall refutes the initial expectation of a negativity bias among high-adversity participants. This outcome should be interpreted cautiously, given the methodological limitations, and underscores the need for replication with larger, more diverse samples and more refined analytic strategies. The finding that negative recall was lowest was unexpected and stands in contrast to prior research on negativity bias (Levens et al., 2016). One possible explanation is emotional avoidance: participants may have subconsciously avoided encoding or recalling negative words as a coping strategy. Alternatively, negative words might increase cognitive load or emotional interference, making them harder to encode and retrieve. These results partially align with Bays & Husain (2008), who argued that attention is preferentially allocated to information perceived as most relevant or least distressing.

A critical issue in this study is the limited control over confounding variables, such as baseline mood and individual differences in coping mechanisms or resilience. Additionally, the reliability of the recall scoring and the use of a short adversity screener may have affected measurement precision. These factors, along with the small sample size and analytic choices (median split), could have influenced the null findings. In contrast to prior studies such as El-Hage et al. (2006) and Ji & Wang (2018), which found adversity impairs memory, our study did not reveal a significant association between adversity and recall, possibly due to these methodological constraints. Although a non-significant trend toward impaired recall with greater adversity was observed, further research is needed to clarify these relationships.

LIMITATIONS AND FUTURE RESEARCH

Our results must be interpreted in light of several limitations of the study. The small, convenience-based sample (N = 18) limits generalizability and increases the risk of Type II error. The correlational design precludes causal conclusions and reduces internal validity. Although some procedural details, such as timing and stimulus presentation, were explicitly controlled, other important aspects, including the reliability of measures, control of confounding variables (e.g., mood, baseline cognitive ability), and randomization procedures, require further development to ensure rigor. The use of a median split for adversity, while facilitating group comparisons, also presents limitations as previously noted.

To address these shortcomings, future research should increase sample size, use random sampling, rigorously control for confounding factors (e.g., mood, cognitive ability, prior trauma), and use validated and reliable measures. Greater procedural clarity, such as reporting inter-rater reliability for scoring recall or explicitly describing counterbalancing, would improve replicability. Studies could also build on Levens et al. (2016) by distinguishing between the effects of recent and distant adversity on VWM to illuminate the role of emotional resilience. Employing more granular adversity measures, such as the full STRAIN survey, would provide richer data. In addition, examining other domains of working memory (e.g., auditory) and considering long-term effects on memory consolidation through longitudinal designs could yield deeper insights. Finally, as the implications of adversity on cognitive functioning are only beginning to be understood, these lines of inquiry could support interventions for at-risk groups, inform cognitive training programs, and influence educational policy.

In conclusion, investigating adversity and its effects on memory is essential for advancing our understanding of human cognition. Because adversity manifests in diverse forms and degrees of severity, appreciating its varied impact is critical. The current findings contribute to theory by challenging the assumption that high adversity is always linked to a negativity bias in memory; instead, the results suggest that emotional factors and individual coping strategies may override adversity-related biases under certain conditions. Practically, these results highlight the importance of considering emotional context and participant characteristics when designing memory interventions for populations with a history of adversity.

REFERENCES

Bays, P. M., & Husain, M. (2008). Dynamic shifts of limited working memory resources in human vision. *Science, 321*(5890), 851–854. https://doi.org/10.1126/science.1158023

Bradley, M. M., Lang, P. J., NIMH Center for the Study of Emotion and Attention, & The Center for Research in Psychophysiology, University of Florida. (1999). Affective Norms for English Words (ANEW): instruction manual and affective ratings. In *Technical Report C-1*. The Center for Research in Psychophysiology, University of Florida.

El-Hage, W., Gaillard, P., Isingrini, M., & Belzung, C. (2006). Trauma-related deficits in working memory. *Cognitive Neuropsychiatry*, 11(1), 33–46. https://doi.org/10.1080/13546800444000164

Ji, S., & Wang, H. (2018). A study of the relationship between adverse childhood experiences, life events, and executive function among college students in China. *Psicologia Reflexão E Crítica*, 31(1). https://doi.org/10.1186/s41155-018-0107-y

Levens, S. M., Armstrong, L. M., Orejuela-Dávila, A. I., & Alverio, T. (2016). The two sides of adversity: the effect of distant versus recent adversity on updating emotional content in working memory. *Cognition & Emotion*, 31(6), 1243–1251. https://doi.org/10.1080/02699931.2016.1197099

Luck, S. J., & Vogel, E. K. (1997). The capacity of visual working memory for features and conjunctions. *Nature, 390*(6657), 279–281. https://doi.org/10.1038/36846

Slavich, G. M. (2022). *Stress and Adversity Inventory (STRAIN) screener for adults*. https://www.uclastresslab.org/pubs/STRAIN-Screener-for-Adults-20-item-v1.0-Released-1-24-2022.pdf

APPENDIX A

Chosen Word Lists

Words were drawn from the Affective Norms for English Words (ANEW) database. Parameters for average word valence were added to ensure a more reliable positive/neutral/ negative rating. On a scale of one to nine, negative words averaged a valence rating of $\lesssim 3$, neutral words averaged ≈ 5, and positive words averaged $\gtrsim 7$. Random words within these parameters were chosen, and placed into randomizers to establish group and order within the group.

Words Categorized:

Group 1: Positive: Joyful, Peaceful, Loved, Grateful, Negative: Sad, Angry, Lonely, Stressed, Neutral: Table, Chair, Door, Book

Group 2: Positive: Happy, Cheerful, Delighted, Thrilled, Negative: Afraid, Guilty, Worried, Horrible, Neutral: Window, Pen, Clock, Floor

Group 3: Positive: Hopeful, Content, Ecstatic, Blissful, Negative: Depressed, Anxious, Frustrated, Terrible, Neutral: Paper, Wall, Roof, Street

Adversity and Visual Working Memory: The Role of Lifetime Adversity When Shaping Visual Working Memory in Emotional Recall

APPENDIX B

Stress and Adversity Inventory (STRAIN) Screener for Adults

The STRAIN survey used is the shortened 20-item version of the original 220-question assessment. This version is dichotomous with "YES"= 1 and "NO"= 0, the summation of the numerical responses are used to score adversity level, 0 pts being the minimum and 20 pts being the maximum. This survey has been modified in some wordings as well as given a third option of "DECLINE TO STATE" ("DECLINE") with the value of 0.

STRAIN Assessment (modified)

Please indicate whether you experienced the situation at **any point during your lifetime...**

Question	Yes	No	DECLINE TO STATE
1) You experienced a difficult move that disrupted your daily life?			
2) You lived without enough space or privacy?			
3) You had difficulty paying for basic things in adulthood, such as food or rent?			
4) You were laid off or fired from a job?			
5) You had difficulty caring for a child (e.g., problems with childcare or paying for basic needs)?			
6) You had an immediate family member move out of the house for an upsetting reason?			
7) You experienced bullying (e.g., name calling, humiliation, rejection) during childhood?			
8) You separated from parent or caregiver for at least one month during childhood?			
9) You found out that a partner was unfaithful to you?			
10) You went through a divorce or serious relationship break-up?			
11) You had major legal problems with a partner or spouse (e.g., financial, custody issues)?			
12) You provided care for a close friend or family member who had a major health problem?			
13) You had a loved one with a mental illness (e.g., severe anxiety, depression, drug problem)?			
14) You had a friend or loved one who was abused (e.g., emotional, physical, or abuse)?			
15) A close friend or loved one passed away?			
16) Your parent/(s) passed away?			
17) You experienced emotional abuse (e.g., invalidated, blamed, threatened, or humiliated)?			
18) You experienced physical abuse (e.g., bruised, hit, restrained, or physically harmed)?			
19) You were assaulted or attacked (e.g., someone tried to hurt, harass, or rape you)?			
20) You experienced ongoing sexual abuse (e.g., raped, molested, or unwanted sexual contact)?			
TOTAL (Sum of 'Yes' responses)			

The Influence of Childhood Parental Support and Irritability on Internalizing Symptoms in Latina Girls

Rabyana B. Iqbal, Department of Psychology
A. Lorena Tafoya, Department of Psychology
Ashley L. Zhang, B.A., Department of Psychology
Matthew S. Kersting, M.A., Department of Psychology
Kalina J. Michalska, Ph.D., Department of Psychology

ABSTRACT

Current research indicates that parental neglect and child irritability are both positively associated with internalizing symptoms. However, minoritized groups, such as preadolescent Latina girls, remain underrepresented in this area of the scientific literature. The present study extends prior research by examining associations among parental support, irritability, and internalizing symptoms in a sample of 27 Latina girls aged 8–13. Multiple linear regression models independently assessed the associations between parental support and irritability with internalizing symptoms, controlling for age and for socioeconomic status via parental income and education. Results indicated a positive association between child irritability and internalizing symptoms. Though our findings are limited due to our small sample size, the association between irritability and internalizing symptoms highlights the importance of further examining child irritability in relation to the development of internalizing symptoms in Latina preadolescent girls.

KEYWORDS: Latina Girls, Parental Support, Irritability, Internalizing Symptoms, Inland Empire

Rabyana Iqbal

Rabyana will be graduating in June 2026 with her B.S. in Psychology and a minor in Philosophy. She works as an undergraduate research assistant in Dr. Kalina Michalska's Kids Interaction and NeuroDevelopment Lab, which explores emotional development of Latina girls in the Inland Empire. She plans to pursue a Clinical Psychology Ph.D. or Psy.D., and focus on child/adolescent populations, after gaining a year of clinical experience post-undergrad.

A. Lorena Tafoya

Lorena is a third-year undergraduate student, double-majoring in Psychology and Education, Society, and Human Development, with a concentration in Learning and Behavioral Studies. She works as an undergraduate research assistant in Dr. Kalina Michalska's Kids Interaction and NeuroDevelopment Lab. She is a University Honors student and serves as the University Honors Co-Chief Ambassador. After graduating from UCR in Spring 2027, she plans to pursue a Clinical Psychology Ph.D. program, with the intention of studying incarcerated youth.

FACULTY MENTOR - Dr. Kalina Michalska, Department of Psychology

Dr. Michalska is an Associate Professor of Psychology at UCR and director of the KIND Lab, with affiliations in the Neuroscience Program and the Department of Psychiatry. She earned her Ph.D. in Developmental Psychology from the University of Chicago and completed a Research Fellowship at NIMH. Her research uses neuroimaging, autonomic measures, and behavioral observations to study emotional processing, childhood behavioral and anxiety disorders, and sociocultural influences on threat neurocircuitry development.

The Influence of Childhood Parental Support and Irritability on Internalizing Symptoms in Latina Girls

INTRODUCTION

Sensitive, responsive caregiving is essential for forming strong parent-child bonds and has lasting psychological consequences. Beyond meeting physical needs, parental support plays a critical role in children's social development, such that positive, mutually engaged interactions are associated with better self-regulation in early childhood and fewer behavioral and mental health issues in adolescence (Lunkenheimer et al., 2020). Conversely, when parental support is inadequate, the resulting social deprivation is linked to increased risk for internalizing symptoms (e.g., anxiety; Calaresi et al., 2025). The present study examines the concurrent association between parental support and internalizing symptoms in a sample of preadolescent Latina girls.

Individual Differences in Parental Support

Parental support may play an important role in shaping the development of internalizing symptoms. However, current research focuses on more extreme adverse experiences, such as emotional abuse and neglect (Strathearn et al., 2020), and there has been less scholarly attention on variability in everyday parental support as a developmental influence on mental health. This gap is especially important for preadolescent Latina girls, who may face immigrant-related stressors that increase susceptibility to psychopathology (Mullins et al., 2024). Despite this, relatively few studies have examined how parental support relates to internalizing symptoms in this population.

Irritability and Internalizing Symptoms

Irritability, defined as an increased proneness to anger relative to one's peers, often expressed through outbursts and reactive aggression (Henriksen et al., 2021), is a strong predictor of anxiety symptoms, and 65% of youth with General Anxiety Disorder experience persistent irritability (Stoddard et al., 2013). The association between irritability and anxiety symptoms is more commonly observed in women and younger populations (Perlis et al., 2009). Additionally, exposure to increased traumatic stressors is associated with a heightened risk of irritability in females compared to males, suggesting underlying differences in how individuals process trauma depending on their sex (Henriksen et al., 2021). Together, these studies suggest a strong positive correlation between irritability and internalizing symptoms, such that anxiety symptoms increase as irritability increases.

Latine Adolescents and Barriers to Mental Health

Individual differences and environmental factors, such as cultural background, gender, preexisting psychological disorders, and socioeconomic status (SES), may influence irritability and internalizing symptoms. Most of the current literature examines samples consisting primarily of non-Hispanic white males, leaving a gap in research on racial and ethnic groups that develop in distinct contexts (Araújo & Borrell, 2006). Latine individuals are more likely to experience greater ethnic-racial discrimination during childhood than white/Caucasian individuals (Pole et al., 2005). Patterns of internalizing symptoms in children, including Latina girls, may be heightened by unique experiences of ethnicity-related stressors, such as discrimination and marginalization (Mullins et al., 2024).

Low-income communities with large populations of undocumented Latines face multiple barriers to accessing mental health services due to exploitation, marginalization, and isolation (Noël, 2018; Shattell et al., 2008), suggesting that youth from under-resourced neighborhoods are more likely to experience poorer emotional outcomes. Similarly, individuals with depression who face financial barriers are more likely to report more severe symptoms than those without economic barriers to medical and mental health care (Pabayo et al., 2021), as limited access restricts treatment and support. These findings suggest that lower SES is associated with receiving care in under-resourced settings, unaffordable medical costs, and increased risk for psychopathology (Abedzadeh-Kalahroudi et al., 2018). This intersectionality suggests overlapping social identities are associated with greater risk for psychopathology (Vu et al., 2019). We aim to expand the current understanding of the impact of parental involvement and irritability on internalizing symptoms in Latina girls, a historically underrepresented population in the literature despite their heightened risk for mental health challenges.

The Influence of Childhood Parental Support and Irritability on Internalizing Symptoms in Latina Girls

Our Study

Our study has two primary aims: (1) to examine the relationship between Latina girls' experiences of parental support during childhood and their self-reported internalizing symptoms, and (2) to examine the relationship between irritability and internalizing symptoms.

We hypothesize that greater parental support will be associated with fewer internalizing symptoms. In contrast, we expect higher levels of irritability to be associated with more frequent internalizing symptoms.

METHODS

Participants

Our data is from an ongoing longitudinal study that began in 2016 and was approved by the Institutional Review Board (#30207). Our current sample consists of 27 Latina girls ages 8 to 13 (M = 9.52, SD = 1.28) from the Inland Empire in Southern California, and their primary caregivers. Participants were recruited from the University of California, Riverside REDCap participant database and contacted via phone and email as part of a larger longitudinal study on socioemotional development.

Parental Support

Latina girls completed 10 items (α = 0 .72) from the Parenting Involvement subscale of the 42-item Alabama Parenting Questionnaire (APQ; Shelton et al., 1996), which assessed perceived parental support from their primary caregiver (e.g., "You have a friendly talk with your [parent]"). This measure uses a 5-point Likert scale (1–5; 1 = *Almost Never*, 5 = *Always*). Items were summed to create a total score.

Irritability

Participants completed the 7-item Affective Reactivity Index (ARI; Stringaris, 2012), a self-reported measure assessing irritability (e.g., "I am easily annoyed by others"). The ARI uses a three-level response scale (0 = *not true*, 1 = *somewhat true*, and 2 = *certainly true*), and total scores were calculated as the sum of the first six items (α = 0.73).

Internalizing Symptoms

Internalizing symptoms were measured using the 41-item Screen for Child Anxiety Related Disorders (SCARED; Birmaher et al., 1999), a self-report measure of anxiety symptoms (e.g., "I worry about things working out for me"). Items are rated on a 3-point Likert scale (0 = *Not True/ Hardly Ever True,* 2 = *Very True/Often True*), and total scores were summed (α = 0.94).

Analysis Plan

To test our first and second hypotheses, we created two multiple linear regression models, regressing APQ and ARI scores onto SCARED scores, respectively.

All models included age, parental income, and mothers' educational attainment as covariates to control for any influence they may have on the association between our variables of interest, as these SES variables may influence available parental support. Maternal educational attainment (M = 4.41, SD = 1.15) was measured using a 6-point Likert scale (1 = "No School," 6 = "Graduate Professional Training (Master's or above)"). Family income (M = 4.93, SD = 1.88), was reported on an 8-point Likert Scale (1 = "under $5,000," 8 = "over $180,000"). Each of these measures was treated as a continuous variable. To correct for multiple comparisons, we applied the Benjamini-Hochberg procedure to all significance values. All analyses were conducted using the R statistical programming language (R Core Team, 2025).

RESULTS

Bivariate correlations for all variables are reported in Table 1. Given the small sample size of N = 27, we conducted a sensitivity analysis to determine the minimum detectable effect size with α = 0.05 and 80% power. The analysis determined the study was powered to detect a large effect, with a minimum $R_p^2 = 0.23$ ($f^2 = 0.30$).

Parental Support and Internalizing Symptoms

We observed no significant association between the APQ Involvement subscale (M = 67.93, SD = 11.89) and SCARED total scores (M = 32.33, SD = 15.72), b = 0.208, 95% CI [-0.46, 0.87], SE = 0.322, $t(22)$ = 0.644, p = 0.526.

The Influence of Childhood Parental Support and Irritability on Internalizing Symptoms in Latina Girls

Irritability and Internalizing Symptoms

We observed a significant association between the ARI (M = 3.30, SD = 2.54) and SCARED total scores, b = 3.639, 95% CI [1.23, 6.04], SE = 1.159, $t(22)$ = 3.139, p = 0.004, such that irritability positively predicted internalizing symptoms. This finding held after Benjamini-Hochberg corrections were applied (p_{adj} = 0.019) and exceeded the minimum threshold determined by the sensitivity analysis, R^2_p = 0.31 (f^2 = 0.45).

Correlations with confidence intervals

Variable	1	2	3	4	5	6
1. Age	--					
2. Maternal Education	-.52* [-.81, -.01]	--				
3. Income	-.31 [-.71, .24]	.42 [-.12, .77]	--			
4. APQ	.45 [-.08, .78]	-.88** [-.96, -.66]	-.39 [-.75, .15]	--		
5. ARI	.21 [-.34, .65]	.08 [-.45, .57]	-.45 [-.78, .08]	-.23 [-.66, .32]	--	
6. SCARED	.10 [-.44, .58]	-.02 [-.52, .50]	-.38 [-.75, .16]	-.04 [-.54, .48]	.67** [.23, .88]	--

Table 1. Correlations with confidence intervals

DISCUSSION

We found no association between parental support and anxiety, leaving our first hypothesis unsupported. However, our results revealed a significant association between irritability and anxiety symptoms, indicating that irritable children may exhibit higher levels of anxiety.

Parental Support and Internalizing Symptoms

Contrary to prior research, we found no significant association between parental support and internalizing symptoms in Latina girls. Strathern and colleagues (2020) reported higher levels of psychopathology among individuals who experienced emotional neglect from caregivers during childhood. Similarly, Calaresi and colleagues (2025) found that social deprivation was associated with internalizing symptoms. These discrepancies may be due to differences in sample populations. Our sample was drawn from the Inland Empire in Southern California, whereas prior studies included individuals from European (Calaresi et al., 2025) or Australian (Strathern et al., 2020) backgrounds. Differences in regional practices or culturally-specific coping strategies among Latina preadolescent girls may help explain these differences (Pierro et al., 2022). Understanding such groups may help inform more culturally responsive mental health services and caregiving practices.

The Influence of Childhood Parental Support and Irritability on Internalizing Symptoms in Latina Girls

Irritability and Internalizing Symptoms

In line with prior research, we found a positive association between irritability and internalizing symptoms, specifically anxiety. This aligns with past literature, which found an association between irritability and anxiety, particularly among women and younger populations (Perlis et al., 2009) and that exposure to stressors is linked to anxiety (Henrickson et al., 2021). Notably, prior studies have largely focused on White samples. Additionally, immigrant-related stressors, such as discrimination, may shape these associations in Latine populations (Mullins et al., 2024). Our study extends these findings to Latina girls in the Inland Empire, a population that remains underrepresented in the literature, suggesting that Latina girls may be susceptible to co-occurring irritability and anxiety symptoms.

Implications

Our findings suggest that anxiety and irritability are positively associated in Latina girls. This association may shed light on the possible importance of how internalizing symptoms uniquely develop in this population. Gaining a better understanding of this relationship could aid in developing methods to reduce irritability in Latina girls. While we did not find associations between parental support and anxiety, future researchers should continue to examine how parenting practices operate within specific cultural contexts. Additionally, immigration-related experiences may influence both parenting and mental health, highlighting the need for more culturally-informed research. Continuing to explore these possible effects in larger Latine samples may allow parental and mental health support systems to better adjust to meet the needs of Latina adolescent and adult women. Future research has the potential to inform practitioners of early intervention strategies, targeting parenting styles and irritability to reduce mental health risks in Latina girls.

LIMITATIONS AND FUTURE DIRECTIONS

This study had a few limitations. First, our sample size was small (N = 27), limiting statistical power and the ability to detect small or moderate effects. Future research should gather larger samples to investigate the uniqueness of the present study's population. Finally, all measures were self-reported measures, which may lead to biased responses due to social desirability or limited self-awareness. Future research should incorporate additional objective measures, such as behavioral or physiological measures, or use multi-informant measures to improve validity.

REFERENCES

1. Abedzadeh-Kalahroudi, M., Razi, E., & Sehat, M. (2018). The relationship between socioeconomic status and trauma outcomes. *Journal of Public Health, 40*(4). https://doi.org/10.1093/pubmed/fdy033.

2. Araújo, B.Y., & Borrell, L.N. (2006). Understanding the link between discrimination, mental health outcomes, and life chances among Latinos. *Hispanic Journal of Behavioral Sciences, 28*(2), 245–266. https://doi.org/10.1177/0739986305285825.

3. Birmaher, B., Brent, D. A., Chiappetta, L., Bridge, J., Monga, S., & Baugher, M. (1999). Psychometric properties of the Screen for Child Anxiety Related Emotional Disorders (SCARED): A replication study. *Journal of the American Academy of Child and Adolescent Psychiatry, 38*(10), 1230–6. https://doi.org/10.1097/00004583-199910000-00011.

4. Calaresi, D., Verrastro, V., Giordano, F., & Saladino, V. (2025). The long-term effects of emotional neglect on family functioning and anxiety symptoms in adolescents. *Journal of Family Violence*, https://doi.org/10.1007/s10896-025-01011-y.

5. Ma, C., Huang, Z., Feng, X., Memon, F. U., Cui, Y., Duan, X., Zhu, J., Tettamanti, G., Hu, W., & Tian, L. (2024). Selective breeding of cold-tolerant black soldier fly (*Hermetia illucens*) larvae: Gut microbial shifts and transcriptional patterns. *Waste Management*, 177, 252–265. https://doi.org/10.1016/j.wasman.2024.02.007.

6. Henriksen, M., Skrove, M., Hoftun, G. B., Sund, E. R., Lydersen, S., Kalvin, C. B., & Sukhodolsky, D. G. (2021). Exposure to traumatic events poses greater risk for irritability in girls than in boys. *Journal of Affective Disorders Reports, 6*, 100204. https://doi.org/10.1016/j.jadr.2021.100204.

7. Lunkenheimer, E., Hamby, C. M., Lobo, F. M., Cole, P. M., & Olson, S. L. (2020). The role of dynamic, dyadic parent–child processes in parental socialization of emotion. *Developmental Psychology, 56*(3), 566–577. https://doi.org/10.1037/dev0000808.

8. Mullins, J. L., Díaz, D. E., Firat, R. B., & Michalska, K. J. (2024). Ethnic–racial discrimination exposure and anxiety in Latina girls: Amygdala volume as an indirect neurobiological pathway. *KZfSS Kölner Zeitschrift für Soziologie und Sozialpsychologie, 76*(3), 627-648. https://doi.org/10.1007/s11577-024-00946-2.

9. Noël, R. A. (2018). U.S. Bureau of Labor Statistics. (Spotlight on Statistics, May 2018). *Race, economics, and social status*. https://www.bls.gov/spotlight/2018/race-economics-and-social-status/pdf/race-economics-and-social-status.pdf.

10 Pabayo, R., Benny, C., Liu, S. Y., Grinshteyn, E., & Muennig, P. (2021). Financial barriers to mental healthcare services and depressive symptoms among residents of Washington Heights, New York City. *Hispanic Health Care International, 20*(3), 154041532110575. https://doi.org/10.1177/15404153211057563.

11. Pierro, R., Ember, C. R., Pitek, E., & Skoggard, I. (2022). Local knowledge and practice in disaster relief: A worldwide cross-cultural comparison of coping mechanisms. *International Journal of Disaster Risk Reduction, 76*, 102988. https://doi.org/10.1016/j.ijdrr.2022.102988.

12. Perlis, R. H., Fava, M., Trivedi, M. H., Alpert, J., Luther, J. F., Wisniewski, S. R., & John Rush, A. (2009). Irritability is associated with anxiety and greater severity, but not bipolar spectrum features, in major depressive disorder. *Acta Psychiatrica Scandinavica, 119*(4), p. 282-289. https://doi.org/10.1111/j.1600-0447.2008.01298.x.

13. Pole, N., Best, S. R., Metzler, T., & Marmar, C. R. (2005). Why are Hispanics at greater risk for PTSD? *Cultural Diversity and Ethnic Minority Psychology, 11*(2) 144-161. https://doi/org/10.1037/1099-9809.11.2.144.

14. R Core Team. (2025). *R: A language and environment for statistical computing*. R Foundation for Statistical Computing. https://www.R-project.org/.

15. Shattell, M. M., Hamilton, D., Starr, S. S., Jenkins, C. J., & Hinderliter, N. A. (2008). Mental health service needs of a Latino population: A community-based participatory research project. *Issues in Mental Health Nursing, 29*(4), 351–370. https://doi.org/10.1080/01612840801904316.

16. Shelton, K. K., Frick, P. J., & Wootton, J. (1996). Assessment of parenting practices in families of elementary school-age children. *Journal of Clinical Child Psychology, 25*(3), 317-329. https://doi.org/10.1207/s15374424jccp2503_8.

17. Stoddard, J., Stringaris, A., Brotman, M. A., Montville, D., Pine, D. S., & Leibenluft, E. (2013). Irritability in child and adolescent anxiety disorders. *Depression and Anxiety, 31*(7), 566–573. https://doi.org/10.1002/da.22151.

18. Strathearn, L., Giannotti, M., Mills, R., Kisely, S., Najman, J., & Abajobir, A. (2020). Long-term cognitive, psychological, and health outcomes associated with child abuse and neglect. *Pediatrics, 146*(4). https://doi.org/10.1542/peds.2020-0438.

19. Stringaris, A., Goodman, R., Ferdinando, S., Razdan, V., Muhrer, E., Leibenluft, E., & Brotman, M.A. (2012). The Affective Reactivity Index: A concise irritability scale for clinical and research settings. *Journal of Child Psychology and Psychiatry, 53*, 1109-1117. https://doi:10.1111/j.1469-7610.2012.02561.x.

20. Vu, M., Li, J., Haardörfer, R., Windle, M., & Berg, C. J. (2019). Mental health and substance use among women and men at the intersections of identities and experiences of discrimination: Insights from the intersectionality framework. *BMC Public Health, 108*(19). https://doi.org/10.1186/s12889-019-6430-0.

Gaps in Knowledge, Receipt, and Acceptance of Measles, Mumps, Rubella Vaccines in a National Sample of Emergency Department

Sahithi Malireddy, Department of Neuroscience
Alexandra Eftimie, UCR School of Medicine
Dr. Shaokui Ge, UCR School of Medicine
Christopher Alvarez, UC San Francisco
Dr. Jesus Torres, UC Los Angeles
Dr. Brian Chinnock, UC San Francisco, Fresno
Dr. Michael Gottlieb,
Rush University Medical Center
Dr. Vijaya Arun Kumar, Wayne State University
Dr. Kristin L. Rising,
Thomas Jefferson University Hospital
Dr. Efrat Rosenzweig Kean,
Thomas Jefferson University Hospital
Dr. Stephanie Eucker,
Duke University School of Medicine
Dr. Robert M. Rodriguez, UCR School of Medicine

ABSTRACT

Measles cases are increasing in the U.S., raising concern about gaps in adult measles, mumps, and rubella (MMR) vaccination, which is poorly captured by current surveillance. Emergency departments (EDs) often act as safety nets for underserved populations and can help identify gaps in adult MMR uptake. We assessed adult MMR up-to-date status, knowledge, and willingness to receive vaccination in the ED, nationally. We conducted a cross-sectional survey of adults aged 18-64 at ten U.S. EDs from April 2024 to December 2024. Participants completed a structured survey assessing MMR knowledge, self-reported vaccination status, reasons for non-receipt, and willingness to receive an MMR vaccine in the ED. Outcomes were summarized as proportions with 95% confidence intervals (CIs). Multivariable logistic regression identified factors associated with not being up to date and with willingness to accept vaccination. Among 2,456 participants, 25.0% (95% CI 23.3–26.7%) had not heard of the MMR vaccine, and 44.0% (42.5–46.4%) were not up to date. Factors associated with being unvaccinated included male sex (OR 2.21 [1.84–2.66]), African American (non-Hispanic) race (OR 2.27 [1.75–2.96]), Hispanic ethnicity (OR 1.98 [1.49–2.62]), non-English speaking (OR 1.53 [1.12–2.09]), and lack of primary care access (OR 1.25 [1.01–1.58]). Among those not up to date, 36.5% (33.6–39.4%) were willing to receive the MMR vaccine if offered in the ED. Substantial gaps in adult MMR vaccination persist, especially among underserved populations. This study aimed to identify the gaps in access to the vaccination by assessing the status, knowledge, and willingness to receive as well as the sociodemographic factors contributing to these access gaps, on a national level. ED-based strategies might support targeted vaccine education and delivery during periods of increased transmission.

KEYWORDS: Vaccine hesitancy; vaccine acceptance; disease resurgence; emergency departments; Measles, Mumps, and Rubella; MMR

FACULTY MENTOR - Dr. Robert Rodriguez, Department of Internal Medicine

Dr. Robert Rodriguez is a Professor of Medicine and Associate Dean of Clinical and Population Health Research at the University of California Riverside School of Medicine. After the University of Notre Dame and Harvard Medical School, he completed a combined Emergency Medicine/Internal Medicine residency at UCLA and a Critical Care Medicine fellowship at Stanford.

SAHITHI MALIREDDY

Sahithi Malireddy is a fourth-year Neuroscience student at UCR. Her research centers on public health, mental health, and healthcare equity, with a focus on improving access to care for marginalized communities. In addition to her work under the mentorship of Dr. Robert Rodriguez, she has also contributed to youth-centered behavioral health and intervention research through the CREER Laboratory under Dr. Lisa Fortuna. Outside of research, Sahithi is involved in mental health advocacy, street medicine, and crisis intervention counseling throughout the Inland Empire. She hopes to pursue a career as a physician focused on advancing equitable, trauma-informed, and community-centered care for historically underserved populations.

Gaps in Knowledge, Receipt, and Acceptance of Measles, Mumps, Rubella Vaccines in a National Sample of Emergency Department

BACKGROUND

The recent resurgence of measles in the United States underscores the need to increase and maintain high levels of Measles, Mumps, and Rubella (MMR) vaccination coverage across the population. Measles is a highly contagious viral illness that can lead to severe medical complications, including pneumonia, encephalitis, and death, particularly in unvaccinated populations. As of March 19, 2026, 1,487 confirmed measles cases have been reported across 32 jurisdictions. Of these cases, 94% (1,398 of 1,487) have been linked to outbreaks, indicating a significant increase in outbreak-associated transmission compared to 2024, when 69% (198 of 285) of cases were outbreak-related [1].

The MMR vaccine is highly effective, and pediatric vaccination rates are monitored throughout the U.S., with approximately 93% of kindergarteners vaccinated [2]. Adults born in or after 1957 are also recommended to receive one or two doses [3]. Despite this, surveys such as the National Health Interview Survey (NHIS) do not assess MMR vaccination, and adult coverage remains poorly described [4]. Additionally, NHIS sampling (in-person household interviews) likely misses medically vulnerable groups, including unhoused persons and immigrants.

Emergency departments (EDs) often serve as healthcare safety nets and access points for underserved populations and are uniquely positioned to examine public health issues, including vaccination coverage [5]. The purpose of this national survey of adult ED patients was to determine: 1) knowledge and uptake of the MMR vaccine; 2) reasons for non-receipt; 3) acceptability if offered in the ED; and 4) reasons for non-acceptance. These data will help identify plausible reasoning for gaps in access and inform healthcare systems with ED-based strategies to increase MMR coverage among underserved populations.

METHODS

We conducted a preplanned secondary analysis of self-reported survey data collected as part of our multicenter emergency department vaccination study published in the CDC Morbidity and Mortality Weekly Report (MMWR). The surveys were conducted across ten EDs in eight U.S. cities (Chicago, IL; Detroit, MI; Durham, NC; Fresno, CA; Los Angeles, CA; Philadelphia, PA; San Francisco, CA; and Sylmar, CA) from April 18, 2024, to December 31, 2024 [6]. Research staff approached non–critically ill adult ED patients (≥18 years) for participation and screened them for eligibility; exclusions included critical illness, altered mental status, incarceration, respiratory precautions, or psychiatric holds. Based on CDC recommendations at initiation (June 2024), patients ≥ 65 years were excluded [7].

After scripted consent, surveys were administered in English and Spanish. Two sites also administered surveys in Mandarin. Questions included: 1) "Have you heard about the MMR vaccine?" with the short plain-language descriptor: "vaccine to prevent measles, mumps, and rubella;" 2) If they responded "yes" or "unsure," they were asked, "Have you received the MMR vaccine?;" 3) if they answered no to question 2, they were asked "Why have you not received it?;" 4) if no to question 1 or 2, they were asked, "Would you accept the MMR vaccine if it were offered to you in the ED?;" and 5) if they answered "no" to question 4, they were asked, "Why would you not accept it?" Patients who stated that they had not heard of the MMR vaccine were only asked questions 4 and 5.

Participants were divided into age quartiles. Outcomes were summarized as percentages with 95% confidence intervals (CIs), excluding missing responses. For the outcome of receipt of the MMR vaccine, only participants who answered yes to both questions 1 and 2 were deemed to have received it, i.e., if they had not heard of the vaccine, they were considered to have not received it.

We used multivariable logistic regression models to assess factors associated with 1) lack of knowledge, 2) lack of receipt, and 3) willingness to receive the vaccine. Independent variables were included as fixed effects, including age (categorical quartiles), sex, city, and factors associated with low vaccination coverage (African American race, Hispanic ethnicity, non-English speaking, no primary care, no insurance) [6]. The study site (or city) was included as a fixed effect to account for geographic variation and healthcare access variation across diverse patient populations. Results are presented as adjusted odds ratios (aORs) with 95% CIs. We managed data using REDCap, a secure,

Gaps in Knowledge, Receipt, and Acceptance of Measles, Mumps, Rubella Vaccines in a National Sample of Emergency Department

web-based platform designed for building online surveys [8] hosted by the University of California, San Francisco, and analyzed the data using RStudio (version 2023.12.1). A sample size of 2401 was required to estimate the prevalence of not being up to date on the MMR vaccination with a 95% confidence interval width of ±2 percentage points. Institutional review board approval was obtained at all sites through the University of California, San Francisco (UCSF) IRB, and STROBE guidelines were followed [9].

RESULTS

Of 4,325 patients approached, 3,275 (75.7%) agreed to participate. We excluded 816 participants who were 65 or older and three participants who had incomplete data, leaving 2,456 participants in this analysis. 1,343 (54.7%) were female, 876 (35.7%) were Latino/a, 695 (28.4%) were African American, and 566 (23.1%) were White non-Latino/a. 463 (18.9%) spoke Spanish primarily, and 622 (25.4%) lacked a primary care provider (Table 1).

Knowledge of the MMR vaccine

A total of 613 participants, or 25.0% (95% CI 23.3–26.7%), had not heard of the MMR vaccine. By age group, 29.1% (95% CI, 25.6–32.6) of those aged 18–30 years, 25.7% (95% CI, 22.3–29.1) of those aged 31–41 years, 21.9% (95% CI, 18.5-25.3%) of those aged 42-53 years, and 23.0% (19.6-26.3%) of those aged 54-64 years had not heard of the MMR vaccine (Table 2).

The following participant characteristics were associated with not having heard of the MMR vaccine: age 18-30 (aOR 1.89; 95% CI 1.39-2.57), male sex (aOR 2.21; 95% CI 1.78-2.71), African American (Non-Hispanic) race (aOR 1.91; 95% CI 1.38-2.62), and non-English as the participants' primary language (aOR 2.17; 95% CI 1.56-3.03). Participation in Sylmar, CA, or Philadelphia, PA, was associated with a greater likelihood of having heard of the vaccine. (Figure 1).

Up to date status of the MMR vaccine

A total of 1,090 participants (44.4%; 95% CI, 42.4–46.4%) were not up to date on the MMR vaccine. By age group, 48.5% (95% CI, 44.6–52.3%) of participants aged 18–30 years, 47.4% (95% CI, 43.4–51.3%) of those aged 31–41 years, 40.4% (95% CI, 36.3-44.4%) aged 42-53 years, and 40.9% (95% CI, 37.0–44.9%) aged 54-64 years were not up to date (Table 2).

The following characteristics were associated with not having received the MMR vaccine: age 18-30 (aOR 1.64; 95% CI 1.26-2.13); age 31-41 (aOR 1.39; 95% CI 1.07-1.79); male sex (aOR 2.21; 95% CI 1.84-2.66); African American (non-Hispanic) (aOR 2.27; 95% CI 1.75-2.96); Hispanic (aOR 1.98; 95% CI 1.49-2.62), non-English as the primary language (aOR 1.53; 95% CI 1.12-2.09); and participation in the cities of Chicago, IL (aOR 1.41; 95% CI 1.02-1.95) or Fresno, CA (aOR 2.01; 95% CI 1.49-2.71). Participation in Sylmar, CA, or Philadelphia, PA, was associated with having received the vaccine (Figure 2).

The most commonly cited reasons for not being up to date on the MMR vaccine were "I didn't know about it/Didn't know I should get it" (29.7%); "I'm not worried about contracting measles, mumps or rubella" (18.2%); "I haven't gotten around to it" (18.2%); and "Other" (19.9%).

Willingness to receive the MMR vaccine in the ED

Among 1,079 participants who were not up to date and had complete data, 394 (36.5%; 95% CI, 34.6–39.4%) reported they would accept the MMR vaccine if offered in the ED. By age group, 31.6% (95% CI, 26.4–36.8%) of those aged 18–30 years, 32.0% (95% CI, 26.6–37.3%) of those aged 31–41 years, 39.0% (95% CI, 32.7–45.2%) of those aged 42-53 years, and 45.7% (95% CI 39.5-52.0%) aged 54-64 years were willing to receive the MMR vaccine (Table 2).

Characteristics associated with greater willingness to receive the MMR vaccine included Hispanic ethnicity (aOR 1.72; 95% CI 1.08-2.75), mixed race (aOR 2.12; 95% CI 1.11-4.07), and participation in the city of Sylmar, CA (aOR 7.45; 95 % CI 3.81-15.49). Characteristics that were associated with a lower willingness to accept the MMR vaccine were participation in Fresno, CA (aOR 0.62; 95% CI 0.41-0.96); Philadelphia, PA (aOR 0.47; 95% CI 0.25-0.85); and Chicago, IL (aOR 0.56; 95% 0.34-0.91) (Figure 3).

The most commonly cited reasons for not accepting the MMR vaccine in the ED were "I need more information about the vaccines and the disease" (39.4%), "I am worried

about side effects from vaccines" (15.2%), "I would rather get them from my doctor or at a pharmacy" (15.2%), and "Other" (36.4%).

DISCUSSION

In this national ED-based study of a diverse adult population, we found gaps in knowledge and receipt of the MMR vaccine. Approximately a quarter of participants had not heard of the vaccine, and nearly half (44.4%) were not up to date. Disparities in knowledge and uptake were especially evident in African Americans, Hispanics, non-English speakers, and participants who lacked primary care. The primary reasons for not having received the MMR vaccine were related to a lack of information and opportunity. Notably, over a third of participants stated they would accept MMR vaccination if offered; if administered to them, this would result in an additional 16% of coverage from 56% to 72% in this population.

While there is substantial data regarding uptake of the MMR in pediatric populations [2], there is no equivalent MMR vaccine surveillance data for U.S. adults. The reliance on in-person household interviews with low response rates limits the validity of other vaccination surveillance studies like those conducted by NHIS [4]. Our sampling of a highly diverse and medically underserved population suggests that there is value in ED-based research to evaluate populations missed by traditional surveillance. Nevertheless, with regard to subpopulation disparities, our study findings are similar to other vaccine surveillance work showing that the characteristics of African American race, Hispanic ethnicity, male sex, and lack of primary care are associated with incomplete vaccination uptake of other vaccines [10-12].

With over 155 million patient visits in 2022, EDs are high-volume healthcare settings [13]. Our findings highlight the potential of leveraging EDs to identify vaccination gaps and provide vaccine messaging in underserved populations who are missed in traditional public health surveillance systems. So as not to interfere with or delay critical ED operations, ED-based vaccination screening and messaging programs must consider workflow dynamics and overburdened staff.

The MMR vaccine is not routinely stocked in EDs. At sites where it is available from central hospital pharmacies, it can be ordered and administered before discharge. At other sites, patients missing the MMR vaccine would likely need referrals to clinics or other vaccination sites. These approaches offer a practical solution to address gaps in MMR coverage, especially for patients who might not engage with conventional healthcare systems.

Beyond routine surveillance, our work informs the development of ED-based programs to respond to measles outbreaks in adults, similar to pediatric efforts [14]. During the first two years of the COVID-19 pandemic, effective ED-centered vaccination programs provided vaccines to underserved adult populations [15–17]. Our data suggest that developing similar targeted programs in outbreak-affected regions is warranted; many adults would accept the MMR vaccine once asked, and others may do so after receiving information.

LIMITATIONS

The greatest limitation of this research is that the United States does not have a centralized adult vaccination registry for most vaccines. We could not verify uptake status through electronic medical records and instead relied on self-reported data. Although this method introduces potential inaccuracies, it is the standard procedure for vaccination surveillance, and previous studies have shown a high level of agreement between self-reported vaccination status and documentation in medical records [18]. Our assumption that participants who had not heard of the MMR vaccine had not received it likely leads to an underestimation of true MMR vaccine uptake rates; it is likely that many received it during childhood and no longer remember now that they are adults. Excluding the group who had not heard of the vaccine still results in uptake rates of 74%, substantially below the 95% uptake rate needed for measles herd immunity [19]. Additionally, all sites were in urban centers, which may limit the external validity of the findings to suburban or rural ED settings; rates of knowledge and uptake may not be representative of patients in these EDs. Finally, stated willingness to receive the vaccine could be influenced by contextual factors, such as social desirability bias.

Gaps in Knowledge, Receipt, and Acceptance of Measles, Mumps, Rubella Vaccines in a National Sample of Emergency Department

CONCLUSION

We found significant gaps in adult MMR vaccine knowledge and coverage, with almost a quarter of ED participants reporting they had never heard of the MMR vaccine, and almost half of them not being up to date. Many patients missing the MMR vaccine would accept it if offered. EDs may serve as effective vaccination surveillance settings to close immunity gaps in underserved populations and reduce the risk of future measles outbreaks. Future studies should focus on the feasibility, implementation strategies, and effectiveness of offering MMR vaccination programs, including specific data on the impact of vaccine uptake and health disparities.

Characteristic	Total (N = 2456)	18–30 years old (N = 651)	31–41 years old (N = 624)	42–53 years old (N = 577)	54–64 years old (N = 604)
Median age. Years (IQR)	41 (30, 53)	25 (22, 28)	36 (33, 39)	47 (44, 51)	59 (56, 62)
Sex					
Female	1343 (54.7%)	405 (62.2%)	377 (60.4%)	289 (50.1%)	272 (45.0%)
Male	1087 (44.3%)	233 (35.8%)	243 (38.9%)	284 (49.2%)	327 (54.1%)
Other	26 (1.1%)	13 (2.0%)	4 (0.6%)	4 (0.7%)	5 (0.8%)
Housing status*					
Marginal	88 (3.6%)	18 (2.8%)	25 (4.0%)	18 (3.1%)	27 (4.5%)
Unstable	132 (5.4%)	18 (2.8%)	40 (6.4%)	33 (5.7%)	41 (6.8%)
Stable	2235 (91.0%)	615 (94.5%)	559 (89.6%)	525 (91.1%)	536 (88.7%)
Race and ethnicity¶					
Black or African American	695 (28.4%)	166 (25.7%)	158 (25.3%)	144 (25.0%)	227 (37.6%)
Asian	93 (3.8%)	44 (6.8%)	18 (2.9%)	18 (3.1%)	13 (2.2%)
Hispanic or Latino	876 (35.7%)	226 (35.0%)	252 (40.4%)	225 (39.0%)	173 (28.6%)
Native American	14 (0.6%)	4 (0.6%)	2 (0.3%)	5 (0.9%)	3 (0.5%)
Native Hawaiian or Pacific Islander	17 (0.7%)	2 (0.3%)	6 (1.0%)	6 (1.0%)	3 (0.5%)
Other	190 (7.8%)	57 (8.8%)	48 (7.7%)	44 (7.6%)	41 (6.8%)
White	566 (23.1%)	147 (22.8%)	140 (22.4%)	135 (23.4%)	144 (23.8%)
Health Insurance					
Affordable Care Act	51 (2.2%)	20 (3.1%)	19 (3.0%)	12 (2.2%)	0 (0.0%)
Community Health Plan	37 (1.6%)	6 (0.9%)	7 (1.1%)	13 (2.4%)	11 (2.1%)
Medi-Cal/ Medicaid	852 (36.3%)	223 (34.3%)	257 (41.2%)	191 (34.8%)	181 (34.5%)
Medicare	204 (8.7%)	25 (3.8%)	32 (5.1%)	56 (10.2%)	91 (17.3%)
Military and Veterans Administration	5 (0.2%)	2 (0.3%)	3 (0.5%)	0 (0.0%)	0 (0.0%)
No Insurance	235 (10.0%)	84 (12.9%)	85 (13.6%)	62 (11.3%)	4 (0.8%)
Other	146 (6.2%)	54 (8.3%)	32 (5.1%)	32 (5.8%)	28 (5.3%)
Private	819 (34.9%)	237 (36.4%)	189 (30.3%)	183 (33.3%)	210 (40.0%)
Primary Language					
English	1931 (78.6%)	553 (84.9%)	487 (78.0%)	422 (73.1%)	469 (77.6%)
Other	62 (2.5%)	20 (3.1%)	11 (1.8%)	15 (2.6%)	16 (2.6%)
Spanish	463 (18.9%)	78 (12.0%)	126 (20.2%)	140 (24.3%)	119 (19.7%)
Have a primary care provider or clinic					
Yes	1829 (74.6%)	460 (70.8%)	452 (72.6%)	440 (76.4%)	477 (79.2%)
No	622 (25.4%)	190 (29.2%)	171 (27.4%)	136 (23.6%)	125 (20.8%)
City of ED visit					
SF	495 (20.2%)	98 (15.1%)	146 (23.4%)	129 (22.4%)	122 (20.2%)
Sylmar	330 (13.4%)	51 (7.8%)	84 (13.5%)	102 (17.7%)	93 (15.4%)
Los Angeles	283 (11.5%)	98 (15.1%)	53 (8.5%)	60 (10.4%)	72 (11.9%)
Fresno	396 (16.1%)	122 (18.7%)	136 (21.8%)	76 (13.2%)	62 (10.3%)
Philadelphia	302 (12.3%)	121 (18.6%)	45 (7.2%)	51 (8.8%)	85 (14.1%)
Chicago	281 (11.4%)	58 (8.9%)	72 (11.5%)	67 (11.6%)	84 (13.9%)
Detroit	209 (8.5%)	57 (8.8%)	48 (7.7%)	56 (9.7%)	48 (7.9%)
Durham	160 (6.5%)	46 (7.1%)	40 (6.4%)	36 (6.2%)	38 (6.3%)

Table 1. Characteristics of 2456 study participants (age 18-64 years) at 10 emergency departments in eight U.S. cities, April 18 - December 31, 2024.

Note: primary care refers to access to a primary care provider (PCP).

Gaps in Knowledge, Receipt, and Acceptance of Measles, Mumps, Rubella Vaccines in a National Sample of Emergency Department

	Total (N=2456)	18-30 (N=651)	31-41 (N=624)	42-53 (N=577)	54-64 (N=604)
Medicare	204 (8.7 %)	25 (3.8 %)	32 (5.1 %)	56 (10.2 %)	91 (17.3 %)
Military and Veterans Administrationt	5 (0.2 %)	2 (0.3 %)	3 (0.5 %)	0 (0.0 %)	0 (0.0 %)
No Insurance	235 (10.0 %)	84 (12.9 %)	85 (13.6 %)	62 (11.3 %)	4 (0.8 %)
Other	146 (6.2 %)	54 (8.3 %)	32 (5.1 %)	32 (5.8 %)	28 (5.3 %)
Private	819 (34.9 %)	237 (36.4 %)	189 (30.3 %)	183 (33.3 %)	210 (40.0 %)
Primary Language					
English	1931 (78.6 %)	553 (84.9 %)	487 (78.0 %)	422 (73.1 %)	469 (77.6 %)
Other	62 (2.5 %)	20 (3.1 %)	11 (1.8 %)	15 (2.6 %)	16 (2.6 %)
Spanish	463 (18.9 %)	78 (12.0 %)	126 (20.2 %)	140 (24.3 %)	119 (19.7 %)
Primary Care					
Yes	1829 (74.6 %)	460 (70.8 %)	452 (72.6 %)	440 (76.4 %)	477 (79.2 %)
No	622 (25.4 %)	190 (29.2 %)	171 (27.4 %)	136 (23.6 %)	125 (20.8 %)
City					
SF	495 (20.2 %)	98 (15.1 %)	146 (23.4 %)	129 (22.4 %)	122 (20.2 %)
Slymar	330 (13.4 %)	51 (7.8 %)	84 (13.5 %)	102 (17.7 %)	93 (15.4 %)
LA	283 (11.5 %)	98 (15.1 %)	53 (8.5 %)	60 (10.4 %)	72 (11.9 %)
Fresno	396 (16.1 %)	122 (18.7 %)	136 (21.8 %)	76 (13.2 %)	62 (10.3 %)
Plil.	302 (12.3 %)	121 (18.6 %)	45 (7.2 %)	51 (8.8 %)	85 (14.1 %)
Chicago	281 (11.4 %)	58 (8.9 %)	72 (11.5 %)	67 (11.6 %)	84 (13.9 %)
Detroit	209 (8.5 %)	57 (8.8 %)	48 (7.7 %)	56 (9.7 %)	48 (7.9 %)
Gurham	160 (6.5 %)	46 (7.1 %)	40 (6.4 %)	36 (6.2 %)	38 (6.3 %)

Table 1 (cont). Characteristics of 2456 study participants (age 18-64 years) at 10 emergency departments in eight U.S. cities, April 18 - December 31, 2024.

Note: primary care refers to access to a primary care provider (PCP).

IQR = interquartile range; ED = emergency department

* Patients were asked, "What is your living situation today?" Stable was defined as a response of, "I have a steady place to live (home, apartment, or other)." Marginal was defined as a response of, "I have a place to live today, but I am worried about losing it in the future." Unstable was defined as a response of, "I do not have a steady place to live (I am temporarily staying with others, in a hotel, in a shelter, living outside on the street, on a beach, in a car, abandoned building, bus or train station, or in a park)."

¶ Persons of Hispanic or Latino origin might be of any race but are categorized as Hispanic

Gaps in Knowledge, Receipt, and Acceptance of Measles, Mumps, Rubella Vaccines in a National Sample of Emergency Department

Table 2
Percentages of 2456 ED patient participants (stratified by age group) who 1) had not heard of the MMR vaccine, 2) were not up to date on the MMR vaccine, and 3) If not up to date, would accept the MMR vaccine if offered in the emergency department.

Patient age (yrs) $N = 2456$	% of participants (95% CI) who had not heard of the MMR vaccine $N = 613$	% of participants (95% CI) who had missed the MMR vaccine (were not up to date) $N = 1090$	% of participants (95% CI) who were not up to date and would accept the MMR vaccine $N = 394$
All ages	25.0 (23.3–26.7)	44.4 (42.5–46.4)	36.5 (33.6–39.4)
18–30	29.1 (25.6–32.6)	48.5 (44.6–52.3)	31.6 (26.4–36.8)
31–41	25.7 (22.3–29.1)	47.4 (43.4–51.3)	32.0 (26.6–37.3)
42–53	21.9 (18.5–25.3)	40.4 (36.3–44.4)	39.0 (32.7–45.2)
54–64	23.0 (19.6–26.3)	40.9 (37.0–44.9)	45.7(39.5–52.0)

ED = emergency department; MMR = measles, mumps and rubella. Conducted in 10 EDs in the cities of Chicago, Illinois, Detroit, Michigan, Durham, North Carolina; Fresno, California; Los Angeles, California; Philadelphia, Pennsylvania; San Francisco, California; and Sylmar, California.

Table 2. Percentage of 2456 emergency department patient participants (stratified by age group) who 1) had not heard of the MMR vaccine, 2) were not up to date on the MMR vaccine, and 3) If not up to date, would accept the MMR vaccine if offered in the emergency department.
MMR = measles, mumps and rubella. Conducted in the cities of Chicago, Illinois; Detroit, Michigan; Durham, North Carolina; Fresno, California; Los Angeles, California; Philadelphia, Pennsylvania; San Francisco, California; and Sylmar, California.

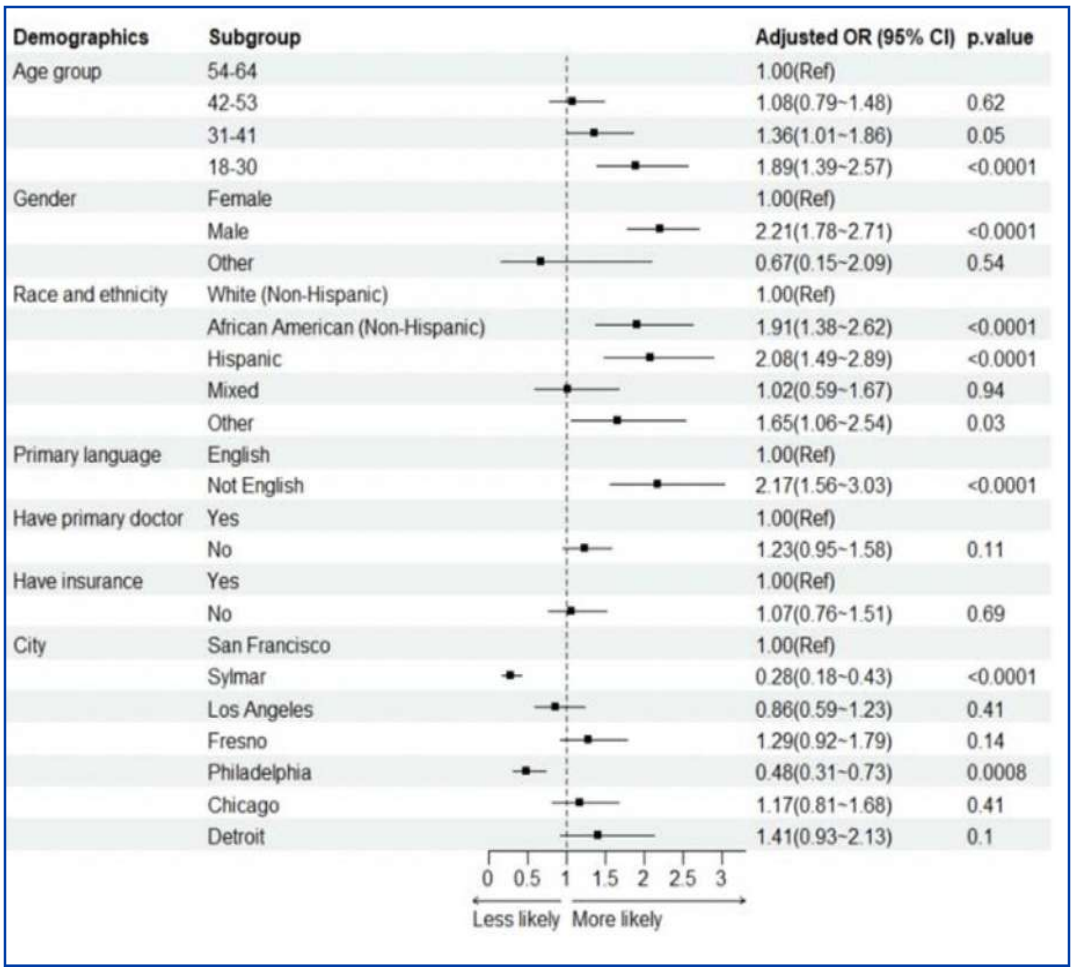

Figure 1: Forest plot of adjusted odds ratios and 95% confidence intervals for characteristics associated with not having heard of the MMR vaccination among adult patients in ten emergency departments in eight U.S. cities, April 18 - December 31, 2024.

Note: the first row is the comparison group to which all other groups were compared.

MMR = measles, mumps and rubella; OR = odds ratio; CI = confidence interval

Gaps in Knowledge, Receipt, and Acceptance of Measles, Mumps, Rubella Vaccines in a National Sample of Emergency Department

Figure 2: Forest plot of adjusted odds ratios and 95% confidence intervals for characteristics associated with not being up to date with MMR vaccination among adult patients in ten emergency departments in eight U.S. cities, April 18 - December 31, 2024.

Note: the first row is the comparison group to which all other groups were compared.

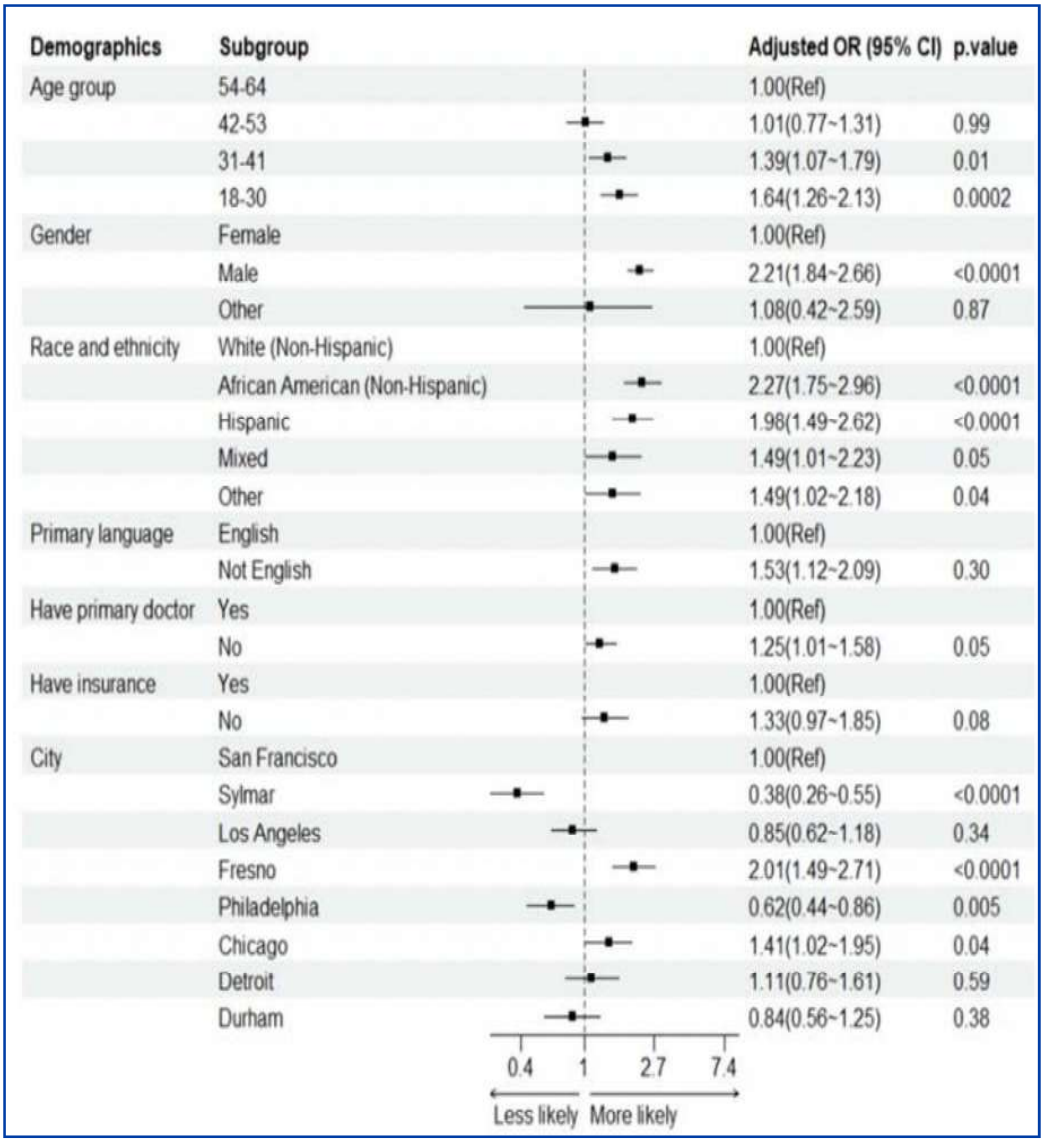

Demographics	Subgroup	Adjusted OR (95% CI)	p.value
Age group	54-64	1.00(Ref)	
	42-53	1.01(0.77~1.31)	0.99
	31-41	1.39(1.07~1.79)	0.01
	18-30	1.64(1.26~2.13)	0.0002
Gender	Female	1.00(Ref)	
	Male	2.21(1.84~2.66)	<0.0001
	Other	1.08(0.42~2.59)	0.87
Race and ethnicity	White (Non-Hispanic)	1.00(Ref)	
	African American (Non-Hispanic)	2.27(1.75~2.96)	<0.0001
	Hispanic	1.98(1.49~2.62)	<0.0001
	Mixed	1.49(1.01~2.23)	0.05
	Other	1.49(1.02~2.18)	0.04
Primary language	English	1.00(Ref)	
	Not English	1.53(1.12~2.09)	0.30
Have primary doctor	Yes	1.00(Ref)	
	No	1.25(1.01~1.58)	0.05
Have insurance	Yes	1.00(Ref)	
	No	1.33(0.97~1.85)	0.08
City	San Francisco	1.00(Ref)	
	Sylmar	0.38(0.26~0.55)	<0.0001
	Los Angeles	0.85(0.62~1.18)	0.34
	Fresno	2.01(1.49~2.71)	<0.0001
	Philadelphia	0.62(0.44~0.86)	0.005
	Chicago	1.41(1.02~1.95)	0.04
	Detroit	1.11(0.76~1.61)	0.59
	Durham	0.84(0.56~1.25)	0.38

MMR = measles, mumps and rubella; OR = odds ratio; CI = confidence interval

Gaps in Knowledge, Receipt, and Acceptance of Measles, Mumps, Rubella Vaccines in a National Sample of Emergency Department

REFERENCES

1. Centers for Disease Control and Prevention. Measles cases and outbreaks [Internet]. Atlanta (GA): CDC; 2025 [cited 2025 Dec 2]. Available from: https://www.cdc.gov/measles/data-research/index.html

2. Seither R, Yusuf OB, Dramann D, et al. Coverage with selected vaccines and exemption rates among children in kindergarten—United States, 2023–24 school year. MMWR Morb Mortal Wkly Rep. 2024;73:925–932. https://doi.org/10.15585/mmwr.mm7341a3

3. Centers for Disease Control and Prevention. Routine MMR vaccination recommendations for providers [Internet]. Atlanta (GA): CDC; 2021 [cited 2025 Dec 2]. Available from: https://www.cdc.gov/vaccines/vpd/mmr/hcp/recommendations.html

4. Hung MC, Srivastav A, Lu PJ, Black C, Lindley MC, Singleton JA. Vaccination coverage among adults in the United States, National Health Interview Survey, 2022 [Internet]. Atlanta (GA): Centers for Disease Control and Prevention; 2022 [cited 2025 Dec 2]. Available from: https://www.cdc.gov/adultvaxview/publications-resources/adult-vaccination-coverage-2022.html

5. Fassas E, Fischer K, Schenkel S, Gatz JD, Gingold DB. Public health interventions in the emergency department: a framework for evaluation. West J Emerg Med. 2024;25(3):415–422.

6. Rodriguez RM, Torres JR, Chinnock B, et al. Emergency department survey of vaccination knowledge, vaccination coverage, and willingness to receive vaccines among underserved populations—eight U.S. cities, April–December 2024. MMWR Morb Mortal Wkly Rep. 2025;74:456–462. https://doi.org/10.15585/mmwr.mm7429a1

7. Centers for Disease Control and Prevention. Adult immunization schedule by age [Internet]. Atlanta (GA): CDC; 2025 [cited 2025 Dec 2]. Available from: https://www.cdc.gov/vaccines/hcp/imz-schedules/adult-age.html

8. Harris PA, Taylor R, Thielke R, Payne J, Gonzalez N, Conde JG. Research electronic data capture (REDCap)—a metadata-driven methodology and workflow process for providing translational research informatics support. J Biomed Inform. 2009;42(3):377–381. https://doi.org/10.1016/j.jbi.2008.08.01010.10

9. von Elm E, Altman DG, Egger M, Pocock SJ, Gøtzsche PC, Vandenbroucke JP; STROBE Initiative. The Strengthening the Reporting of Observational Studies in Epidemiology (STROBE) statement: guidelines for reporting observational studies. Ann Intern Med. 2007;147(8):573–577. https://doi.org/10.7326/0003-4819-147-8-200710160-00010

10. Lu PJ, O'Halloran A, Williams WW, Lindley MC, Farrall S, Bridges CB. Racial and Ethnic Disparities in Vaccination Coverage Among Adult Populations in the U.S. Am J Prev Med. 2015 Dec;49(6 Suppl 4):S412-25. doi: 10.1016/j.amepre.2015.03.005. Epub 2015 Aug 18.

11. Lu PJ, Hung MC, Srivastav A, Grohskopf LA, Kobayashi M, Harris AM, Dooling KL, Markowitz LE, Rodriguez-Lainz A, Williams WW. Surveillance of Vaccination Coverage Among Adult Populations -United States, 2018. MMWR Surveill Summ. 2021 May 14;70(3):1-26. doi: 10.15585/mmwr.ss7003a1.

12. Molina MF, Nichol G, Eucker SA, Addo N, Rising K, Arreguin M, et al. COVID-19 booster vaccine hesitancy in the emergency department. Ann Emerg Med. 2023;S0196-0644(23)00296-2. https://doi.org/10.1016/j.annemergmed.2023.04.009

13. Cairns C, Ashman JJ, Kang K. Emergency department visit rates by selected characteristics: United States, 2022 [Internet]. Hyattsville (MD): National Center for Health Statistics; 2024 [cited 2025 Dec 2]. Available from: https://www.cdc.gov/nchs/products/databriefs/db503.htm

14. Schlenker TL, Risk I, Harris H. Emergency department vaccination of preschool-age children during a measles outbreak. Ann Emerg Med. 1995;26(3):320–323. https://doi.org/10.1016/S0196-0644(95)70080-3

15. Rodriguez RM, Nichol G, Eucker SA, Chang AM, O'Laughlin KN, Pauley A, et al. Effect of COVID-19 vaccine messaging platforms in emergency departments on vaccine acceptance and uptake: a cluster randomized clinical trial. JAMA Intern Med. 2023;183(2):115–123. https://doi.org/10.1001/jamainternmed.2022.5909

16. Chary A, Thomas Y, Suh M, Ordonez E, Buehler G. Strategies in emergency department–based COVID-19 vaccination. West J Emerg Med. 2022;23(4):536–539. https://doi.org/10.5811/westjem.2022.4.55043

17. Cooper C, Zack S, Shah S. Implementation of a COVID-19 vaccination program in the emergency department. Hosp Pharm. 2022;57(5):599–602. https://doi.org/10.1177/00185787221095773

18. Rolnick SJ, Parker ED, Nordin JD, et al. Self-report compared to electronic medical record across eight adult vaccines: do results vary by demographic factors? Vaccine. 2013;31:3928–3935. https://doi.org/10.1016/j.vaccine.2013.06.041

19. Plans-Rubió P. Measles Vaccination Coverage and Anti-Measles Herd Immunity Levels in the World and WHO Regions Worsened from 2019 to 2023. Vaccines (Basel). 2025 Feb 5;13(2):157. doi: 10.3390/vaccines13020157. PMID: 40006704

The Effects of Cold Smoke on Hummingbird Behavior and Lung Physiology

Isabelle Rose Loaisiga; Department of Evolution, Ecology, and Organismal Biology
Keziyah Yisrael, Ph.D.; Division of Biomedical Sciences, School of Medicine
Hovanness Dingilian, Department of Chemical and Environmental Engineering
Javier Asin, DMV, Ph.D.; California Animal Health And Food Safety Laboratory
David Lo, M.D., Ph.D.; Division of Biomedical Sciences, School of Medicine
Christopher J. Clark, Ph.D.; Department of Evolution, Ecology, and Organismal Biology

ABSTRACT

This study investigates the effects of cold smoke exposure on the behavior and lung health of twelve wild-caught and acclimated Anna's hummingbirds. Half of the group was placed inside an environmental chamber and exposed to cold wood smoke at a 1,419 $\mu g/m^3$ concentration for 4 hours (smoke group). The remaining six birds were placed in a separate environmental chamber without smoke (control group). At the end of the exposure, half of each group was euthanized immediately in order to study short-term effects, and the other half were euthanized two weeks later in order to study long-term effects. A necropsy was performed on all the birds, and their lungs were processed for histology and analyzed after hematoxylin and eosin (H&E) staining. Each bird's lung histology was graded on the amount of anthracosis present to determine if exposed birds had a greater amount of anthracosis in their lungs compared to unexposed birds. We also investigated if the later-euthanized group had more anthracosis compared to the immediately euthanized group. No significant differences in anthracosis were observed between exposed and control groups or across euthanasia time points. Observational results showed no differences in behavior between the two groups during the experiment. Statistical analyses (t-tests) showed no significant differences in food consumption between the smoke and control groups or in body mass change after the experiment. T-tests did show that the males ate more than the females. Overall, this research aims to advance our understanding of avian respiratory physiology and behavior as well as to enhance our knowledge of the size and density of particulates that affect hummingbird lungs after wildfires.

KEYWORDS: hummingbird, lungs, wildfires, smoke, Anna's hummingbird, anthracosis, hummingbird behavior

FACULTY MENTOR - Dr. Christopher J. Clark;
Department of Evolution, Ecology, and Organismal Biology

Dr. Christopher J. Clark has been a professor at UC Riverside since 2013. An expert on hummingbirds, his research focuses on sounds produced by hummingbird and owl flight. In 2001 he received an undergraduate degree in Zoology at Washington State University, a Ph.D. in Integrative Biology at UC Berkeley in 2009.

Isabelle Rose Loaisiga

Isabelle Loaisiga graduated *cum laude* from the University of California, Riverside with a Bachelor's of Science in Biology in 2025, where she was the president of the pre-veterinary club, part of the Honors program, and worked as a necropsy assistant at the California Animal Health and Food Safety Laboratory. She is currently in her second year at the University of Pennsylvania School of Veterinary Medicine, where she is working toward her future goal of improving animal health and welfare while advancing animal science through research. She is particularly interested in pathology, surgery, and translational medicine, but is open to the variety of paths veterinary school has to offer.

The Effects of Cold Smoke on Hummingbird Behavior and Lung Physiology

INTRODUCTION

Wildfires have recently become a severe crisis for California because of their abnormal frequency. Long periods of drought, in addition to the Santa Ana Winds, have led to California facing three times the annual average burned area in 2020-2023 (1.8 million acres) compared to the 2010s (0.6 million acres) (Yu, 2025). Depending on the winds and other climate conditions, wildfire smoke can travel hundreds of miles (LA County DPH, 2025). Humans can escape the harmful smoke from wildfires by staying indoors. However, wild animals have fewer ways of escaping this smoke, making them more vulnerable to wildfires.

When a wildfire starts, it first emits hot smoke. This smoke is hazardous because it contains gaseous pollutants, hazardous air pollutants (HAPs), particulate matter (PM), and numerous other volatile organic compounds (VOCs) (Jaffe et al., 2020). The primary concern with hot smoke is that it immediately kills animals because carbon monoxide binds tightly to hemoglobin, starving the body of oxygen (Varon et al., 1999).

As smoke physically cools, it undergoes a series of chemical reactions and transformations, creating secondary pollutants, including ozone (O3) and secondary organic aerosols (SOA) (Jaffe et al., 2020), while VOCs largely dissipate, leaving the PM behind. This "cold smoke" remains a hazard. Depending on its size, the PM can penetrate through an animal's respiratory tract and reach the lungs, posing a serious threat to the animal's health. Particles measuring 2.5-10 micrometers in diameter may be inhaled and penetrate the lungs (Stone et al., 2019). PM 2.5 micrometers in diameter or less are known as fine inhalable particles and are more dangerous since they have more significant health risks (Stone et al., 2019).

Scientists already understand the effects of hot smoke leading to death because of CO, but cold smoke's physiological and behavioral effects have not been as clear. There is very little research about how different species, specifically birds, behaviorally respond to cold smoke from the wildfires around them. Additionally, there is limited research on how harmful, if at all, cold smoke could be to bird lung health. Birds are crucial to the ecosystem and directly impact our health, economy, and food production through pollination, spreading seeds, keeping coral reefs alive, controlling pests, and more. The animal model used in this experiment was Anna's hummingbirds (Calypte anna). Their smaller body size makes them more sensitive to pollutants and respiratory damage compared to larger birds, allowing a more sensitive test of a bird's threshold to cold smoke. Additionally, they are abundant in Southern California, where our lab is located, and which specializes in hummingbird research.

Birds may be more vulnerable to the effects of cold smoke than other animals because of their physiology. Avian metabolism is very high due to the high energy demands of flight, leading to high rates of gas exchange, making them susceptible to inhaling more PMs (Munshi-South et al., 2010). Unlike mammals, birds' respiratory system includes densely packed, narrow capillaries with unidirectional airflow through their lungs and air sacs (Brown et al., 1997). This contributes to their highly efficient gas exchange but can be problematic for trapping particles. Their trachea is relatively longer than those of mammals and contains mucus-secreting cells and cilia that work together to remove harmful particles (Jacob and Pescatore, 2013). A recent study comparing the lung health of different zoo animals found that avian species have a higher occurrence of anthracosis than do mammals (Leya et al., 2023). Anthracosis is a condition that is caused by the "accumulation of carbon in the lungs due to…exposure to air pollution or inhalation of smoke" (Mirsadraee, 2014). Anthracosis poses a serious threat to human and avian respiratory health because it causes chronic lung inflammation and immunodeficiency and invites potential parasitic conditions such as lophomoniasis (Tajik Jalayeri et al., 2024).

This experiment studied hummingbird behavioral response to cold smoke particulates through observational assessment. We compared normal day-to-day hummingbird behavior in the lab to their behavior while exposed to smoke in the smoke exposure chamber, noting signs of stress (e.g., decreased activity, fluffed feathers, mouth opening, slow blinking, decreased food consumption) and normal health (e.g., flying around occasionally, perching, regular food consumption). We hypothesized that birds exposed to smoke will show behavioral signs of stress compared to the control group, which will show signs of normal health.

The Effects of Cold Smoke on Hummingbird Behavior and Lung Physiology

This experiment also studied the physiological effects of cold smoke on avian lungs by comparing the amount of anthracosis between the control and exposed groups on histopathology. Anthracotic granules (black pigment) may be located inside or outside of alveolar macrophages, in the perivascular, or in the peribronchiolar area, along with inflammatory infiltrates and accompanied by edema (Leya et al., 2023). We hypothesized that the smoke group will have more anthracosis from smoke irritation in the lungs compared to the control group. Furthermore, we also examined the effects of smoke on recovery time after exposure. Half of the birds from each group, smoke and control, were euthanized two weeks after smoke exposure to study long-term effects, and the other half were euthanized immediately to study short-term effects. We predicted that the birds euthanized two weeks after smoke exposure will show long-term effects, such as an increased amount of anthracosis due to impaired respiratory recovery from smoke damage. Birds euthanized immediately were expected to show acute physiological effects in lung histology, such as lower levels of anthracosis.

MATERIALS AND METHODS

(a) Bird Care

Twelve Anna's Hummingbirds (Calypte anna), eight females and four males, were captured in the wild on the campus of the University of California, Riverside (UCR). All components of the experiment and treatment of birds followed the approved California Department of Fish and Wildlife collecting permit (#S-183160004-19092), U.S. Fish and Wildlife Service (USFWS) collecting permit (MBPER3871689), and UCR IACUC protocol (#30063). The birds were acclimated to individual cages and housed in captivity. Birds were also weighed and monitored daily.

(b) Chamber and Smoke Details

This experiment used two environmental chambers (one for the smoke-exposure group and the other for the control group) constructed from transparent acrylic sidings that were 0.635 cm think. The dimension of each chamber was 101.6 x 81.3 x 63.6 cm.

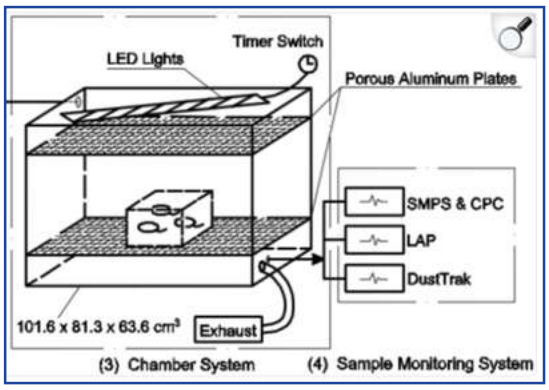

Figure 1: (3) Chamber system used during the experiment along with the SMPS in (4) sample monitoring system (Image from Peng et al, 2019).

Each chamber had controlled airflow, with approximately one air change per hour. According to The Guide For the Care of and Use of Laboratory Animals, by the National Research Council, this is below the 10-15 air changes per hour recommendation. However, a hummingbird's metabolic rate is approximately 40 mL O_2/g/hr; therefore, six flying hummingbirds are estimated to consume about 1 L of O_2 per hour, or approximately 1% of the chamber volume (Clark and Dudley, 2010).

Smoke simulating wildfire conditions was generated using a food smoker inside a fume hood. The device heated wood chips on a metal plate, with charcoal and fatwood used as the heat source beneath it. Once a target temperature was reached, the chips released smoke that was then drawn into the tubing toward the environmental chamber. Before reaching the chamber, the smoke was filtered with activated charcoal to remove harmful pollutants, such as carbon monoxide (CO). However, some CO could still reach the smoke chamber, so a CO monitor was used to track levels the birds were exposed to and ensure the amount of CO did not impact the hummingbirds' welfare. If the CO monitor inside the environmental chamber exceeded 50 ppm, we reduced the flame.

Particles of 2 nm to 1000 nm were measured and characterized using a Scanning Mobility Particle Sizer (SMPS) (Model 3080 Electrostatic Classifier using Kr85, TSI, Minnesota, USA) system. Every 130 seconds the SMPS

The Effects of Cold Smoke on Hummingbird Behavior and Lung Physiology

captured the concentration of smoke being exposed to the birds (27 scans/hour).

(c) Acclimation

We acclimated the birds to the insect cages (30.5 x 30.5 x 30.5 cm) and the environment they would be in during the experiment to decrease their stress on experiment day. On Days 1 and 2, birds were placed in individual mesh insect cages for 5 hours daily. The insect cages were meant to separate each bird and allow for PM to be inhaled during the experiment. On Day 3, a test run of the experiment was conducted to ensure minimal behavioral stress for the birds on the experiment day. The birds were placed in their designated mesh insect cages and separated into two groups: smoke-exposed (N=6) and control (N=6). Each group had 4 females and 2 males. Birds were placed into their designated environmental chambers for 3 hours without any exposure to smoke.

(d) Smoke Exposure

On Day 4, the experiment was conducted. All birds were weighed at 07:30 h and transported to the experimental facility. The birds were placed in their individual mesh insect cages with a perch and 30 mL of nectar solution. Then, at 08:30 h, six birds inside the insect cages were placed in the smoke environmental chamber, while the remaining 6 were placed in the control environmental chamber. Between 11:00 h and 16:00 h, the smoke-exposed group was exposed to filtered smoke particles that were 0.2 pm -1 pm at an average concentration of 1,419 $\mu g/m^3$. There were approximately 108 scans for smoke particle concentration during the entire experiment. The maximum concentration was 3574.73 $\mu g/m^3$, and the minimum was 715.62 $\mu g/m^3$. Fluctuations in concentration were attributed to changes in airflow, fuel addition, and carbon monoxide control (i.e., increasing airflow into the chamber following rises in CO levels), while maintaining the flame.

(e) After the Experiment

Immediately after the experiment, each bird's weight was recorded. Three birds (one male and two females) from each group were euthanized using isoflurane. The six birds then received a post-mortem necropsy with a prosection from the sternum to the cloaca and then soaked in 10% neutral buffered formalin for 24 hours. The lungs were extracted and sent to University of California, Irvine (UCI) Health for tissue processing and paraffin embedding.

After exposure, the remaining six birds were returned to their original housing cages. They were observed four times daily, for one hour each throughout the day for respiratory distress, behavioral changes, and health concerns such as lethargy, weight loss, nasal discharge, lack of grooming, hunched posture, mouth breathing and opening, decreased flight, and fluffed feathers. After 15 days, the remaining six birds were euthanized following the same protocol as above.

(f) Hematoxylin and Eosin (H&E) Staining

Once all the tissue sections were returned from processing, all 12 slides were stained with hematoxylin and eosin (H&E) for histopathological analysis. First, the slides were deparaffinized. Each slide was placed in xylene twice for 5 min, followed by 100% ethanol (EtOH) twice for 5 min each. The slides were then rehydrated through a graded ethanol series of 95%, 70%, 50%, and 30% EtOH for 2 min each, and subsequently immersed in phosphate-buffered saline (PBS) for 10 min . After deparaffinization, slides were immersed in hematoxylin for 4 min, rinsed in tap water (10 dips), and briefly immersed in phosphate-buffered saline (PBS) for 1 min. The slides were then stained with eosin for 5 min and rinsed again in tap water (10 dips). Following staining, the slides were dehydrated through a graded ethanol series: 50% EtOH (3 dips), 70% EtOH (3 dips), 95% EtOH (1 dip), and 100% EtOH (3 dips), followed by clearing in xylene twice for 5 min each. Finally, the slides were mounted and allowed to dry for 24 hours prior to examination.

(g) Analysis

Following the histological staining, slides were sent to a veterinary anatomical pathologist for blind analysis and evaluation. Each lung slide was graded for anthracosis from 0 to 3 (none, mild, moderate, severe).

(h) Statistics

We used JMP statistical software for the analysis. In JMP, an ordinal logistic fit was performed for anthracosis (on a scale from 0 to 3) found in the hummingbird lungs. Anthracosis was the dependent variable, and the independent

The Effects of Cold Smoke on Hummingbird Behavior and Lung Physiology

variables were treatment (smoke exposure), sex, and time of euthanasia (immediately or two weeks post-exposure).

JMP was used to perform t-tests to compare food consumption and body mass change before and after the experiment. Smoke exposure and sex were used as grouping variables in separate analyses. One female hummingbird in the control group was excluded from these two T-tests because she did not eat at all and was an outlier.

RESULTS

(a) Engineering particles/density results

Scans of the smoke inside the chamber were conducted from 09:00 to 16:00 h The first 2 hours were excluded due to clogging-related errors in the tubing system delivering smoke to the chamber. Starting at 11:00 h, SMPS scanned the chamber 108 times during 4 hours, showing fluctuations in the concentration of smoke levels. The average concentration of smoke particles was 1,419 μg/m^3. The maximum concentration was 3574.73 μg/m^3, and the minimum was 715.62 μg/m^3.

(b) Behavioral analysis

Hummingbird behavior was assessed by observation. Both groups showed no significant differences before, during, or after the experiment. Both control and exposed groups flew around occasionally, perched most of the time, drank their nectar solution, and showed no signs of stress (e.g. slow blinking eyes, opening their mouth, fluffed feathers, and decreased movement).

(c) Food consumption and weight gained

For the analysis of food consumed and body mass change, one bird was dropped as an outlier because it had consumed no food. For the remaining 11 birds, there was also no effect of smoke on body mass ($t(9) = 0.615$, $p = 0.554$). However, there was a significant effect of sex, with male hummingbirds gaining more weight than females ($t(9) = 2.613$, $p = 0.028$).

There was no effect of smoke on food consumed during the experiment ($t(10) = 0.882$, $p = 0.399$) or of sex ($t(10) = 2.103$, $p = 0.062$).

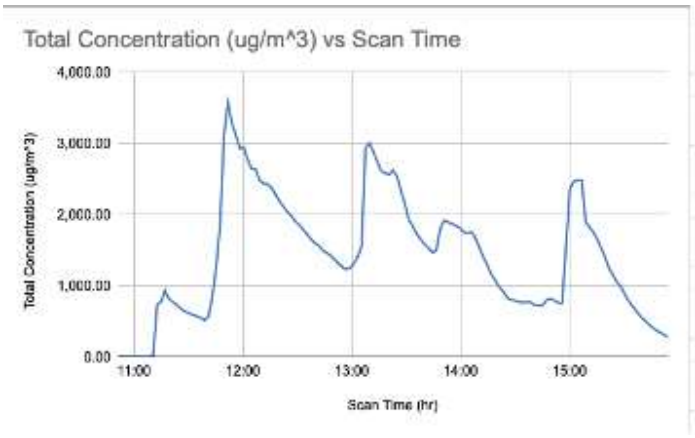

Figure 2: Total concentration of smoke particles (μg/m^3) fluctuated over the course of 4 hours. The concentration ranges from 3574.73 μg/m^3 to 715.62 μg/m^3.

(d) Histology evaluation

Hummingbird lung histology showed variations of anthracosis between all groups studied and no patterns when comparing groups. There was no significant effect of cold smoke on anthracosis (Ordinal Logistic Fit, $p = 0.336$, $df = 10$), nor were there significant effects of time after smoke exposure ($p = 0.552$) or sex ($p = 0.618$).

Scans of the smoke inside the chamber were conducted from 09:00 to 16:00 h The first 2 hours were excluded due to clogging-related errors in the tubing system delivering smoke to the chamber. Starting at 11:00 h, SMPS scanned the chamber 108 times during 4 hours, showing fluctuations in the concentration of smoke levels. The average concentration of smoke particles was 1,419 μg/m^3. The maximum concentration was 3574.73 μg/m^3, and the minimum was 715.62 μg/m^3.

DISCUSSION

This study showed that exposure to an average of 1,419 μg/m^3 smoke particles for four hours did not affect any of the measured variables.

The degree of anthracosis in the hummingbirds' lungs did not show any significant differences between smoke and control groups or between euthanasia time points. This does not support our hypothesis that the smoke group

The Effects of Cold Smoke on Hummingbird Behavior and Lung Physiology

would show more pathogenesis in histology compared to the control group. It also contradicts our hypothesis that there would be long-term effects of smoke exposure on the later-euthanized group versus short-term effects on the immediately-euthanized group. Considering that both groups had some degree of anthracosis, we can infer that ambient air in the study environment contains harmful pollutants capable of irritating their respiratory systems.

Exposure to smoke also showed no effect on the amount of food consumed and body mass change between the groups. Our hypothesis that the smoke group would have a larger body mass change and would eat less than the control group was not supported. This implies that the smoke did not cause stress.

During the experiment, the smoke and control groups showed no signs of stress and behaved as if in good health (e.g., flying around occasionally, perching, and regular food consumption). This does not support our hypothesis that birds exposed to smoke would show behavioral signs of stress compared to the control group.

The unexpected results of this study may be due to the small sample size and limited duration of the experiment. One day, for four hours may have been too short an exposure time for the smoke to affect the birds' behavior and physiological processes in the lungs. This short duration and length of exposure could allow the birds to recover more easily and not be as affected by the smoke. Having longer exposures, such as every day for a month and for more hours in the day, such as 8 hours, would more realistically mimic the effects of a true wildfire. This type of experiment would focus on the physiological processes to overcome constant exposure (which would be faced in a real wildfire) and test the bird's immune system.

Additionally, the smoke concentration might have constrained our results by being too weak to affect the birds' behavior and lung health. Based on the Air Quality Index (AQI), the smoke particle concentrations used in this experiment fell within the upper end of the "Hazardous" category (purple range), corresponding to $PM_{2.5}$ concentrations of ≥222.5 μg/m³ (IQAir). Although this is a large amount of smoke inhaled by the birds, since it was

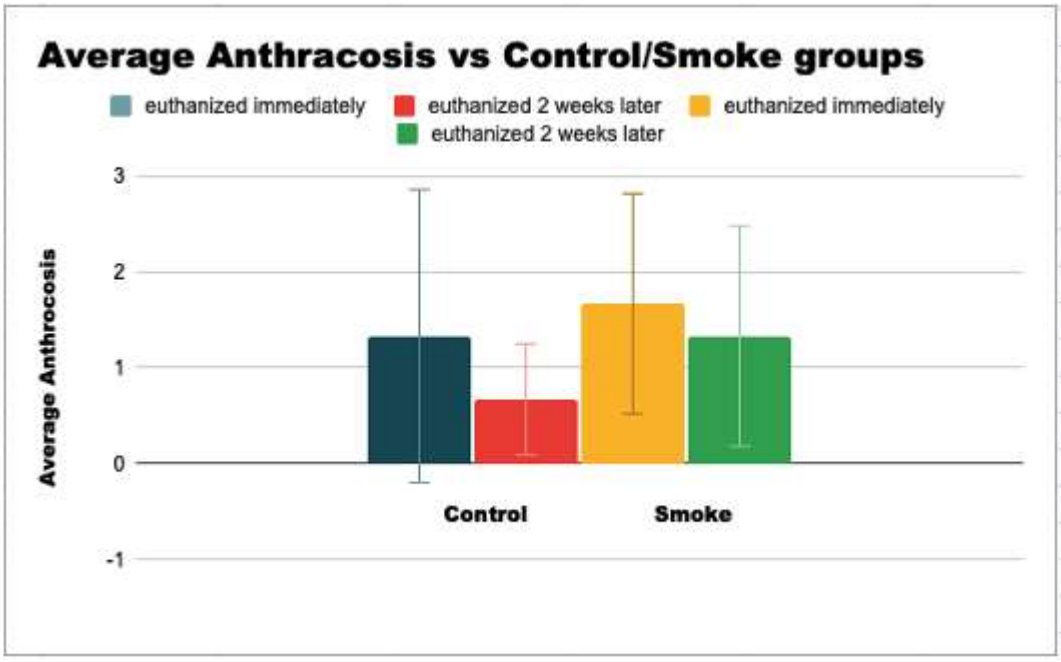

Figure 2: Anthracosis scaling (0-3) for all control groups (euthanized immediately and euthanized 2 weeks later) and smoke groups (euthanized immediately and euthanized 2 weeks later). There are no significant differences between groups. Error bars capture +/- 1 SD.

The Effects of Cold Smoke on Hummingbird Behavior and Lung Physiology

for only four hours in one day, this type of exposure may be recoverable. By increasing the concentration of smoke and duration of exposure, we can better test how resilient the birds are.

Finally, the mechanism for creating smoke was limiting because of the need to continuously maintain a flame, add fuel, change air flows, and control CO. For instance, once the CO monitor inside the environmental chamber reached >50 ppm, we reduced the flame. However, reducing the flame also led to a lower concentration of PM to which the birds were exposed. We had to find the right balance between feeding the flame to increase particulate concentration and reducing the flame to not expose the birds to overwhelming amounts of CO. This caused some fluctuations in the PM concentration over time. This led to the birds not inhaling the expected higher, consistent amounts of PM for an extended period and, therefore, not affecting their respiratory systems as intended.

For future projects on this topic, we suggest modifying some factors, including more frequent exposures, no CO emissions, and pure PM to create a more realistic scenario that reflects actual exposure to cold smoke in the wild. Periodically exposing birds to smoke, such as every day for a month, or exposing them to higher acute concentrations, such as 10,000 $\mu g/m^3$, would ensure the birds are inhaling enough PM to test their resistance and tolerance to extreme cases of smoke. Researchers could then study the birds' responses and histological pathologies (both long- and short-term) and identify physiological resilience or effects and behavioral changes over time. Also, using a different metric of lung pathology would give greater insight into the damage occurring in the respiratory tract. This could include measuring inflammatory cells, edema, and necrosis. Additionally, gathering histology on the air sacs, other organs, and lymph nodes could provide more insight into the physiological effects, since they play a vital role in hummingbird breathing and contribute to the unidirectional flow through the lungs.

Although this project did not show significant differences between the behavior and amounts of anthracosis in the lungs of cold smoke-exposure compared to the control, further research is important to better understand bird respiratory physiology and immunology that contributes to them possibly being resilient creatures. Ultimately, it is important to better understand how cold smoke affects bird lung health and behavior as they play a crucial role in our ecosystem and wildfire cold smoke may pose a major threat to their health and survival.

The Effects of Cold Smoke on Hummingbird Behavior and Lung Physiology

REFERENCES

Brown, Richard E., et al. "The Avian Respiratory System: A Unique Model for Studies of Respiratory Toxicosis and for Monitoring Air Quality." *Environmental Health Perspectives*, vol. 105, no. 2, Feb. 1997, p. 188, DOI: 10.2307/3433242.

Clark, C. J. and Dudley, R. "Hovering and Forward Flight Energetics in Anna's and Allen's Hummingbirds." *Physiological and Biochemical Zoology*, vol. 83, no. 4, 2010, pp. 654-662.

"IQAIR: What Is AQI?" *IQAir*, www.iqair.com/us/newsroom/what-is-aqi?srsltid=AfmBOorVNENzfJrnW-OGZ9jJzgBeCyLBhYfGmK_qVkdpaPTDVM29xfRN. Accessed 16 Apr. 2025.

Jacob, Jacquie, and Tony Pescatore. ASC-200: *Avian Respiratory System*, Nov. 2013, www2.ca.uky.edu/agc/pubs/ASC/ASC200/ASC200.pdf.

Jaffe, Daniel A., et al. "Wildfire and prescribed burning impacts on air quality in the United States." *Journal of the Air & Waste Management Association*, vol. 70, no. 6, 2 June 2020, pp. 583–615. https://www.tandfonline.com/doi/full/10.1080/10962247.2020.1749731.

Leya, Mwense, et al. "The Presence of Anthracosis is Associated with the Environmental Air Quality of Zoo, Wildlife, and Companion Animals in Jeollabuk-do Province, South Korea." *American Journal of Veterinary Research*, vol. 84, no. 6, 2023. https://doi.org/10.2460/ajvr.23.01.0016.

Los Angeles County Department of Public Health. "Wildfire Smoke in Los Angeles County." www.publichealth.lacounty.gov/eh/safety/wildfire-smoke.htm#:~:text=Smoke%20from%20wildfires%20can%20drift,and%20your%20family%20from%20smoke. Accessed 17 Apr. 2025.

Mirsadraee, M. "Anthracosis of the Lungs: Etiology, Clinical Manifestations and Diagnosis: A Review." Tanaffos. vol.13, no.4, 2014; pp. 1-13.

Munshi-South, Jason, and Gerald S. Wilkinson. "Bats and Birds: Exceptional Longevity Despite High Metabolic Rates." *Aging Research Reviews*, vol. 9, no. 1, 2010, pp. 12–19. https://www.sciencedirect.com/science/article/abs/pii/S1568163709000488?via%3Dihub.

National Research Council. *Guide For the Care and Use of Laboratory Animals*. 8th ed., National Academies Press, 2011, https://grants.nih.gov/grants/olaw/guide-for-the-care-and-use-of-laboratory-animals.pdf.

Peng X., et al. "Establishment and Characterization of a Multi-Purpose Large Animal Exposure Chamber for Investigating Health Effects. *Review of Scientific Instruments*, vol.90, no.3, 2019. article 035115. https://pubmed.ncbi.nlm.nih.gov/30927824/.

Stone, Susan L., et al. *Wildfire Smoke: A Guide for Public Health Officials*. United States Environmental Protection Agency, 2019.

Tajik Jalayeri, Mohammad Hadi, et al. "Diagnosis of Pulmonary Lophomoniasis in an Elderly Anthracosis Patient with Resistant Respiratory Symptoms: A Literature Review and a Case Report Study." *Clinical Case Reports*, vol. 12, no. 6, June 2024. https://doi.org/10.1002/ccr3.9085.

United States Environmental Protection Agency. "Particulate Matter (PM) Basics." www.epa.gov/pm-pollution/particulate-matter-pm-basics. Accessed 16 Apr. 2025.

Varon, Joseph, et al. "Carbon Monoxide Poisoning: a Review for Clinicians." *The Journal of Emergency Medicine*, vol. 17, no. 1, 1999, pp. 87–93. https://pubmed.ncbi.nlm.nih.gov/9950394/.

"Ventilation Design Handbook on Animal Research Facilities Using Static Microisolators - Volumes I and II." *National Institutes of Health, U.S. Department of Health and Human Services*, orf.od.nih.gov/TechnicalResources/Bioenvironmental/Pages/execsummary_vent.aspx. Accessed 2 Mar. 2025.

Yu, Manzhu. "Q&A: Causes, Spread and Solutions for California's Wildfire Crisis." *Penn State Institute of Energy and the Environment*, 15 Jan. 2025, https://iee.psu.edu/news/blog/californias-wildfire-crisis-expert-insights-causes-spread-and-solutions. 65433.2023.2294745.

Evaluating Acid Activation Parameters of Biochar for Ammonia Adsorption

Melina Caraballo, Department of Chemical and Environmental Engineering
Amanda Rupiper, Ph.D; Department of Chemical and Environmental Engineering

MELINA BELEN CARABALLO

Melina Caraballo is a fourth year Environmental Engineering major. She conducts research under Dr. Amanda Rupiper, investigating the ammonia adsorption performance of various biochar strains made from agricultural feedstock. She is passionate about sustainability and circular systems and plans to pursue a career in environmental consulting.

ABSTRACT

Ammonia emissions from agricultural systems are an ongoing environmental challenge, and gas adsorption is a common treatment approach. Biochar is charred organic material, usually made from wood or agricultural straw, that has proven to be a low-cost and effective adsorbent for ammonia removal. However, its performance often depends on production modifications such as acid activation. Although acid activation is known to enhance adsorption capacity, the influence of its preparation parameters remains insufficiently understood. This study investigates the effect of particle size (ground and unground), phosphoric acid concentration (15%, 30%, and 45%), and rinsing method (two rinses, five rinses, and a 1-hour soak) on biochar produced from cherry wood chips pyrolyzed at 500°C for 15 minutes. A total of 18 treatment combinations were evaluated in duplicate. The pH was measured before and after activation and used as an indirect indicator of ammonia adsorption potential, as increased surface acidity is associated with enhanced ammonia binding. Post-activation pH values ranged from 2.2 to 3.3, compared to initial values between 7.87 and 9.78. Unground biochar consistently exhibited lower pH values than ground samples, suggesting greater acid retention due to differences in particle structure. Higher acid concentrations produced lower pH values, while more extensive rinsing increased pH due to the removal of residual acid. These results demonstrate that preparation parameters influence biochar surface chemistry and should be optimized to improve ammonia adsorption performance.

KEYWORDS: Biochar, Ammonia, Adsorption, Acid Activation, Surface Functional Groups, Phosphoric acid, pH

FACULTY MENTOR - Dr. Amanda Rupiper,
Department of Chemical and Environmental Engineering

Amanda Rupiper is an Assistant Professor of Teaching in Chemical and Environmental Engineering at UCR. Her research and teaching focus on environmental engineering systems, sustainability, and data-driven modeling, with a strong emphasis on undergraduate research and mentorship.

Evaluating Acid Activation Parameters of Biochar for Ammonia Adsorption

INTRODUCTION AND BACKGROUND

Ammonia emissions from agricultural activities remain an environmental concern, and biochar is one of the many mitigation strategies available. However, raw biochar often exhibits a relatively limited adsorption capacity. Previous studies have determined that modified biochar can adsorb greater amounts of ammonium in liquid solutions compared to unmodified biochar (Zhang et al., 2020). Despite this, the parameters for acid activation are not well documented, and how different methods affect the adsorption potential remains unclear. Therefore, the objective of this study is to evaluate how variations in acid activation influence the properties of biochar.

Ammonia is a colorless gas that indirectly contributes to climate change by breaking down in the atmosphere and forming nitrous oxide, a greenhouse gas. In the United States, approximately 90% of ammonia emissions originate from agricultural activities such as livestock activity and the use and production of fertilizers (Ro et al., 2015). In addition to environmental impacts, ammonia emissions also affect air and water quality. Ammonia can react in the atmosphere and form fine particulate matter (PM2.5), which is associated with respiratory issues and premature mortality (Wyer et al., 2022). These impacts highlight the need to capture and remove ammonia emissions to protect both environmental and human health.

Biochar is a carbon-rich material that is made from organic biomass such as rice husks, wood chips, poultry litter, coconut shavings, corn husks, etc. It is widely used as an adsorbent, similar to activated carbon. Biochar is formed through pyrolysis, a process in which biomass is heated in a low-oxygen environment ranging from 300 to 600°C for 15 to 60 minutes, depending on the desired outcome. Biochar has several advantages, including ease of production, low cost, environmental friendliness, and sustainability (Tang et al., 2025). Due to its porous structure and surface chemistry, biochar has emerged as a promising approach for pollutant control.

Biochar can be modified through various physical and chemical activation methods, such as thermal treatment, steam activation, and chemical modification. Among these, phosphoric acid activation has been shown to improve ammonia adsorption by increasing the number of acidic surface functional groups, which play an important role in ammonia binding (Ro et al., 2015). As a result, acid-activated biochar has been reported to achieve greater reductions in ammonia emissions compared to non-activated biochar, which highlights its effectiveness for ammonia removal (Baral et al., 2023).

Acid activation modifies biochar by treating it with an acid solution, typically phosphoric or nitric acid, for a set period of time. During this process, the acid diffuses across the surface and into the pores of the biochar. In doing so, it alters the surface chemistry and internal pore structure. These changes increase the number of available adsorption sites and enhance the interactions between the acidic biochar surface and the basic ammonia gas. In other words, acid activation of biochar after pyrolysis promotes acid-base interactions between the biochar surface and ammonia gas (NH3), which improves overall adsorption capacity.

When the surface chemistry of biochar is altered during acid activation, new functional groups are formed on the material's surface. These newly formed functional groups increase the acidity of the biochar and become chemically bound to the carbon structure. Furthermore, studies have reported a linear correlation between the breakthrough capacity of ammonia and the number of surface functional groups present on the biochar (Huang et al., 2008). The presence of these groups increases the overall surface acidity of the biochar and provides additional active sites for ammonia adsorption. Acid modification has been shown to improve ammonium adsorption by increasing the concentration of oxygen-containing functional groups, such as carboxylic and lactonic groups (Vu et al., 2017). These groups enhance adsorption by allowing the biochar surface to retain ammonia molecules more effectively. Therefore, understanding how different acid activation parameters influence biochar surface chemistry is important for improving ammonia adsorption performance.

Previous work from this laboratory reported a pH of 8.94 for non-acid-activated biochar (Howlett et al.), which confirms the neutral or alkaline nature of untreated materials and the necessity of acid activation to enhance ammonia adsorption yield. As the effectiveness of acid activation has

Evaluating Acid Activation Parameters of Biochar for Ammonia Adsorption

been well established in the literature, this study does not seek to re-evaluate its benefit over untreated biochar. Instead, this study builds upon these findings to address a gap in the literature regarding how specific preparation parameters, such as particle size, acid concentration, and rinsing method, influence the pH of the biochar. By varying these conditions, this study aims to identify an optimal acid activation procedure for improving ammonia adsorption capacity.

METHODS

Experimental Design

This experiment was designed to evaluate the effects of particle size, phosphoric acid concentration, and post-treatment rinsing method on biochar pH. The variables included two particle sizes (ground and unground), three phosphoric acid concentrations (15%, 30%, and 45%), and three rinsing treatments (two rinses, five rinses, and a 1-hour soak), which resulted in 18 unique treatment combinations. A baseline condition representing standard activation practice for woodchip biochar was defined as a ground sample treated with 30% phosphoric acid and subjected to five rinses. This condition served as a reference point for comparison, with other treatment combinations representing deviations from this baseline. Each condition was prepared using 1 gram of biochar and conducted in duplicate, yielding a total of 36 experimental samples. Initial pre-activation pH values were measured for the samples and used as a baseline for comparison with post-activation measurements.

Biochar Production

The biochar used in this experiment was produced from cherry woodchip shavings and was pyrolyzed at 500°C for 15 minutes using a muffle furnace. Production was conducted between January 16 and January 27, 2026, in which over 60 grams of biochar were produced. Excess biochar was produced to allow for duplicate testing. One of the parameters tested was particle size. For the unground biochar, the woodchips were simply used as received, and for the ground biochar, the woodchips were reduced to a smaller and more uniform size using a mortar and pestle prior to pyrolysis. Samples were placed in crucibles, covered with aluminum foil, and sealed with a lid in order to achieve the low oxygen conditions required for pyrolysis. After 15 minutes, the crucibles were removed from the muffle furnace and left to cool before weighing and packaging.

Acid Activation Procedure and Storage

Three phosphoric acid solutions were prepared at 15%, 30%, and 45% dilution; 100 mL of each solution was prepared. For each treatment condition, 1 gram of biochar was placed into a 50 mL beaker, and 3 mL of phosphoric acid was added. This volume was selected to ensure complete wetting and coating of the biochar surface and was kept consistent across all samples. Samples were thoroughly mixed to promote uniform contact between the acid and biochar. Beakers were then sealed with Parafilm and stored in a dark cabinet overnight for approximately 15 hours to allow for sufficient interaction time while preventing the acid from volatilizing and the mixture from drying out.

Rinsing method and post-treatment

After being left undisturbed overnight, the biochar was removed from the 50 mL beakers and underwent a rinsing treatment to remove the acid. For the rinsing treatment, the biochar was transferred to funnels that were lined with filter paper and placed over graduated cylinders. The filter paper was pre-wetted with water before the biochar was added. For the 1-hour soak treatment, a layer of Parafilm was placed beneath the filter paper to ensure the water stayed in place. A 20 mL volume of DI water was used for the soak, which allowed all the biochar to be submerged during the treatment, and in order to keep conditions consistent, 20 mL was used for the rinses as well. Each rinse was timed, averaging from 1 to 1.5 minutes per rinse. Afterward, the filter papers were placed on brick plates, and the biochar was evenly spread out into a thin layer before being placed in a drying oven at 100°C for 1 hour to remove residual moisture while avoiding burning the filter paper.

Final pH Measurements

After drying, the biochar was gently brushed off the filter paper and transferred to a weigh boat to obtain the post-activation weight before being placed into a 50 mL beaker. A 30 mL volume of DI water was added to each beaker and stirred thoroughly before measuring the final post-activation pH. In order to maintain consistency, the pH meter was calibrated every two weeks and before each use.

Evaluating Acid Activation Parameters of Biochar for Ammonia Adsorption

Two measurements were taken per trial and then averaged to obtain a more accurate reading.

DISCUSSION

Biochar Sample Identification and pH Measurements

Tables 1 and 2 summarize the identification system used for each sample, along with its pre- and post-activation pH measurements. The naming convention goes as follows: letter–particle size–acid concentration–rinsing method. (e.g. A-UG-15%-2x). The pre- and post-activation weights of the samples were recorded in order to verify consistency and detect mass loss during processing. Some samples had slightly higher final weights than their initial weights, which is likely attributable to filter paper residue that transferred over after the drying process. Only minor changes in mass were observed, which suggests that the activation and rinsing procedures did not substantially alter the amount of biochar used in the final pH measurements. The final pH values measured for each biochar sample following activation and rinsing are summarized below.

Trends in Final pH Measurements

Trial 1 was conducted on January 30–31, 2026, and trial 2 was conducted on February 14 to 15, 2026. The initial pH for trial 1 was measured on January 29 and showed an unground pH of 8.82 and a ground pH of 9.78. The initial pH for trial 2 was measured on February 14 and showed an unground pH of 7.87 and a ground pH of 8.92. This variation may be attributed to the storage period between trials. Trial 2 was conducted approximately two weeks after the first trial, during which the stored biochar samples could have adsorbed atmospheric compounds present in the laboratory environment.

A similar trend can be observed in the final pH measurements, as shown in Figure 1, where the final pH measurements for trial 2 were generally slightly higher than those from trial 1. Trial 1 had pH ranges as low as 2.29 and

Sample ID	Trial 1 Final pH Average	Trial 2 Final pH Average
A-UG-15%-2x	2.64	2.695
B-UG-30%-2x	2.55	2.605
C-UG-45%-2x	2.32	2.395
D-UG-15%-5x	3.005	3.195
E-UG-30%-5x	2.9	3.035
F-UG-45%-5x	2.835	2.86
G-UG-15%-1 hr	2.83	2.88
H-UG-30%-1 hr	2.415	2.545
I-UG-45%-1hr	2.295	2.375

Table 1: Final pH measurements for Unground Biochar following acid activation with an initial UG pH of 8.82 for trial 1 and 7.87 for trial 2.

Sample ID	Trial 1 Final pH Average	Trial 2 final pH Average
J-G-15%-2x	2.885	2.94
K-G-30%-2x	2.54	2.595
L-G-45%-2x	2.485	2.46
M-G-15%-5x	3.27	3.325
N-G-30%-5x	3.08	2.985
O-G-45%-5x	2.995	2.915
P-G-15%-1hr	2.74	2.73
Q-G-30%-1hr	2.465	2.515
R-G-45%-1hr	2.3	2.365

Table 2: Final pH Measurements for Ground Biochar following acid activation with an initial G pH of 9.78 for trial 1 and 8.92 for trial 2.

Evaluating Acid Activation Parameters of Biochar for Ammonia Adsorption

as high as 3.27, whereas trial 2 had a range from 2.36 to 3.33. Despite this difference, the overall trends in the data remain consistent. Ground samples had higher pH values than their unground counterparts. Additionally, pH decreased with increasing acid concentration, and samples rinsed five times had higher pH values compared to those rinsed twice. The standard error was calculated for each data point, with values ranging from 0.005 to 0.095, indicating minimal variation between the replicate trials. A one-way ANOVA test confirmed that differences in pH across the 15%, 30%, and 45% acid concentrations were statistically significant ($p=0.0025$), supporting the observed trend of decreasing pH with increasing acid concentration.

Effect of Activation Parameters on Final pH

The difference in particle size is illustrated in Figure 2, where sample C represents the unground and sample Q represents the ground. Unground samples consistently exhibited lower final pH values than did ground samples. One possible explanation is that larger particles retain more acid in their pore structure, which limits acid removal during rinsing. Residual acid trapped within these pores may contribute to lower measured pH values. In contrast, the smaller and more uniform structure of the ground samples may facilitate more effective rinsing, resulting in higher final pH values. However, this mechanism was not directly tested and would require further characterization to confirm.

The influence of acid concentration on final pH was also evident. Lower pH values in the 45% phosphoric acid-treated biochars indicate that the stronger acid concentration had a more significant effect on the biochar's final pH. Similarly, the 15% acid-treated strains had higher final pH values, suggesting that higher acid concentrations result in greater surface acidity after activation. This trend is also seen in Figure 1, where the final pH values for unground samples, rinsed twice, linearly decreased as the acid concentration increased.

The rinsing method had a distinct effect for the two and five-time rinse treatments; however, the 1-hour soak was inconsistent. Samples that underwent 5 rinses generally showed higher final pH values than samples rinsed only twice, suggesting that additional rinsing removed residual acid from the biochar surface. The 1-hour soak treatments produced more variable pH values, which suggests that this method might not be consistent in removing residual phosphoric acid.

RESULTS

The overall trends in the data indicate that unground biochar treated with 45% phosphoric acid produced the lowest final pH values across the tested conditions. Additionally, the samples subjected to five rinses consistently exhibited higher final pH values than those rinsed only twice, suggesting a

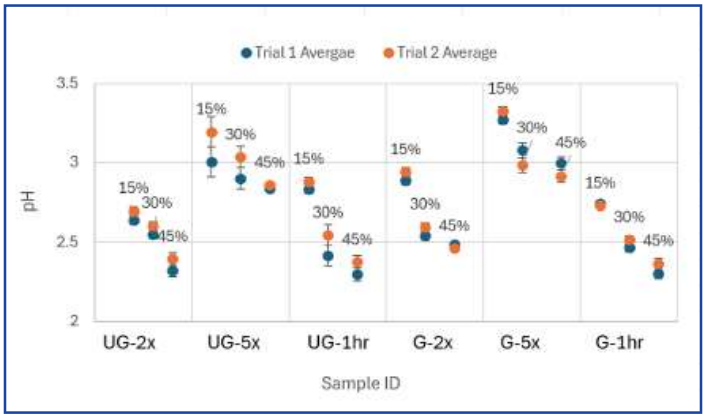

Figure 1: Average Final pH Values of Biochar Samples for Trials 1 and 2

Figure 2: Visual Comparison of Particle Size in Ground vs. Unground Samples

more effective removal of residual phosphoric acid. These results demonstrate that both feedstock preparation and acid activation play significant roles in influencing the surface acidity of acid-activated biochar.

EXPERIMENTAL LIMITATIONS

While the final pH of the biochar provides a useful indicator of surface acidity and potential adsorption, additional testing would be required to quantify the adsorption performance under each treatment. Additionally, it is important to consider that some rinsing procedures might not have fully removed residual activating acid from the biochar surface. Samples subjected to fewer rinses or soaking treatments may have retained trace amounts of acid, which could artificially lower pH measurements. This interpretation is also supported by qualitative observations, as a majority of samples treated with two rinses or the 1-hour soak retained a noticeable acidic odor after their rinse treatment. This further suggests that residual phosphoric acid may still have been present. Residual acid is important to consider as it may react with the ammonia differently than a biochar surface containing only bound acidic functional groups. Surface functional groups are chemically bound to the carbon structure of the biochar and promote the adsorption of ammonia gas. If residual phosphoric acid remained on the biochar, adsorption would be less likely to occur, and a direct acid-base reaction between phosphoric acid (H_3PO_4) and ammonia (NH_3) would occur instead.

FUTURE DIRECTIONS

While pH provides a useful indicator of surface acidity, it does not directly quantify ammonia adsorption capacity. Therefore, the next step in this research is to perform ammonia adsorption experiments in order to directly determine how these activation parameters influence adsorption performance. Future testing will focus on evaluating adsorption capacity and assessing whether the two-times rinse or 1-hour soak preparations artificially raise adsorption capacity.

In addition to adsorption testing, future work will include scanning electron microscopy (SEM) analysis to directly examine biochar surface structure. SEM imaging will allow for visual characterization of differences in pore structure and surface texture resulting from different biochar samples and activation parameters. This analysis aims to provide a more complete picture of how the acid preparation process influences biochar surface chemistry. These future directions will bridge the gap between the pH-based findings of this study and direct measurements of surface properties and adsorption performance.

CONCLUSION

The goal of this study was a better understanding of the acid activation parameters of biochar used for ammonia adsorption. Parameters such as particle size, acid concentration, and rinsing method were tested to see how they affected the pH of the biochar after pyrolysis. The results suggest that activation conditions influence the pH and surface acidity of biochar, which is a valuable indicator of the potential ammonia adsorption yield. In general, treatments that result in a lower pH while still ensuring no residual acid remains to react with the ammonia may be favorable indicators of surface activity, and optimizing acid activation conditions is an effective strategy for improving the performance of biochar as a low-cost adsorbent for ammonia emissions.

Studies have shown that in agricultural systems, biochar can improve pH, porosity, and water availability in soils, which helps increase nutrient uptake by plants (Joseph et al., 2021). When biochar is used to reduce these emissions, the captured ammonia remains adsorbed onto the surface of the biochar. Once the biochar is saturated and is no longer able to capture ammonia, it can be applied to the soil and become an additional nutrient source for plants. The trends observed in this study suggest that acid-activated biochar may offer dual benefits by both capturing ammonia emissions and subsequently serving as a nutrient source when applied to soil. These findings emphasize the importance of controlling activation conditions when producing biochar in order to ensure that it is both effective for ammonia adsorption and suitable for environmental applications after it has been spent.

Evaluating Acid Activation Parameters of Biochar for Ammonia Adsorption

REFERENCES

Baral, K. R., McIlroy, J., Lyons, G., & Johnston, C. (2023). The effect of biochar and acid activated biochar on ammonia emissions during manure storage. *Environmental Pollution*, 317, 120815. https://www.sciencedirect.com/science/article/pii/S0269749122020309

Howlett, T., Ocampo, A., Rupiper, A. *Ammonia Adsorption Performance of Biochars from Agricultural Waste Feedstocks: Implications for Air Pollution Control*. Unpublished manuscript, Department of Chemical and Environmental Engineering, University of California Riverside, in preparation.

Huang, C.-C., Li, H.-S., & Chen, C.-H. (2008). Effect of Surface Acidic Oxides of Activated Carbon on Adsorption of Ammonia. *Journal of Hazardous Materials, 159*(2-3), 523-527. https://doi.org/10.1016/j.jhazmat.2008.02.051

Joseph, S., Cowie, A. L., Van Zwieten, L., Bolan, N., Budai, A., Buss, W., Cayuela, M. L., Graber, E. R., Ippolito, J. A., Kuzyakov, Y., Luo, Y., Ok, Y. S., Palansooriya, K. N., Shepard, J., Stephens, S., Weng, Z. (Han), & Lehmann, J. (2021). How biochar works, and when it doesn't: A review of mechanisms controlling soil and plant responses to biochar. *GCB Bioenergy*, 13(11), 1731-1764. https://doi.org/10.1111/gcbb.12885

Ro, K., Lima, I., Reddy, G., Jackson, M., & Gao, B. (2015). Removing Gaseous NH3 Using Biochar as an Adsorbent. *Agriculture*, 5(4), 991-1002. https://doi.org/10.3390/agriculture5040991

Tang, L., Chen, S., Wang, N., & Jiang, X. (2025). Comparative study of adsorption and slow-release performance and mechanism of phosphoric acid and ammonia-modified biochars on 2,4-dichlorophenoxyacetic acid. *Separation and Purification Technology*, 358, 130470. https://doi.org/10.1016/j.seppur.2024.130470

Vu, T. M., Trinh, V. T., Doan, D. P., Van, H. T., Nguyen, T. V., Vigneswaran, S., & Ngo, H. H. (2017). Removing ammonium from water using modified corncob-biochar. *The Science of the Total Environment*, 579, 612-619. https://doi.org/10.1016/j.scitotenv.2016.11.050

Wyer, K. E., Kelleghan, D. B., Blanes-Vidal, V., Schauberger, G., & Curran, T. P. (2022). Ammonia emissions from agriculture and their contribution to fine particulate matter: A review of implications for human health. *Journal of Environmental Management*, 323(116285), 116285. https://doi.org/10.1016/j.jenvman.2022.116285

Zhang, M., Song, G., Gelardi, D. L., Huang, L., Khan, E., Mašek, O., Parikh, S. J., & Ok, Y.S (2020). Evaluating biochar and its modifications for the removal of ammonium nitrate, and phosphate in water. *Water Research*, 186, 116303. https://doi.org/10.1016/j.watres.2020.116303

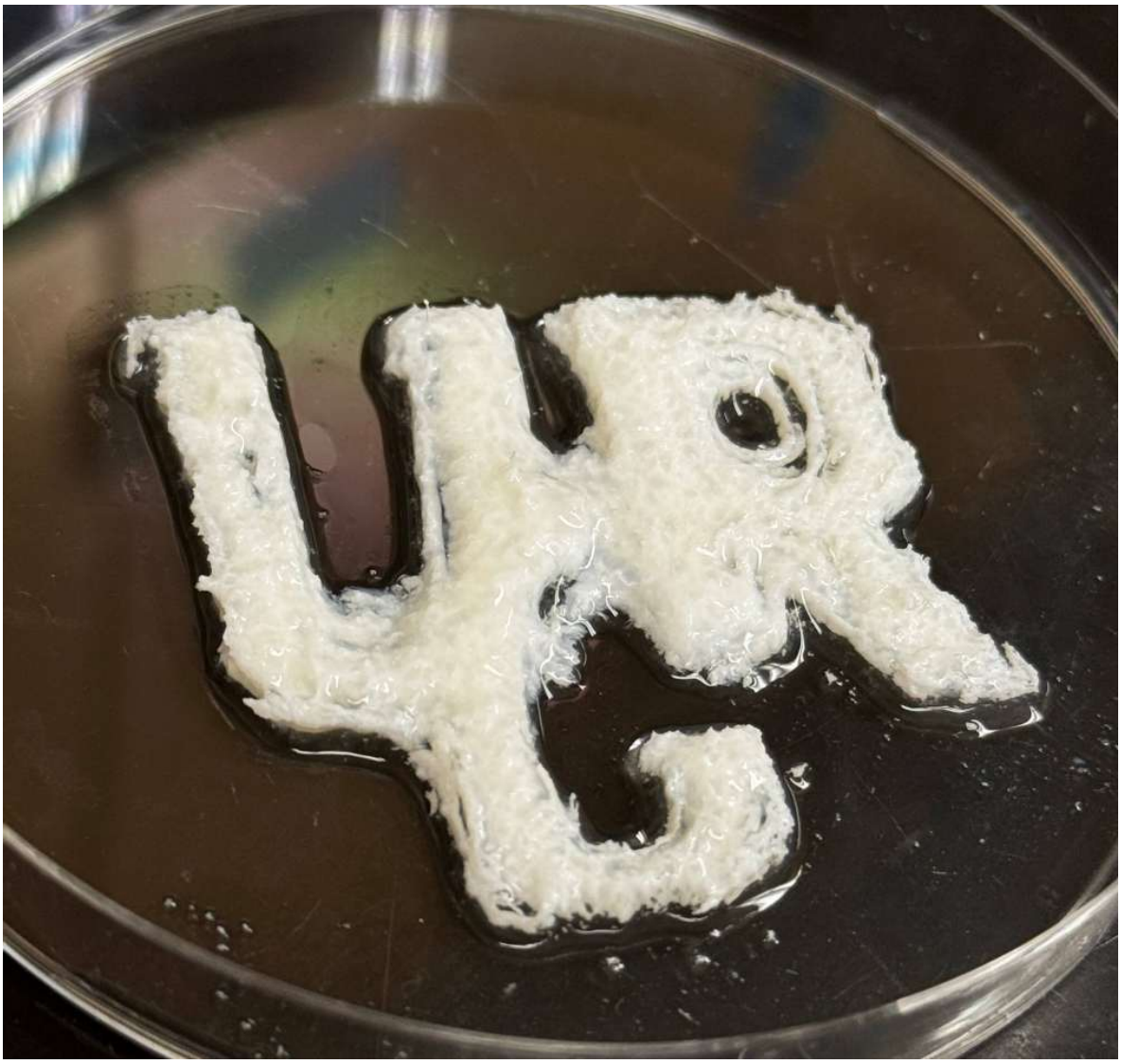

This image was created by Amariah Peedikayil. It shows a printed BIPORES scaffold in the UCR logo shape. This scaffold was created in Dr. Iman Noshadi's Biomaterial laboratory by Varun Vemuri and Andres Perdigon. Cells will be seeded on the material to create a tissue engineering construct.

Impact of Fluid Flow on Mechanical Stress and Deformation in Healthy and Senescent Endothelial Cells

Keyanna-Milenia Pinzon, Department of Bioengineering
Ethan Liu, Department of Bioengineering
Kai Lin, Department of Bioengineering
Adarsh Mattappally, Department of Bioengineering
Victor G Rodgers, Ph.D.; Department of Bioengineering

ABSTRACT

Endothelial cells are continuously exposed to shear stress from blood flow, which plays a critical role in mechanotransduction and the regulation of cellular behavior. These forces induce cellular deformation and transmit stress to intracellular structures, including the nucleus. Cellular senescence is associated with increased stiffness, which alters how mechanical forces are distributed within the cell. However, there is a lack of computational models that directly compare healthy and senescent endothelial cells under identical flow conditions.

In this study, a computational model was developed using COMSOL Multiphysics® to evaluate the mechanical responses of healthy and senescent endothelial cells under steady-state, incompressible laminar flow. Material properties were defined using atomic force microscopy measurements, and both the cell body and nucleus were modeled as isotropic, linearly elastic materials.

Results showed that healthy cells exhibit approximately 20-40 times greater deformation than senescent cells across all regions. Additionally, Von Mises stress analysis revealed a reduction of approximately 29.5% in stress transmission to the nucleus in senescent cells. These findings indicate that increased cellular stiffness significantly reduces both deformation and internal force propagation.

Overall, this study demonstrates that senescence impairs the mechanical responsiveness of endothelial cells, which may contribute to altered mechanotransduction and dysfunction in vascular systems.

FACULTY MENTOR - Dr. Victor G Rodgers, Department of Bioengineering

Dr. Rodgers applies transport phenomena, mathematical modeling, thermodynamics, and kinetics to biomedical engineering problems. The Rodgers Lab develops medical devices to reduce edema and deliver drugs for severe stroke, spinal cord injury, and TBI patients, and studies the thermodynamics of crowded protein systems.

KEYANNA-MILENIA PINZON

Keyanna-Milenia Pinzon is a third-year Bioengineering honors student. She is a Chancellor's Research Fellow and Bilderback Bioengineering Scholar, and plans to pursue a Ph.D. in biomedical engineering focused on biological therapeutics.

ETHAN LIU

Ethan Liu is a third-year bioengineering major. He plans to pursue a career developing engineered biological components for medicine.

KAI LIN

Kai Lin is a third-year Bioengineering major. He plans to pursue a Ph.D. in biophysics and medical device development.

ADARSH MATTAPPALLY

Adarsh Mattappally is a third-year Bioengineering major. He is president of the Undergraduate Research Club and plans to pursue an M.D.

Impact of Fluid Flow on Mechanical Stress and Deformation in Healthy and Senescent Endothelial Cells

INTRODUCTION

Endothelial cells form a monolayer lining on the interior surface of blood vessels and play a critical role in maintaining vascular homeostasis via signaling pathways (Figure 1). These cells regulate processes such as vascular permeability, inflammation, blood clotting, and vascular flow (Bloom et al., 2024). As blood moves through vessels, it exerts fluid shear stress on the endothelial cell membrane, creating mechanical forces that influence cell behavior and function.

An important property of cells is their ability to transform mechanical stimuli into biochemical or electrical signals, a process known as mechanotransduction. Shear stress applied at the membrane is transmitted through the cytoskeleton and reaches the nucleus. Previous studies have shown that the nuclear-to-cytoplasmic (cell body) stiffness ratio determines how mechanical stress is distributed throughout the cell (Angom et al., 2022).

Cellular senescence occurs when the DNA of a cell is damaged, causing cell cycle arrest, but the cell continues to be metabolically active. Senescence naturally occurs in our bodies as we age and is an entry path to apoptosis, or cell death. It is believed to be a cause of many age-related diseases, including cardiovascular disease. Senescent cells exhibit higher stiffness, reflected by a higher Young's Modulus (Angom et al., 2022). These mechanical changes affect how cells respond to forces and the permeability of the membrane. Unfortunately, there is a lack of models that simulate senescent conditions in endothelial cells. Having a model to understand the behavior in relation to fluid flow can offer a useful tool to researchers.

In order to investigate these mechanical effects, a computational model was developed to simulate healthy and senescent endothelial cells under fluid flow and to quantify the forces acting on the cells. In this study, COMSOL Multiphysics® (Version 6.2, Burlington, MA, USA; referred to as COMSOL) is used due to the program's ability to couple fluid dynamics and solid mechanics, enabling analysis of shear stress, cell deformation, and stress gradients that are transmitted to the nucleus. Governing equations from fluid mechanics and linear elasticity were used to capture the interaction between fluid flow and cellular response, allowing deformation magnitude and stress distributions to be quantified. The parameters were chosen to evaluate how differences in cellular stiffness influence the mechanical response of endothelial cells to shear flow.

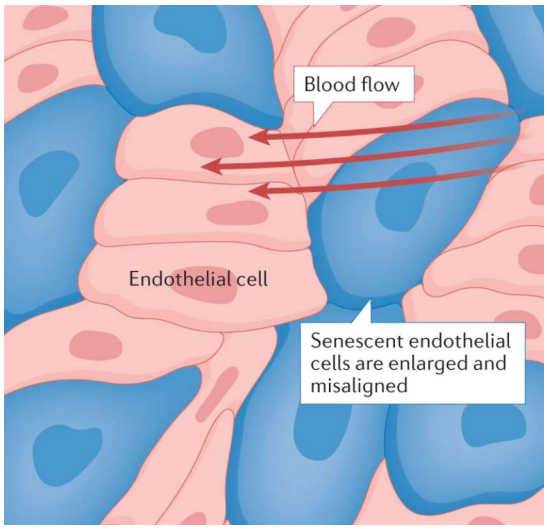

Figure 1. Morphological differences in senescent and healthy endothelial cells. Senescent cells (blue) become enlarged and misaligned to the blood flow. They exhibit higher stiffness and less deformation.
Bloom et al., Mechanisms and consequences of endothelial cell senescence, 2022.

THEORY

To model healthy and senescent endothelial cells under identical shear flow conditions, simulations were conducted under the Navier-Stokes equation implemented in COMSOL. The Navier-Stokes equation governs fluid motion and incorporates parameters that determine shear stress, including fluid density, dynamic viscosity, and the velocity field. The model will show how fluid flow generates shear forces at the cell surface, enabling direct comparison of mechanical responses between healthy and senescent cells.

Impact of Fluid Flow on Mechanical Stress and Deformation in Healthy and Senescent Endothelial Cells

$$\rho\,(u \cdot \nabla)u \;=\; \nabla \cdot [-\,pI \;+\; K] \;+\; F$$

ρ = fluid density
u = fluid velocity vector
p = pressure
I = identity tensor
K = viscous stress tensor
F = external force

In addition to the conservation of momentum described by the Navier-Stokes equation, the conservation of mass within the fluid domain is enforced by the continuity equation:

$$\nabla \cdot u \;=\; 0$$

Both governing equations describe an incompressible fluid flow within the system. To solve the equations, the flow was assumed to be a fully developed laminar flow; the velocity profile remains constant along the direction of flow with no acceleration. This assumption simplifies the governing equations by making the spatial derivative of velocity equal to zero. Incompressible flow was assumed, and the density remained constant throughout the model. The cell body and the nucleus were linearly elastic, allowing deformation to occur using the constant material properties.

In the model, the fixed constraint was where the cell adheres to the endothelial wall at z = 0. The fluid was given the same properties as water. The model was unable to support the dynamic viscosity of blood, but rather than modeling blood rheology, our aim was to compare the difference in shear stress while keeping fluid type constant. The cells were simplified into a hemisphere. The cell was split in the y-direction, assuming symmetry.

METHODS

Assumptions - To enable tractable computation and isolate the effect of cellular stiffness, multiple assumptions were made to ensure efficiency of COMSOL simulations and the model within the scope of this analysis. The model was a stationary model; the fluid flow was fully developed and could be characterized by laminar flow, allowing for a constant profile along the direction of flow. Additionally, the material of the cell body and nucleus was modeled as an isotropic linearly elastic material, enabling deformation to be calculated using constant material properties.

Additionally, the fluid was treated as incompressible with constant density, which is appropriate for biological fluids under low-speed conditions where density variations are negligible.

Geometry - A three-dimensional model was constructed to represent a single endothelial cell within a surrounding fluid domain. The fluid domain was defined as a cube with side lengths of 5.4 μm. The cell was modeled as a quarter sphere positioned on the bottom surface of the domain, representing adhesion to the vessel wall. For the healthy cell, the radius of the sphere was set to 1.35 μm to reflect the measured cell height from the literature (Bloom et al., 2024). The nucleus was modeled as a hemisphere with a radius of 0.25 μm, positioned concentrically within the cell body and elevated 0.5 μm above the base surface. The final geometry for the healthy cell is shown in Figure 2. For the senescent cell model shown in Figure 3, only the radius of the cell body was modified to 0.89 μm while all other geometric parameters were held constant to allow for direct comparison.

Subdomain - Because the primary focus of this study was the relative difference in mechanical responses between healthy and senescent endothelial cells, rather than precise replication of blood rheology, the fluid was modeled using properties equivalent to water. This simplification was necessary due to limitations in representing the dynamic viscosity of blood within the model. While this assumption did not capture the full complexity of physiological flow, it enabled consistent comparison of shear stress and deformation between the two cell conditions under identical fluid properties. The fluid was modeled using properties equivalent to water, with a density of 1000 kg/m^3, along with the dynamic viscosity of 0.001 Pa-s.

The mechanical properties of the cell body were assigned based on literature values, with Young's modulus set to 0.81 kPa for the healthy cell and 4.52 kPa for the senescent cell. The nucleus was assigned a constant Young's modulus of

Impact of Fluid Flow on Mechanical Stress and Deformation in Healthy and Senescent Endothelial Cells

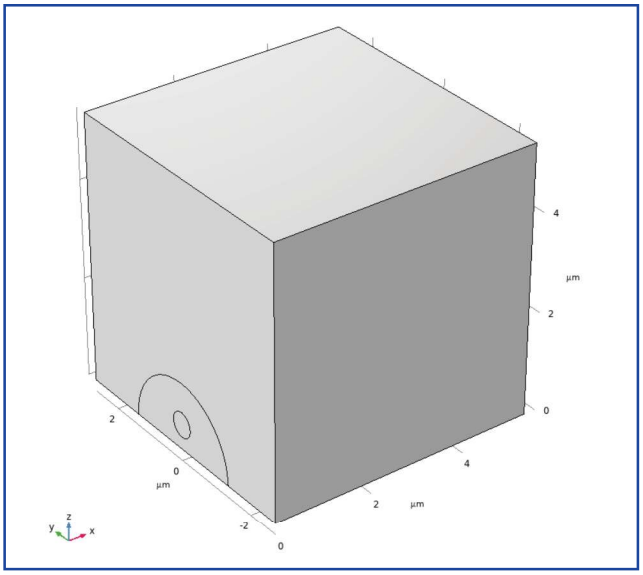

Figure 2: Fluid with velocity over a healthy endothelial cell. Fluid is represented by the cube. The cell membrane is shown as a hemisphere and the nucleus is represented as a sphere. Both are split in the y-direction assuming symmetry.

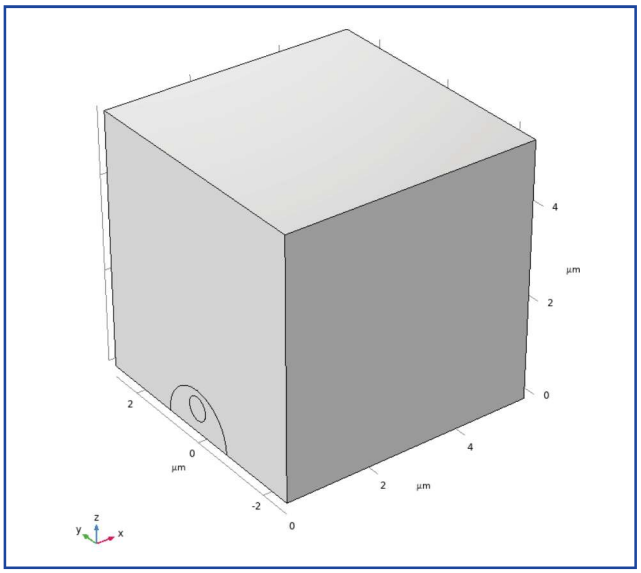

Figure 3: Fluid with velocity over a senescent endothelial cell. Compared to Fig. 2, the distance between the highest y-value of the cell and the nucleus is smaller due to senescence.

5 kPa for both cases. The Young's modulus stiffness values were taken from atomic force microscopy techniques on endothelial cells (Angom et al., 2022). A Poisson's ratio of 0.3 was assumed for both the cell body and the nucleus, consistent with literature values (Angom et al., 2022).

Boundary - A symmetry boundary condition was applied along one face of the fluid domain. The inlet and outlet were defined along the y-direction, with the inlet assigned a uniform velocity of 0.015 m/s and the outlet set to a reference pressure of 0 Pa. A fixed constraint was applied at the base of the cell. An attachment was set to the surfaces between the nucleus and the cell body. The remaining boundaries were set to no-slip. The shear stress transmitted from the cell body to the cell nucleus was analyzed. The cell was divided into three regions to quantify deformation.

The three regions characterized the spatial distribution of deformation throughout the cell. Shear stress was evaluated at the cell surface and around the nucleus, enabling comparison between membrane stress and internally propagated stress toward the nucleus.

RESULTS & DISCUSSION

The stress and deformation values were averaged across 25 sample points within each region. To quantify the mechanical response of healthy and senescent cells, we analyzed deformation and Von Mises stress distributions resulting from fluid flow. Cell deformation represented how the cell changes shape under shear stress, providing insight into how forces propagate through the structure. Displacement magnitudes were evaluated across three regions: the upper region exposed to flow, the middle region near the nucleus, and the adhesion site where the cell was fixed to the vessel wall.

The healthy cell exhibited much greater deformation across all regions compared to the senescent model (Figure 4). In the upper region, the healthy cell deformed by 1.12 ± 0.06 µm, compared to 0.03 ± 0.01 µm by the senescent cell. In the middle region around the nucleus, deformation dropped from 0.53 ± 0.06 µm in the healthy cell to 0.02 ± 0.01 µm in the senescent, and from 0.13 ± 0.02 µm to 0.01 ± 0.01 µm at the adhesion site.

Impact of Fluid Flow on Mechanical Stress and Deformation in Healthy and Senescent Endothelial Cells

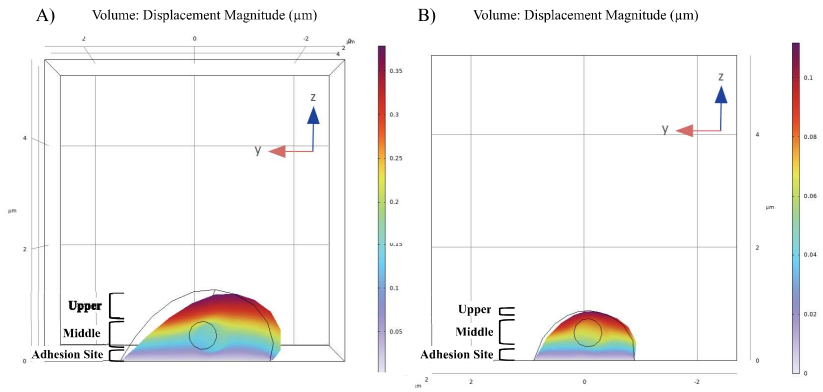

Figure 4. Magnitude of the volume of displacement of a healthy cell (A) and a senescent cell (B).

The upper region is classified the distance between the nucleus and the surface of the cell. The middle region is the diameter of the nucleus. The adhesion site is located below the nucleus. The healthy cell model faces a noticeably increased deformation compared to the senescent cell model.

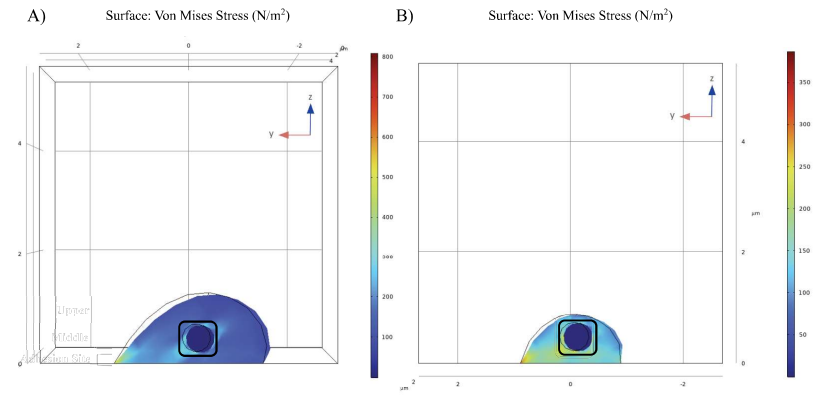

Figure 5. Distribution of stress in the membrane of a healthy cell (A) and a senescent cell (B).

The boxed region indicates the area averaged to calculate stress around the nucleus. Referencing the scale, the healthy cell model has a noticeably increased internal stress distribution compared to the senescent cell.

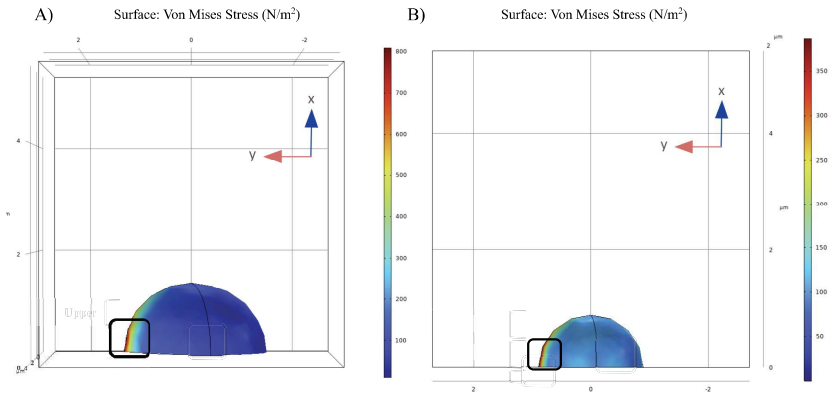

Figure 6. The distribution of stress on the surface of a healthy cell (A) and a senescent cell (B).

The boxed region indicates the area averaged to calculate shear surface force. The healthy cell has a noticeably greater surface shear stress compared to the senescent cell.

Impact of Fluid Flow on Mechanical Stress and Deformation in Healthy and Senescent Endothelial Cells

This difference in deformation behavior directly influences the internal stress distribution, which was evaluated using Von Mises stress. Stress was evaluated in two locations, the outer cell surface and inner body just around the nucleus.

Like the deformation models, at the surface of the cell, the healthy cell experienced 763.42 ± 17.91 N/m^2 stress compared to the senescent model's 284.23 ± 13.72 N/m^2 (Figure 5).

Around the nucleus, the Von Mises stress decreased from 325.59 ± 17.72 N/m^2 in the healthy cell model to 229.35 ± 9.33 N/m^2 in the senescent cell model.

The results presented by the COMSOL simulation indicate that senescent endothelial cells experienced significantly lower Von Mises stress at both the cell membrane and around the nucleus compared to healthy cells.

This reduction reflected a decreased transmission of mechanical stress through the cellular structure. These findings are consistent with literature reports, which observed an approximate ~56% reduction in shear stress transmitted to the nucleus from healthy Human Umbilical Vein Endothelial Cells (HUVEC) to aged senescent HUVEC cells (Walther et al., 2023). In comparison, the present model predicted a reduction of approximately ~29.5% when observing the Von Mises transmitted to the nucleus. While the magnitude differs, both computational results and experimental findings agree on the trend of cellular senescence reducing nuclear mechanosensing. Reduced deformation and stress transmission observed in the senescent cell model suggest that increased cellular stiffness limits the cell's ability to mechanically respond to shear loading. This diminished mechanical responsiveness may impair mechanotransduction, as lower deformation reduces the propagation of forces to intracellular structures such as the nucleus, potentially altering shear-sensitive signaling pathways.

The discrepancy between the simulations and the experimental results (Walther et al., 2023) can be attributed to several simplifying assumptions in the model. First, the use of an idealized hemispherical geometry does not capture the complex morphology of endothelial cells, which may influence local stress distributions, force transmission pathways, and assumptions within the Navier-Stokes equation. Additionally, modeling the cell body and nucleus as linearly elastic materials neglects the viscoelastic behavior of biological tissues, potentially affecting the magnitude and temporal response of deformation. The use of water properties instead of blood further simplifies the fluid environment, omitting non-Newtonian effects that can alter shear stress profiles. Among these assumptions, geometric simplification was expected to have the most direct impact on spatial stress distribution, while the material and fluid assumptions primarily influenced the magnitude of the predicted responses.

To enable tractable computation and to isolate the effect of cellular stiffness, several simplifying assumptions were applied to the Navier–Stokes formulation. The flow was assumed to be steady-state, eliminating time-dependent terms and allowing the velocity field to remain constant over time. This assumption was reasonable because the study focused on the comparative mechanical response of cells under constant shear conditions, rather than transient pulsatile blood flow.

The flow was also assumed to be fully developed and laminar, meaning the velocity profile did not change along the direction of flow, and inertial effects were minimal. This is consistent with microscale flow conditions typical of small vessels and ensures that shear stress remains uniform and comparable across simulations.

Additionally, the fluid was treated as incompressible with constant density, which is appropriate for biological fluids under low-speed conditions where density variations are negligible. Together, these assumptions simplified the governing equations while preserving the dominant shear-driven forces acting on the cell surface.

Although these simplifications did not capture the full complexity of physiological blood flow, they provided a controlled framework for consistently evaluating how differences in cellular stiffness influenced deformation and stress transmission under identical flow conditions. These findings suggest that increased cellular stiffness alters how mechanical forces are distributed within

Impact of Fluid Flow on Mechanical Stress and Deformation in Healthy and Senescent Endothelial Cells

the cell, which may influence how external stimuli are experienced at a structural level. The presented model offers a framework for understanding how changes in mechanical properties affect cellular response to fluid flow. In vascular systems, disrupted mechanotransduction has been associated with endothelial dysfunction, increased inflammation, and the progression of cardiovascular diseases such as atherosclerosis. The presented model offers a simplified yet informative framework for understanding how age-related mechanical changes may contribute to vascular pathology under fluid-flow conditions.

Future work should extend this model by incorporating viscoelastic material properties to better capture time-dependent cellular deformation. Additionally, implementing more realistic endothelial cell geometries would improve the accuracy of predictions of stress distribution and force transmission. Incorporating non-Newtonian fluid properties would further enhance physiological relevance by accounting for shear-dependent viscosity effects in blood flow.

CONCLUSION

This study used computational modeling to investigate how differences in cellular stiffness influenced the mechanical response of endothelial cells under fluid shear stress. Using coupled fluid dynamics and solid mechanics in COMSOL, healthy and senescent cells were analyzed under identical laminar flow conditions to quantify deformation and stress transmission.

Results show that cellular stiffness plays a critical role in how mechanical forces are distributed within the cell. Healthy cells, characterized by a lower Young's modulus, exhibited ~20–40 times greater deformation than did senescent cells. In contrast, senescent cells showed minimal deformation and a more uniform stress distribution. Analysis of Von Mises stress further revealed differences in force transmission to the nucleus, with healthy cells exhibiting localized stress concentrations, while senescent cells distributed stress more broadly. These findings indicate that increased stiffness reduces the cell's ability to mechanically adapt to external flow.

The computational trends observed in this study are consistent with findings reported in the literature (Walther et al., 2023), which demonstrated a substantial reduction in shear stress transmitted to the nucleus in senescent endothelial cells compared to healthy cells. While this model predicts a ~29.5% reduction compared to ~56% experimentally, both demonstrate the same overall trend of decreased stress transmission with increased stiffness. These results highlight the role of cellular stiffness in regulating how forces are experienced within the cell.

Location of Deformation	Average Deformation of Healthy Cell	Average Deformation of Senescent Cell
Upper Region	1.12 ± 0.06 μm	0.03 ± 0.01 μm
Middle Region	0.53 ± 0.06 μm	0.02 ± 0.01 μm
Adhesion Site	0.13 ± 0.02 μm	0.01 ± 0.01 μm

Table 1. Average deformation values of the healthy and senescent cell models from three distinct regions. Values shown were averaged from 20 random points along the corresponding region. Standard deviation calculated through Google Sheets.

Location of Shear	Healthy Cell	Senescent Cell
Cell Membrane	764.07 ± 18.01 N/m^2	284.23 ± 13.72 N/m^2
Around the Nucleus	325.59 ± 17.72 N/m^2	229.35 ± 9.33 N/m^2

Table 2. Average Von Mises stress values of the healthy and senescent cell models from both the outer cell membrane and inner area around the nucleus. Values shown were averaged from 25 random points along the corresponding region. Standard deviation calculated through Google Sheets.

Impact of Fluid Flow on Mechanical Stress and Deformation in Healthy and Senescent Endothelial Cells

APPENDIX

Healthy Cell Membrane			
X	Y	Z	Value [N/m^2]
0.0058452	1.3472	0.0032849	753.39
0.033107	1.3408	0.0068658	751.98
0.058435	1.3388	0.0034157	771.08
0.080632	1.3329	0.0076866	765.86
0.10775	1.329	0.0069109	777.52
0.13139	1.3271	0.0036908	795.34
0.15503	1.3252	4.73×10^{-4}	806.18
0.19267	1.3155	0.0070636	782.97
0.23845	1.3084	0.0066602	784.78
0.29291	1.299	0.0080607	766.25
0.32336	1.2949	0.0068125	750.51
0.28293	1.2982	0.012364	758.18
0.2508	1.3008	0.016718	748.69
0.20333	1.3079	0.017353	751.23
0.15416	1.3152	0.018211	752.94
0.10968	1.3247	0.013942	757.01
0.075909	1.3274	0.018542	731.55
0.051926	1.3352	0.011597	744.21
0.019648	1.3411	0.010158	737.44
0.20467	1.312	0.009824	773.6
0.26435	1.2988	0.016329	748.59
0.29486	1.2963	0.012229	754.37
0.18424	1.3161	0.0082195	780.31
0.28918	1.3027	0.0026576	782.4
0.30486	1.2964	0.0093682	755.47
0.24196	1.3065	0.0091169	772.23
0.17237	1.3179	0.0083781	780.94
0.13348	1.3203	0.015084	761.37
0.1657	1.3176	0.010762	774.44
0.18957	1.3124	0.013364	764.44
0.22483	1.3112	0.0055905	784.37
0.12999	1.3222	0.012634	767.94
0.081073	1.3253	0.020757	726.66

Healthy Cell Nucleus			
X	Y	Z	Value [N/m^2]
1.91×10^{-18}	0.08796	0.23065	280.33
1.42×10^{-17}	-0.094474	0.21152	341.08
1.33×10^{-17}	-0.082884	0.21304	335.23
1.30×10^{-17}	-0.10036	0.2006	306.68
1.45×10^{-17}	-0.097919	0.21138	342.99
1.30×10^{-17}	-0.079965	0.21173	332.87
1.35×10^{-17}	-0.088432	0.20711	335.34
1.20×10^{-17}	-0.064265	0.21986	327.8
1.33×10^{-17}	-0.084665	0.21047	334.92
1.20×10^{-17}	-0.063703	0.22134	327.75
1.40×10^{-17}	-0.096499	0.2071	335.06
1.20×10^{-17}	-0.0689	0.21181	326.57
1.43×10^{-17}	-0.10281	0.20785	331.69
1.41×10^{-17}	-0.091437	0.21521	341.25
1.43×10^{-17}	-0.095204	0.21185	341.67
1.16×10^{-17}	-0.059871	0.21867	322.27
1.36×10^{-17}	-0.08198	0.22075	338.69
1.17×10^{-17}	-0.054792	0.23058	320.31
1.13×10^{-17}	-0.052543	0.22581	316.45
1.34×10^{-17}	-0.083571	0.21424	336.24
1.39×10^{-17}	-0.090737	0.21116	338.75
1.29×10^{-17}	0.12171	0.4816	308.31
1.25×10^{-17}	0.11654	0.50583	266.63
1.30×10^{-17}	0.11441	0.47788	320.14
1.31×10^{-17}	0.10696	0.45176	293.48
1.34×10^{-17}	-0.080122	0.21961	337.04
1.43×10^{-17}	-0.094454	0.21345	342.07
1.25×10^{-17}	-0.070964	0.21771	330.8
1.19×10^{-17}	-0.058378	0.22904	324.38
1.34×10^{-17}	-0.085296	0.21155	335.84
1.23×10^{-17}	-0.11633	0.21427	319.68
1.33×10^{-17}	-0.097832	0.20281	317.51
1.32×10^{-17}	-0.081713	0.21309	334.58

Table 3. Points used to calculate average Von Mises stress of the healthy endothelial cell in the membrane and around the nucleus.

Impact of Fluid Flow on Mechanical Stress and Deformation in Healthy and Senescent Endothelial Cells

APPENDIX

Senescent Cell Membrane			
X	Y	Z	Value
4.99×10^{-1}	7.09×10^{-1}	2.66×10^{-2}	2.67×10^{2}
4.54×10^{-1}	7.38×10^{-1}	3.13×10^{-2}	2.72×10^{2}
4.16×10^{-1}	7.60×10^{-1}	4.63×10^{-2}	2.67×10^{2}
3.75×10^{-1}	7.90×10^{-1}	3.70×10^{-2}	2.82×10^{2}
3.32×10^{-1}	8.14×10^{-1}	4.37×10^{-2}	2.84×10^{2}
3.03×10^{-1}	8.20×10^{-1}	4.08×10^{-2}	2.88×10^{2}
2.83×10^{-1}	8.24×10^{-1}	4.14×10^{-2}	2.88×10^{2}
2.73×10^{-1}	8.26×10^{-1}	4.17×10^{-2}	2.88×10^{2}
2.47×10^{-1}	8.32×10^{-1}	3.87×10^{-2}	2.92×10^{2}
2.17×10^{-1}	8.38×10^{-1}	3.96×10^{-2}	2.92×10^{2}
1.97×10^{-1}	8.42×10^{-1}	4.02×10^{-2}	2.93×10^{2}
1.85×10^{-1}	8.44×10^{-1}	4.06×10^{-2}	2.93×10^{2}
1.35×10^{-1}	8.53×10^{-1}	4.21×10^{-2}	2.93×10^{2}
1.18×10^{-1}	8.57×10^{-1}	4.27×10^{-2}	2.93×10^{2}
1.05×10^{-1}	8.59×10^{-1}	4.31×10^{-2}	2.93×10^{2}
9.54×10^{-2}	8.61×10^{-1}	4.34×10^{-2}	2.93×10^{2}
8.30×10^{-2}	8.63×10^{-1}	4.37×10^{-2}	2.92×10^{2}
7.31×10^{-2}	8.65×10^{-1}	4.40×10^{-2}	2.92×10^{2}
4.94×10^{-2}	8.71×10^{-1}	4.09×10^{-2}	2.94×10^{2}
3.48×10^{-2}	8.73×10^{-1}	4.05×10^{-2}	2.95×10^{2}
2.54×10^{-2}	8.66×10^{-1}	7.20×10^{-2}	2.72×10^{2}
6.19×10^{-2}	8.60×10^{-1}	7.35×10^{-2}	2.69×10^{2}
9.49×10^{-2}	$8.55 \times 10^{-1}1$	7.03×10^{-2}	2.71×10^{2}
1.58×10^{-1}	8.42×10^{-1}	7.22×10^{-2}	2.69×10^{2}
2.14×10^{-1}	8.32×10^{-1}	6.66×10^{-2}	2.72×10^{2}
2.34×10^{-1}	$8.28 \times 10^{-1}1$	6.60×10^{-2}	2.71×10^{2}
2.34×10^{-1}	8.28×10^{-1}	6.60×10^{-2}	2.71×10^{2}
2.46×10^{-1}	8.26×10^{-1}	6.56×10^{-2}	2.71×10^{2}
2.85×10^{-1}	8.16×10^{-1}	7.60×10^{-2}	2.61×10^{2}
4.87×10^{-2}	8.61×10^{-1}	7.65×10^{-2}	2.68×10^{2}
1.81×10^{-2}	8.67×10^{-1}	7.17×10^{-2}	2.73×10^{2}
2.12×10^{-2}	8.76×10^{-1}	3.64×10^{-2}	2.99×10^{2}
1.22×10^{-2}	$8.81 \times 10^{-1}1$	2.55×10^{-2}	3.07×10^{2}
6.97×10^{-3}	8.84×10^{-1}	1.82×10^{-2}	3.13×10^{2}
2.65×10^{-2}	8.80×10^{-1}	1.86×10^{-2}	3.12×10^{2}

Senescent Cell Nucleus			
X	Y	Z	Value
1.34×10^{-17}	-0.0130835862	0.2342515173	234.8014022
1.22×10^{-17}	0.0148688136	0.2409398488	226.2279059
1.17×10^{-17}	0.0123754513	0.2308238869	222.8892878
1.24×10^{-17}	0.00436739726	0.2314481258	228.1496562
1.32×10^{-17}	-0.01070637129	0.23259773	233.3058142
1.32×10^{-1}	-0.01779303865	0.233123154	232.9608628
1.32×10^{-1}	-0.02346240121	0.233543392	232.6847876
1.34×10^{-1}	-0.02583957016	0.2351973981	234.1806201
1.08×10^{-1}	-0.03617604262	0.2358975266	225.9071143
8.68×10^{-18}	-0.042762473	0.2392747713	221.0481733
5.66×10^{-18}	-0.05316858733	0.2399658664	211.4774932
3.12×10^{-18}	-0.06111734304	0.2433383237	208.1069221
5.24×10^{-18}	-0.06034842854	0.2196827981	201.6473199
8.62×10^{-18}	-0.04784334948	0.2219726332	209.1591788
8.69×10^{-18}	-0.04148901545	0.2435971162	224.0976488
1.17×10^{-17}	-0.03065476471	0.2443448008	234.7633915
1.36×10^{-17}	-0.02254758501	0.2364306125	235.951897
1.36×10^{-17}	-0.01546099362	0.2359051693	236.2968177
1.38×10^{-17}	-0.01358618521	0.2372440346	237.9997419
1.34×10^{-17}	0.001522183738	0.2419798131	234.9948985
1.30×10^{-17}	0.009264056951	0.245795138	232.0422036
1.39×10^{-17}	0.004015666365	0.2520953662	238.3332448
1.41×10^{-17}	-7.01×10^{-4}	0.2495170897	240.0094979
1.40×10^{-17}	-0.00105699276	0.2480718138	239.5324973
1.32×10^{-17}	0.002500538635	0.2404303872	233.6411832
1.27×10^{-17}	0.007839126498	0.2400143903	230.1344204
1.25×10^{-17}	0.0105085473	0.239806403	228.3809658
1.27×10^{-17}	0.007839126498	0.2400143903	230.1344204
1.25×10^{-17}	0.002676435139	0.2301069683	228.5494668
1.32×10^{-17}	-0.007871662035	0.2323875545	233.4437938
1.32×10^{-17}	-0.01212359971	0.2327028008	233.2368222
1.32×10^{-17}	-0.01212359971	0.2327028008	233.2368222
1.34×10^{-17}	-0.02017024809	0.234777171	234.4567019
1.36×10^{-17}	-0.01687835898	0.2360102479	236.2278165
1.36×10^{-17}	-0.001147101267	0.2421881197	236.7484231

Table 4. Points used to calculate average Von Mises stress of the senescent endothelial cell in the membrane and around the nucleus.

Impact of Fluid Flow on Mechanical Stress and Deformation in Healthy and Senescent Endothelial Cells

APPENDIX

Upper			
X	Y	Z	Value [µm]
0	-0.1736334	1.167815	0.3541
0	0.08118816	1.156571	0.3621063
0	-0.5673889	1.19391	0.3549113
0	-0.2726956	1.246524	0.3712426
0	0.2049733	1.1523419	0.3699916
0	0.2854135	1.105685	0.3636345
0	-0.0365238	1.117433	0.3460238
0	-0.3420992	1.149606	0.3463025
0	-0.6727333	1.069807	0.3242520
0	-0.936547	1.054061	0.3239967
0	-0.7661938	1.045624	0.31891
0	-0.405778	1.023230	0.3130519
0	-0.0211170	1.014048	0.318149
0	0.2810838	1.091508	0.3593633
0	0.1545570	1.139602	0.3630868
0	0.4126326	1.056818	0.3605648
0	0.206336	1.05135410	0.3427521
0	-0.1330747	1.151077	0.3510638
0	-0.0757103	1.1408	0.3502866
0	-0.3149755	1.198453	0.3584111

Middle			
X	Y	Z	Value [µm]
0	0.9488621	0.4442371	0.1994230
0	0.66276296	0.46484002	0.18437065
0	0.49813228	0.51297236	0.18982360
0	0.35642295	0.52152677	0.18303225
0	0.33507972	0.56507038	0.19630346
-2.40×10^{-17}	-0.3088916	0.64252747	0.18709257
-1.44×10^{-17}	-0.4322415	0.62069455	0.19360741
0	-0.5456737	0.56656564	0.18179239
0	-0.6801116	0.56487681	0.18499485
0	-0.8092071	0.54305043	0.18341194
0	-1.0239740	0.53651058	0.19238764
0	-1.1562063	0.44474696	0.17568859
0	-1.1714071	0.44247577	0.17659052
0	-0.9715200	0.49761262	0.17725606
0	-0.8278222	0.48865987	0.16805285
0	-0.7210485	0.53579703	0.17832296
0	-0.6167453	0.53464955	0.17473135
0	-0.5277893	0.57997368	0.18479075
-7.57×10^{-19}	-0.4868377	0.63933871	0.19985351
-8.09×10^{-19}	-0.4948364	0.5273310	0.17152950

Adhesion Site			
X	Y	Z	Value [µm]
0	1.21483428	0.12453770	0.06614605
0	0.99095860	0.09890715	0.04182225
0	0.88117104	0.10922278	0.04479769
0	0.64035193	0.15258422	0.05991435
0	0.34775256	0.12135022	0.04778366
0	0.05284874	0.14425678	0.05590380
7.99×10^{-19}	-0.0814964	0.13256072	0.05427280
0	-0.1975314	0.11180923	0.04736328
0	-0.3119772	0.17683210	0.07286809
0	-0.4656101	0.14919623	0.05493930
0	-0.8240378	0.09525245	0.03318312
0	-1.0217821	0.11613717	0.04555904
0	-1.1573642	0.09686997	0.04187022
0	-1.2153930	0.16448396	0.07666321
0	-1.2636392	0.09537088	0.04771613
0	-1.0975083	0.14220523	0.05931331
0	-0.8965323	0.14724106	0.05351260
0	-0.7207538	0.11899181	0.04146544
0	-0.5957637	0.12825113	0.04525249
0	-0.4790656	0.09922869	0.03593792

Table 5. Points used to calculate average deformation values of a healthy endothelial cell in three sites.

Impact of Fluid Flow on Mechanical Stress and Deformation in Healthy and Senescent Endothelial Cells

APPENDIX

Upper			
X	Y	Z	Value [µm]
0	0.39340771	0.72742507	0.03484600
0	0.32732432	0.73892209	0.03432316
0	0.25174556	0.79303362	0.03584859
0	0.20121915	0.79330064	0.03542962
4.15×10^{-18}	0.11969325	0.79431210	0.03481885
6.98×10^{-18}	0.07697428	0.79533169	0.03448685
8.78×10^{-18}	0.04978384	0.79599680	0.03428128
7.75×10^{-18}	0.01610702	0.81239134	0.03533840
7.95×10^{-18}	-0.0148320	0.81325501	0.03527222
5.21×10^{-18}	-0.0610775	0.81459949	0.03538612
3.53×10^{-18}	-0.0764758	0.81505900	0.03545325
1.52×10^{-19}	-0.1112090	0.81219678	0.03554190
0	-0.1351765	0.79738302	0.03480342
0	-0.1392450	0.79363191	0.03460718
0	-0.1430975	0.79372475	0.03462429
0	-0.1552736	0.78245188	0.03406822
0	-0.1783114	0.78295856	0.03425576
0	-0.2013638	0.78343513	0.03442453
-2.34E-18	-0.2456950	0.74166809	0.03268597
-5.92E-18	-0.2540424	0.72635460	0.03209320

Middle			
X	Y	Z	Value [µm]
0	0.73816335	0.34276547	0.02273521
0	0.67887371	0.34447022	0.02176854
0	0.60531037	0.40394414	0.02398639
0	0.44612070	0.42612535	0.02342833
0	0.42209540	0.43311827	0.02355787
0	0.39071489	0.43311603	0.02324127
0	0.34220373	0.43643918	0.02305835
0	0.32483640	0.43639699	0.02295104
3.33×10^{-19}	0.31789352	0.43633853	0.02291588
6.08×10^{-18}	0.27303655	0.44589383	0.02299578
1.27×10^{-17}	0.22786636	0.45474817	0.02291163
-4.08×10^{-17}	-0.2790138	0.47353178	0.02444622
-2.00×10^{-17}	-0.3306844	0.47186522	0.02403718
-6.15×10^{-18}	-0.3652000	0.47134210	0.02390351
0	-0.3963241	0.47101453	0.02376260
0	-0.4513632	0.47097834	0.02393357
0	-0.4656326	0.45701592	0.02344653
0	-0.5069523	0.45718915	0.02358272
0	-0.5799972	0.43682266	0.02312439
0	-0.6872570	0.41735359	0.02321695

Adhesion Site			
X	Y	Z	Value [µm]
0	0.80468886	0.03708650	0.00232567
0	0.75700163	0.04733361	0.00296826
0	0.70520342	0.04741652	0.00293428
0	0.64988782	0.04770941	0.00281425
0	0.63241315	0.04431309	0.00259210
0	0.55993208	0.04431309	0.00259210
0	0.38736082	0.04432918	0.00259460
0	0.29415769	0.04428549	0.00258244
0	0.22504593	0.04421839	0.00250379
0	0.12827590	0.04431754	0.00237261
0	0.05911139	0.04450486	0.00223866
0	-0.0264253	0.05870181	0.00303432
0	-0.1125988	0.05894690	0.00319386
0	-0.3260567	0.06593845	0.00373093
0	-0.3918838	0.06241597	0.00347236
0	-0.4402725	0.06238468	0.00339915
0	-0.4989793	0.06237566	0.00336635
0	-0.5612335	0.06238458	0.00324383
0	-0.6026514	0.06238458	0.00324383
0	-0.7474746	0.06309619	0.00360418

Table 6. Points used to calculate average deformation values of a senescent endothelial cell in three sites.

Impact of Fluid Flow on Mechanical Stress and Deformation in Healthy and Senescent Endothelial Cells

REFERENCES

Angom RS, Kulkarni T, Wang E, Kumar Dutta S, Bhattacharya S, Das P, et al. Vascular endothelial growth factor receptor-1 modulates hypoxia-mediated endothelial senescence and cellular membrane stiffness via YAP-1 pathways. *Front Cell* Dev Biol. 2022;10.

Bloom SI, Islam MT, Lesniewski LA, Donato AJ. Mechanisms and consequences of endothelial cell senescence. *Nat Rev* Cardiol. 2022;20(1).

Cabrera AP, Bhaskaran A, Xu J, Yang X, Scott HA, Mohideen U, et al. Senescence increases choroidal endothelial stiffness and susceptibility to complement injury: Implications for choriocapillaris loss in AMD. *Invest Ophthalmol Vis Sci.* 2016;57(14):5910–5918.

Chala N, Moimas S, Giampietro C, Zhang X, Zambelli T, Exarchos V, et al. Mechanical fingerprint of senescence in endothelial cells. *Nano Lett.* 2021;21(12):4911–4920.

Cheng CK, Wang N, Wang L, Huang Y. Biophysical and biochemical roles of shear stress on endothelium: A revisit and new insights. *Circ Res.* 2025;136(7):752–772.

Keshavanarayana P, Spill F. A mechanical modeling framework to study endothelial permeability. *Biophys J.* 2024;123(3):334–348.

Kliche K, Jeggle P, Pavenstädt H, Oberleithner H. Role of cellular mechanics in the function and life span of vascular endothelium. *Pflugers Arch.* 2011;462(2):209–217.

Ma D, Ren J, Qian X. Enhanced viscoelasticity as a biomechanical signature in senescent vascular endothelial cells. *Cell Rep Phys Sci.* 2025;6(9):102844.

Silvani G, Romanov V, Cox CD, Martinac B. Biomechanical characterization of endothelial cells exposed to shear stress using acoustic force spectroscopy. *Front Bioeng Biotechnol.* 2021;9.

Singam A, Bhattacharya C, Park S. Aging-related changes in the mechanical properties of single cells. *Heliyon.* 2024;10(12):e32974.

Walther BK, Sears AP, Mojiri A, Avazmohammadi R, Gu J, Chumakova OV, et al. Disrupted stiffness ratio alters nuclear mechanosensing. *Matter.* 2023;6(10):3608–3620.

World Health Organization. Cardiovascular diseases.

Zhai Y, Colmenarez JA, Mendoza VO, Dong P, Nunes K, Suh D, et al. Multiscale mechanical characterization of cornea with AFM, SEM, and uniaxial tensile test. *Proc ASME Int Mech Eng Congr Expo.* 2023;5.

Evaluating Severity and Long-Term Outcomes in Pediatric Anoxic Brain Damage and Stroke Utilizing TriNetX

Christina Meien Zhu, Department of Biology
Daniel Novak, Ph.D.; Department of Social Medicine, Population, & Public Health

ABSTRACT

Pediatric anoxic brain damage (ABI) and pediatric stroke are both significant causes of mortality and long-term neurodevelopmental disabilities in children. Although they arise from different mechanisms, both can lead to similar complications. Comparing outcomes between these two conditions may help us better understand how different mechanisms of early brain injury impact long-term comorbidity profiles and clinical care needs. However, there is currently no large-scale comparative study of multi-system comorbidity burden between infants with ABI and hemorrhagic stroke. In this retrospective observational cohort study, we use the clinical data in TriNetX, a large, multicenter electronic health record (EHR) network, to look at risk difference, risk ratio, and odds ratios for the prevalence of respiratory, cardiovascular, neurological, metabolic, developmental, and inflammatory co-morbidities in 19,172 infants aged 0-1 diagnosed with ABI versus those with hemorrhagic stroke. Outcomes were assessed from the time of injury through a 3-year follow-up window, and patients with overlapping diagnoses were excluded. Infants with ABI were found to have significantly higher burden of multi-system complications, including increased risk of respiratory failure (RR=2.412) and cardiac arrest (RR=10.148) compared to hemorrhagic stroke patients. Neurological complications were also significantly more frequent in the ABI group, while hydrocephalus, inflammatory central nervous system diseases, and retinopathy of prematurity were more frequent in the hemorrhagic stroke group. These findings suggest that infants with ABI may require more comprehensive monitoring and multidisciplinary management strategies to address the wide range of potential long-term complications.

KEYWORDS: Pediatric anoxic brain injury, Pediatric stroke, Neonatal brain injury, TriNetX, Retrospective cohort study, Electronic health records, Neurological outcomes

FACULTY MENTOR - Dr. Daniel Novak;
Department of Social Medicine, Population, & Public Health

Daniel Novak, an associate professor in the Department of Social Medicine, Population, and Public Health and Director of Scholarly Activities in the UCR School of Medicine. He earned his doctorate in Learning Sciences from the University of Washington. His research focuses on cutting-edge educational technologies to support professional development.

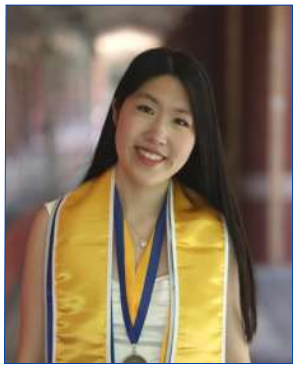

Christina Zhu

Christina Zhu is a Biology graduate from UC Riverside and an alumna of University Honors, where she served as Co-Chief Honors Ambassador. Supported by the University Honors Leadership and Excellence in Research Scholarships, she completed her capstone under the guidance of Dr. Daniel Novak and received the University Honors Pillars of Excellence Award. Zhu currently volunteers in a clinic in San Francisco's Chinatown, conducts research at the Feng Lab and Ferriero Lab at UC San Francisco, and plans to attend medical school.

Evaluating Severity and Long-Term Outcomes in Pediatric Anoxic Brain Damage and Stroke Utilizing TriNetX

INTRODUCTION

Despite significant advances in pediatric critical care, anoxic brain damage, also called anoxic brain injury (ABI), and hemorrhagic stroke remain two devastating causes of neurologic disability and death in young children (Rawanduzy et al., 2022). ABI in children occurs when the brain is deprived of oxygen, leading to widespread neuronal and systemic damage, as well as high mortality rates (Khot et al., 2006; Messina et al., 2025; Magalhães et al., 2005). Pediatric stroke is a significant cause of neurologic morbidity and long-term disability in children (Boulouis et al., 2019). The types of stroke include ischemic stroke,[1] which occurs when blood flow to a part of the brain is blocked by a clot or narrowing of the arteries, and hemorrhagic stroke, which occurs when a blood vessel in the brain ruptures, resulting in bleeding into or around the brain. Hemorrhagic stroke often leads to localized mechanical injury and hydrocephalus due to bleeding and inflammation (Aronowski et al., 2011; Sigal et al., 2014; Magid-Bernstein et al., 2022). Early recognition of both conditions can be challenging because symptoms are often nonspecific and may be mistaken for other conditions. ABI symptoms may be initially subtle, and in acute cases, the patients are in a vegetative state (Ishaque et al., 2022). In addition, around 50% of pediatric stroke cases are initially misdiagnosed due to low clinical suspicion (Janas et al., 2023). Delayed diagnosis may contribute to differences in treatment initiation and long-term outcomes.

The existing literature on pediatric ABI and pediatric hemorrhagic stroke has largely focused on outcomes of these conditions in isolation, with ABI more strongly associated with impacting multiple organ systems, and hemorrhagic stroke more strongly associated with focal deficits (Ham et al., 2017; Kriel et al., 1994). However, no studies have directly contrasted outcomes within the same analytic framework, and most existing work lacks standardized risk quantification (e.g. risk ratios or odds ratios) across outcomes (Shaklai et al., 2014). This study addresses these gaps by analyzing real-world, multi-hospital data to provide direct comparisons of outcomes and provide more representative estimates of morbidity and mortality patterns.

Children who survive ABI or hemorrhagic stroke often experience long-term neurological complications that affect cognition, independence, and overall quality of life. Despite these shared outcomes, anoxia and stroke differ significantly in their standard treatment approaches (Carney et al., 2017). Pediatric stroke management often includes targeted pharmacologic or surgical interventions (Ferriero et al., 2019), whereas ABI management is mostly supportive or rehabilitative (Schultz et al., 2017). Comparative data on long-term complications across these conditions may help clinicians anticipate each condition's common comorbidities and tailor monitoring, rehabilitation planning, and family counseling.

METHODOLOGY

While reviewing the existing literature, we found limited research directly comparing the rates of respiratory, cardiovascular, neurological, metabolic, and other developmental complications in infants with ABI versus hemorrhagic stroke. To address this gap, we conducted a retrospective cohort study using the TriNetX research platform comparing clinical outcomes between infants aged 0 to 1 diagnosed with ABI to those diagnosed with non-traumatic intracerebral hemorrhage. Cohorts were constructed with the ABI group defined by ICD-10-CM code G93.1 and the intracerebral hemorrhage group defined by ICD-10-CM code I61. Patients with overlapping diagnoses of both ABI and hemorrhagic stroke were excluded to maintain distinct comparison groups. An age at event filter of 0-1 yr was applied to observe injuries during early infancy, a critical period of brain development that is highly vulnerable to hypoxic and vascular injury.[2] Clinical outcomes were selected based on prior literature on complications of ABI and hemorrhagic stroke, as well as the availability of sufficiently large cohorts in the database. They

1. This study focused on hemorrhagic stroke rather than ischemic stroke to limit variation within the stroke cohort and allow for a clearer comparison with ABI.

2. Due to data availability limitations, the study was not able to look at only neonates (0-28 days), which could have introduced more variability in developmental stages and early-life exposures.

Evaluating Severity and Long-Term Outcomes in Pediatric Anoxic Brain Damage and Stroke Utilizing TriNetX

were then identified using ICD-10 diagnostic codes (Table 2) and categorized into organ-system domains (Table 2) as defined in the TriNetX platform. Outcomes were assessed from the index event through three years of follow-up, and same-day events were included because complications of neonatal brain injury frequently arise within hours of the initial injury. The TriNetX US Collaborative Network includes de-identified electronic medical records from 120 million patients across 71 healthcare organizations. The data for this study were extracted from TriNetX on January 29, 2025. Baseline characteristics, including age at index event, sex, and race/ethnicity, were summarized between cohorts (Table 1).[3]

We used TriNetX's built-in analytic tools to conduct measures of association analyses, including risk differences, risk ratios, and odds ratios to compare the likelihood of an outcome occurring between the two cohorts. Risk difference is the difference in the probability of an outcome occurring between cohorts. Risk ratio compares the relative likelihood of an outcome occurring in one cohort versus the other, and odds ratio compares the odds (the chance of having vs. not having the outcome) between cohorts. All calculations used 95% confidence intervals, and statistical significance was assessed using z-tests, with p-values <0.05 considered significant. We used Kaplan-Meier survival curves to show time-to-event probabilities of the outcome occurring from the initial injury through the three years of follow-up. At the end of the study, survival probabilities were compared between the two cohorts. A log-rank test was also used to determine if differences between the two cohorts were statistically significant.

Because this study used only de-identified, aggregated data from the TriNetX network, it did not involve direct interaction with human subjects or access to identifiable private information. Under IRB guidelines, analyses of such de-identified datasets are typically not considered human subjects research. The aggregation of data from several global sources in TriNetX also makes it extremely difficult to identify individual patients.

RESULTS

This analysis compared the prevalence and risk of respiratory, cardiovascular, neurological, metabolic, developmental, and inflammatory domains in children aged 0-1 diagnosed with ABI versus those with hemorrhagic stroke, using real-world data extracted from a large, multicenter electronic health record network. The following sections summarize these findings and are organized by clinical domain.

Summary of Respiratory and Cardiovascular Outcomes

Patients with ABI tended to have worse outcomes across several organ systems when compared to patients with hemorrhagic stroke. Respiratory failure, for example, was significantly more common among the ABI cohort, affecting 45.4% of patients vs. 18.8% in the hemorrhagic stroke group. This translated to an associated risk ratio (RR) of 2.41 (95% CI, 2.30–2.53), indicating a significantly higher risk of respiratory complications. Similarly, other forms of heart disease occurred more frequently in the ABI group (38.5% vs. 16.7%), corresponding to an RR of 2.31 (95% CI, 2.18–2.44). Cardiac arrest showed one of the largest disparities, with ABI patients having a tenfold greater risk (27.6% vs. 2.7%; RR = 10.15, 95% CI, 9.07–11.36). Hypotension was nearly three times as common in the anoxic cohort (13.9% vs. 4.7%; RR = 2.96, 95% CI, 2.67–3.28). Overall, these findings show a clearly higher burden of respiratory and cardiovascular complications associated with ABI compared to hemorrhagic stroke in this population.

Summary of Neurological Complications

Across a broad range of neurological outcomes, patients with ABI had substantially worse morbidity than those with hemorrhagic stroke. Disorders of electrical activity and episodic dysfunction, including unspecified convulsions, episodic and paroxysmal disorders, and epilepsy, were more common among the ABI cohort, with risk ratios ranging from 1.68 to 2.30. Movement disorders were also significantly elevated, with ABI patients experiencing extrapyramidal symptoms, dystonia, and motor paralysis (paraplegia or quadriplegia) at rates 3–5 times higher

3. No formal propensity score matching or other covariate balancing techniques were performed. Future studies should incorporate these methods to further reduce potential confounding.

Evaluating Severity and Long-Term Outcomes in Pediatric Anoxic Brain Damage and Stroke Utilizing TriNetX

Table 1: Patient Demographics

Cohorts	# of Patients	Female (%)	Hispanic or Latino (%)	White (%)	Black (%)	Unknown/Other Race (%)	Asian (%)	Native Hawaiian or Other Pacific Islander (%)	Current Age Mean +/- SD	Age at Index Mean +/- SD
Anoxic Brain Injury	6,145	42.96%	16.67%	47.99%	23.78%	23.72%	3.33%	1.18%	8.11 ± 4.95	0.3 ± 0.46
Hemorrhagic Stroke	13,027	41.78%	19.35%	50.91%	23.73%	20.61%	3.70%	1.05%	7.07 ± 4.71	0.3 ± 0.46

than those with hemorrhagic stroke. Severe neurological complications demonstrated some of the largest differences. Coma and persistent vegetative state were both dramatically more prevalent among ABI patients, with risk ratios exceeding 6.0. Similarly, the incidence of brain death was substantially elevated (RR=23.26), underscoring the devastating consequences of global hypoxic injury relative to focal hemorrhagic events. While ABI patients generally had higher risks for most complications, hydrocephalus was an exception. It occurred significantly more often in hemorrhagic stroke patients and was consistent with the known sequelae of intraventricular hemorrhage. This inverse association (RR = 0.29) provides internal validation of the contrasting pathophysiological mechanisms between the two conditions. It seems that ABI in early life is associated with a much broader and severe spectrum of neurological morbidity compared to hemorrhagic stroke. The pattern of elevated risks across both functional and structural outcomes highlights the extensive and lasting impact of global hypoxic injury on brain development and patient survival.

Summary of Metabolic Complications

Patients with ABI demonstrated a much higher burden of metabolic complications compared to those with hemorrhagic stroke. Metabolic disorders, both inherited and acquired abnormalities, were significantly more common among ABI patients (45.3% vs. 26.5%; ARD = 18.8%, $p < 0.0001$), corresponding to an RR of 1.71 (95% CI, 1.64–1.79) and an odds ratio (OR) of 2.30 (95% CI, 2.14–2.47). Survival analysis also confirmed this elevated risk, with a highly significant log-rank test ($p < 0.0001$). Similarly, disorders of fluid, electrolyte, and acid-base balance occurred at higher rates in the ABI cohort (38.3% vs. 17.7%; ARD = 20.6%, $p < 0.0001$). The RR for these conditions was 2.16 (95% CI, 2.05–2.28), and the OR was 2.88 (95% CI, 2.68–3.11). Consistent with these findings, it had a highly significant log-rank result ($p < 0.0001$). Together, these findings highlight a pattern of metabolic dysregulation following ABI. The higher rates of both generalized metabolic disorders and specific disturbances in homeostasis, like electrolyte disturbances, suggest that global hypoxic injury causes widespread effects beyond just the central nervous system and affects the whole body.

Summary of Other Developmental Disorders

Analysis of developmental and inflammatory outcomes revealed that cerebral palsy occurred significantly more often in the ABI cohort (22.7% vs. 14.1%; ARD = 8.6%, $p < 0.0001$), with an RR of 1.61 (95% CI, 1.51–1.72), reflecting a much higher risk of motor disability. Similarly, coagulation defects were more prevalent among ABI patients (9.5% vs. 2.4%; ARD = 7.1%, $p < 0.0001$), corresponding to an RR of 3.90 (95% CI, 3.40–4.46). In contrast, inflammatory diseases of the central nervous system were less frequent in ABI patients compared to hemorrhagic stroke patients (3.0% vs. 4.9%; ARD = –1.9%, $p < 0.0001$), with a RR of 0.60 (95% CI, 0.51–0.71). Similarly, retinopathy of prematurity was much less common among ABI patients (1.2% vs. 22.2%; ARD = –21.0%, $p < 0.0001$), with an RR of 0.05 (95% CI, 0.04–0.07), indicating a disparity possibly caused by differences in underlying pathophysiology and neonatal risk factors.

Mortality

Patients with ABI had a much higher risk of mortality compared to patients with hemorrhagic stroke (26.4% [1,535/5,814] vs. 4.8% [616/12,825]; ARD = 21.6%, $p < 0.0001$). The RR was 5.50 (95% CI, 5.03–6.00), and the OR was 7.11 (95% CI, 6.44–7.86). The log-rank test was highly significant ($p < 0.0001$), indicating a consistently higher risk of death in patients with ABI. The significantly higher mortality risk observed in patients with ABI likely stems from ABI's more global and irreversible nature compared to hemorrhagic stroke. ABI deprives the entire brain of oxygen

Evaluating Severity and Long-Term Outcomes in Pediatric Anoxic Brain Damage and Stroke Utilizing TriNetX

and leads to neuronal death, disrupting brainstem functions and regions that control respiration, cardiac function, and autonomic regulation, leading to multi-organ failure. In comparison, hemorrhagic stroke can cause significant focal injury, as well as secondary complications such as hydrocephalus. However, many patients may retain the brainstem and regulatory pathways, allowing for survival.

SUMMARY ACROSS ALL OUTCOMES

Infants with ABI faced worse outcomes across nearly every system. Respiratory and cardiovascular complications were most prevalent, with ABI patients having 2.4 times higher rates of respiratory failure and over 10 times higher risk of cardiac arrest compared to stroke patients. Neurological outcomes also showed large disparities. ABI patients faced much greater risks of seizures (both unspecified convulsions and epilepsy), episodic and paroxysmal disorders, extrapyramidal

Table 2: Risk Ratios for all Outcomes[4]

Outcome Name	ICD-10	% ABI	% HS	Risk Ratio	95% CI (RR)	p Value (RR)
Respiratory and Cardiovascular Outcomes						
Respiratory failure	J96	45.4	18.8	2.412	2.296–2.533	0.0
Heart Disease	I30-I52	38.5	16.7	2.306	2.184–2.435	0.0
Cardiac arrest	I46	27.6	2.7	10.148	9.067–11.358	0.0
Hypotension	I95	13.9	4.7	2.96	2.671–3.280	0.0
Neurological Complications						
Seizures	R56.9	42.8	22.5	1.899	1.811–1.991	0.0
Paroxysmal disorders	G40-G47	39.5	23.5	1.682	1.603–1.764	0.0
Epilepsy	G40	35.2	15.3	2.297	2.171–2.431	0.0
Movement disorders	G20-G26	13.4	3.9	3.426	3.072–3.820	0.0
Paralysis	G82	9.6	2.0	4.782	4.137–5.527	0.0
Dystonia	G24	8.1	2.5	3.239	2.818–3.723	0.0
Coma	R40.2	9.9	1.6	6.205	5.306–7.256	0.0
Hydrocephalus	G91	4.5	15.6	0.292	0.257–0.332	0.0
Brain death	G93.82	6.3	0.3	23.256	16.465–32.848	0.0
Degenerative CNS diseases	G30-G32	4.3	2.2	1.941	1.641–2.296	0.0
PVS	R40.3	0.9	0.1	10.653	5.569–20.379	0.0
Metabolic Complications						
Metabolic disorders	E70-E88	45.3	26.5	1.712	1.638–1.789	0.0
Electrolyte disorders	E87	38.3	17.7	2.162	2.051–2.279	0.0
Other Developmental Disorders						
Cerebral palsy	G80	22.7	14.1	1.609	1.507–1.717	0.0
Coagulation defect	D68.9	9.5	2.4	3.896	3.401–4.464	0.0
CNS Inflammatory diseases	G00-G09	3.0	4.9	0.603	0.510–0.714	0.0
ROP	H35.1	1.2	22.2	0.053	0.041–0.067	0.0
Mortality						
Mortality	R99	26.4	4.8	5.497	5.033–6.004	0.0

4. Outcome labels were simplified for readability. Abbreviation: ABI, anoxic brain injury; RR, risk ratio; CI, confidence interval; CNS, central nervous system; HS, hemorrhagic stroke; ROP, retinopathy of prematurity; PVS, persistent vegetative state.

symptoms, motor paralysis, dystonia, coma, and persistent vegetative state. For many of these conditions, the risk ratios exceeded 3.0. Metabolic imbalances were also more common among those with ABI. Risk ratios for these outcomes were nearly doubled relative to the hemorrhagic stroke cohort, suggesting that systemic homeostasis is broadly disrupted after anoxic events. Developmental outcomes showed similar patterns. ABI was associated with increased prevalence of cerebral palsy and coagulation defects. However, hydrocephalus and inflammatory diseases of the central nervous system were less common among patients with ABI. Retinopathy of prematurity was also less frequent in the ABI group. Overall, ABI was found to be associated with widespread and severe complications to the brain, heart, and metabolic regulation systems.

DISCUSSION

This study shows consistently greater morbidity across the multiple organ systems we looked at for patients with ABI compared to patients with hemorrhagic stroke. However, it is important to note that findings may be affected by differences in severity and physiologic status at presentation and should be interpreted as observational associations. Infants with ABI showed significantly higher rates of respiratory failure, cardiac arrest, other forms of heart disease, hypotension, seizures, coma, persistent vegetative state, and brain death. Unlike hemorrhagic stroke, which is typically associated with more localized injury (Aronowski et al., 2011), ABI is associated with injury across multiple brain regions and widespread neuronal dysfunction (Khot et al., 2006; Messina et al., 2025). Notably, the risk of brain death is much higher in patients with ABI. Metabolic disturbances were also more prevalent in the ABI group, suggesting that the effects of hypoxic injury extend far beyond the central nervous system. Hypoxic injury has been shown to induce mitochondrial dysfunction and oxidative stress (Magalhães et al., 2005), which may contribute to the metabolic dysregulation observed in this group. However, not all outcomes were worse in the ABI group. Patients with hemorrhagic stroke had higher rates of hydrocephalus, inflammatory diseases of the central nervous system, and retinopathy of prematurity. This may be due to hemorrhage in the brain obstructing the flow of cerebrospinal fluid, as well as inflammation that arises after stroke, both of which can increase the risk of hydrocephalus (Aronowski et al., 2011; Magid-Bernstein et al., 2022).

While past studies looked at survival metrics and outcomes associated with hypoxic-ischemic brain injury or hemorrhagic stroke, few have directly compared the breadth and severity of complications caused by these two types of brain injury side-by-side. This study addresses a key gap in the literature by providing a large, quantitative analysis of the multi-system impact of each condition. In our study, we observed that the ABI group had significantly greater systemic and neurological morbidity than hemorrhagic stroke. It is especially important to note the association between ABI and increased risk of systemic metabolic imbalances. Together, these findings suggest that ABI may be associated with a multi-system cascade of injury. As such, it presents a critical need for comprehensive guidelines and management strategies that include respiratory, cardiovascular, and metabolic monitoring and support.

LIMITATIONS AND FUTURE RESEARCH

This study has several limitations. Because it relied on real-world electronic health record (EHR) data from multiple hospitals, variability in coding practices and data documentation could have affected data consistency. We also could not ensure that patients had complete data across all variables of interest, such as functional status, cognitive outcomes, imaging results, or longitudinal recovery trajectories, limiting the depth of outcome analysis. Due to data availability limitations, the study included all infants 0 to 1 years old instead of only neonates to increase the sample size, which likely introduced variability in developmental stages and early-life exposures. Although baseline characteristics were summarized, no propensity score matching or other covariate balancing techniques were performed between cohorts, which may have resulted in confounding due to baseline differences between groups. Additionally, the retrospective observational design means that we cannot establish causal relationships between brain injury type and subsequent comorbidities. Although we used

Evaluating Severity and Long-Term Outcomes in Pediatric Anoxic Brain Damage and Stroke Utilizing TriNetX

standardized risk metrics, including risk ratios and odds ratios to quantify associations, the lack of randomization and controls means that there are possible confounding factors. These could be differences in the severity of the injury, differences in treatments, comorbid medical conditions, or socioeconomic factors. To confirm the associations identified in this study, future research should include controlled experimental research and use a smaller age range.

CONCLUSION

In this multi-institutional study, infants diagnosed with ABI demonstrated a far greater burden of systemic, neurological, metabolic, and developmental complications compared to those with hemorrhagic stroke. These included severe respiratory failure, cardiac arrest, seizures, coma, metabolic imbalances, and lasting neurodevelopmental disability. In comparison, infants with hemorrhagic stroke exhibited higher rates of hydrocephalus, inflammatory diseases of the central nervous system, and retinopathy of prematurity.

These findings suggest that ABI in infancy results in more widespread downstream morbidity than hemorrhagic stroke. This has important implications for both early and longitudinal care management. Infants with ABI may require more cardiopulmonary and metabolic surveillance, as well as coordinated inter-specialty care. Meanwhile, infants with hemorrhagic stroke may benefit from targeted surveillance for hydrocephalus and neuroinflammation.

Future research should focus on refining risk-stratification tools that integrate clinical, imaging, and biomarker data to support early diagnosis and predict patients at higher risk of facing systemic and neurological outcomes after each type of injury. Long-term follow-up assessing patients' functional abilities and developmental progress beyond three years of age would also strengthen our understanding of recovery outcomes.

ACKNOWLEDGMENT

I would like to sincerely thank Dr. Novak for his mentorship and guidance throughout my research journey. His support was instrumental in making this project possible, and working with him has been one of the most transformative parts of my undergraduate experience. I am deeply grateful for his encouragement, expertise, and dedication. I am also grateful to Dr. Ponthenkandath and Dr. Jiang for their advice and clinical insight into pediatric brain injuries, which greatly enriched and shaped the direction of this project. Additionally, I thank University Honors for providing the resources and opportunities that enabled me to pursue and complete this research. Finally, I am grateful to my friends and family for all their support.

Evaluating Severity and Long-Term Outcomes in Pediatric Anoxic Brain Damage and Stroke Utilizing TriNetX

REFERENCES

Aronowski, J., & Zhao, X. (2011). Molecular pathophysiology of cerebral hemorrhage. *Stroke, 42*(6), 1781–1786. https://doi.org/10.1161/strokeaha.110.596718

Boulouis, G., Blauwblomme, T., Hak, J. F., Benichi, S., Kirton, A., Meyer, P., Chevignard, M., Tournier-Lasserve, E., Mackay, M. T., Chabrier, S., Cordonnier, C., Kossorotoff, M., & Naggara, O. (2019). Nontraumatic pediatric intracerebral hemorrhage. *Stroke, 50*(12), 3654–3661. https://doi.org/10.1161/strokeaha.119.025783

Carney, N., Totten, A. M., O'Reilly, C., Ullman, J. S., Hawryluk, G. W. J., Bell, M. J., Bratton, S. L., Chesnut, R., Harris, O. A., Kissoon, N., Rubiano, A. M., Shutter, L., Tasker, R. C., Vavilala, M. S., Wilberger, J., Wright, D. W., & Ghajar, J. (2017). Guidelines for the management of severe traumatic brain injury, fourth edition. *Neurosurgery, 80*(1), 6–15. https://doi.org/10.1227/neu.0000000000001432

Ferriero, D. M., Fullerton, H. J., Bernard, T. J., Billinghurst, L., Daniels, S. R., DeBaun, M. R., deVeber, G., Ichord, R. N., Jordan, L. C., Massicotte, P., Meldau, J., Roach, E. S., & Smith, E. R. (2019). Management of stroke in neonates and children: A scientific statement from the American Heart Association/American Stroke Association. *Stroke, 50*(3), e51–e96. https://doi.org/10.1161/str.0000000000000183

Ham, P. B., & Raju, R. (2017). Mitochondrial function in hypoxic ischemic injury and influence of aging. *Progress in Neurobiology, 157*, 92–116. https://doi.org/10.1016/j.pneurobio.2016.06.006

Heindl, U., & Laub, M. (1996). Outcome of persistent vegetative state following hypoxic or traumatic brain injury in children and adolescents. *Neuropediatrics, 27*(02), 94–100. https://doi.org/10.1055/s-2007-973756

Ishaque, M., Manning, J. H., Woolsey, M. D., Franklin, C. G., Tullis, E. W., Beckmann, C. F., & Fox, P. T. (2017). Functional integrity in children with anoxic brain injury from drowning. *Human Brain Mapping, 38*(10), 4813–4831. https://doi.org/10.1002/hbm.23745

Janas, A. M., Barry, M., & Lee, S. (2023). Epidemiology, causes, and morbidities of stroke in the young. *Current Opinion in Pediatrics, 35*(6), 641–647. https://doi.org/10.1097/mop.0000000000001294

Khot, S., & Tirschwell, D. (2006). Long-term neurological complications after hypoxic-ischemic encephalopathy. *Seminars in Neurology, 26*(4), 422–431. https://doi.org/10.1055/s-2006-948323

Kriel, R. L., Krach, L. E., Luxenberg, M. G., Jones-Saete, C., & Sanchez, J. (1994). Outcome of severe anoxic/ischemic brain injury in children. *Pediatric Neurology, 10*(3), 207–212. https://doi.org/10.1016/0887-8994(94)90024-8

Magalhães, J., Ascensão, A., Soares, J. M., Ferreira, R., Neuparth, M. J., Marques, F., & Duarte, J. A. (2005). Acute and severe hypobaric hypoxia increases oxidative stress and impairs mitochondrial function in mouse skeletal muscle. Journal of *Applied Physiology, 99*(4), 1247–1253. https://doi.org/10.1152/japplphysiol.01324.2004

Magid-Bernstein, J., Girard, R., Polster, S., Srinath, A., Romanos, S., Awad, I. A., & Sansing, L. H. (2022). Cerebral hemorrhage: pathophysiology, treatment, and future directions. *Circulation Research, 130*(8), 1204–1229. https://doi.org/10.1161/circresaha.121.319949

Messina, Z., Hays Shapshak, A., & Mills, R. (2025). Anoxic encephalopathy. In StatPearls. StatPearls Publishing. http://www.ncbi.nlm.nih.gov/books/NBK539833/

Tagin, M. A., Woolcott, C. G., Vincer, M. J., Whyte, R. K., & Stinson, D. A. (2012). Hypothermia for neonatal hypoxic ischemic encephalopathy. *Archives of Pediatrics & Adolescent Medicine, 166*(6). https://doi.org/10.1001/archpediatrics.2011.1772

Rawanduzy, C. A., Earl, E., Mayer, G., & Lucke-Wold, B. (2022). Pediatric stroke: a review of common etiologies and management strategies. *Biomedicines, 11*(1), 2. https://doi.org/10.3390/biomedicines11010002

Schultz, B. A., & Bellamkonda, E. (2017). Management of medical complications during the rehabilitation of moderate-severe traumatic brain injury. *Physical Medicine and Rehabilitation Clinics of North America, 28*(2), 259–270. https://doi.org/10.1016/j.pmr.2016.12.004

Shaklai, S., Peretz, R., Spasser, R., Simantov, M., & Groswasser, Z. (2014). Long-term functional outcome after moderate-to-severe paediatric traumatic brain injury. *Brain Injury, 28*(7), 915–921. https://doi.org/10.3109/02699052.2013.862739

Cross-Cultural Communication: Examining Translation Gaps Between Korean and English

Elizabeth Park, Department of Comparative Literature and Languages
Emily Graham, Ph.D; Department of Comparative Literature and Languages

ELIZABETH PARK

Elizabeth Park is a recent graduate from the University of California, Riverside with a Bachelor's degree in Linguistics. Her work focuses on cross-cultural communication, analyzing translation gaps between the Korean and English languages. This research was completed as a capstone project under the guidance of Dr. Emily Graham in the Comparative Literature and Languages Department. Elizabeth hopes to further explore language and communication studies alongside plans to apply to a graduate program in Speech-Language Pathology.

ABSTRACT

In an increasingly global society, varying media entertainment presents different languages and cultures through the assistance of subtitles. In particular, Korean films have become popular in English-speaking countries through the prevalence of English subtitles. While this enables viewers to interact with Korean culture and language, studies reveal that English translations frequently overlook nuances of the Korean language, producing inaccurate or misleading interpretations. Through the examination of language and power dynamics in the Korean film, *Parasite*, this research explores power dynamics and cultural implications revealed through the Korean language by the use of honorifics. However, in English language subtitles, these crucial elements of the Korean language are almost completely absent. This analysis, then, presents an argument for how broad and inaccurate translations often erase central elements of a culture and further lend to misconceptions of non-Anglocentric societies.

KEYWORDS: language, translations, honorifics, film

FACULTY MENTOR - Dr. Emily Graham,
Department of Comparative Literature and Languages

Emily Graham is Assistant Professor of Linguistics, and her primary research interests lie in psycholinguistics and phonetics. She has conducted research on sentence-level processing, specifically how we link pronouns to their antecedents as well as the neurophysiological processing of determiner phrases.

Cross-Cultural Communication: Examining Translation Gaps Between Korean and English

INTRODUCTION AND BACKGROUND

In recent years, the rise of Korean culture and media has popularized Korean films, which in turn have increased their global exposure and broadened their viewership. A common way to reach this extended audience has been through subtitle translations, where one language is translated into another. While this has created opportunities for many viewers to engage with Korean culture and language, research indicates that many translations contain inaccurate or misleading interpretations of the Korean language. Subtitles often omit the role of social hierarchy standards and variations in social relationships that warrant different types of language use.

Using Bong Joon Ho's 2019 film *Parasite*, my research aims to specifically bridge the gap between Korean and English translation discrepancies and the cultural understandings that stem from the reflection of these languages. Language is often a major indicator in the representation of social positionings, relations, and hierarchy systems (Alisoy, 2024). Because these social positions, status markers, and hierarchical rank are affiliated with cultural values, the use of language can reveal deeper implications within a society's cultural viewpoint and perspective. Therefore, examining how language operates within these contexts provides valuable insights into the power dynamics at play, illustrating how linguistic choices not only reflect cultural ideologies but also reinforce social hierarchies.

LITERATURE REVIEW

Examining this issue raises questions about how language use reflects respective language ideologies (Feng, 2008) and if appropriate language modes are communicated in translations. The role of translations in conveying linguistic ideologies holds particular relevance as the linguistic ideologies of a language often reflect and adhere to certain cultural values, views and beliefs. Differences in a culture's language system can reveal stark variations in reactions, interpretations, and implications. When comparing Korean and English, it is important to examine if the ideologies of the Korean language and culture are communicated adequately in English translations.

The pragmatics of the Korean and English languages present striking dissimilarities, especially the use of honorifics and intersubjectification in the Korean language (Cho, 2022). Prioritizing social status and identity encourages a shift towards a more pronounced awareness of the hearer's position and status when communicating with others. Similarly, Korean strongly emphasizes the speaker-addressee's perspective, a language approach that dictates speech styles based on the social relationship of the individuals. For example, if a speaker is addressing a hearer who is older, they will generally choose to use honorifics and language markers used in formal speech. However, if the speaker and addressee have a close friendship, these honorifics may not be used, and instead the speaker may use *banmal*, language markers indicating casual speech. This focus on relationships and interpersonal communication makes the Korean language system intricate due to the varying grammatical and discourse functions; these distinctions are found most commonly in the different suffixes and "sentence-enders" in the Korean language.

Korean honorifics are linguistic markers that relay social positions and status between two or more speakers Commonly used in verb endings, these markers, such as -요 (-yo), -읍니다 (-imnida,) or -에요 (ehyo), vary by situation and can be categorized into two different categories: hearer honorifics and referent honorifics. Within hearer honorifics, there are several subcategories that can be applied to almost every utterance, regardless of the content of the individual statement or larger conversation (Brown & Yeon, 2015). Each subcategory refers to different contextual scenarios depending on the relationship between two speakers, such as ones "used when addressing strangers, non-intimates and superiors" (Brown & Yeon, 2015, p. 305). Referent honorifics, although similar in the way they indicate relative social positionings, are forms that specifically refer to a sentence referent.

Like hearer honorifics, there are several categories of referent honorifics that depend on the status and social position of the referent, such as a child, doctor, or grandparent. These honorifics may be used simultaneously and serve parallel purposes in defining hierarchical and social status. Changes are made to both the speaker's and hearer's speech patterns to reflect their respective status. In addition

Cross-Cultural Communication: Examining Translation Gaps Between Korean and English

to honorifics, the Korean language also utilizes *banmal* or non-honorific speech that signifies more intimate and casual speech. These markers occupy the same word positionings as honorifics, typically appearing in verb endings or sentence-final particles. These forms often express familiarity and comfort within relationships and signal one's social status as an equal, friend, or, in some cases, can be used by a superior to belittle the hearer.

Based on the specific nuances between honorifics and *banmal*, one might predict a rigidity in the use of these formalities. However, these usage patterns are often flexible, with speakers frequently shifting between different speech styles to reflect varying intentions (Brown & Yeon, 2015). Although there are many uses of this shift in speech styles, upgrading from *banmal* to honorific or downgrading from honorific to *banmal* are often the most jarring to listeners. As these shifts occur, ulterior motives or other purposes for a shift usually become apparent. In instances where non-honorific speech is upgraded to honorific, the shift may be perceived as sarcastic or like an insincere form of politeness (Brown & Yeon, 2015) or as a proactive attempt to enforce unnatural and unnecessary respect or courtesy. Conversely, shifting from honorific to non-honorific speech may be used to express greater intimacy or familiarity, or to showcase a conscious effort to be impolite (Brown & Yeon, 2015). In either case, any speech style shifting is seen as purposeful, apparent, and jarring to all parties involved, including external third parties such as audiences. These shifts are especially disruptive for the addressee, as these modifications usually conflict with standard relationships based on social positions.

In contrast, the English language generally focuses on the intended meaning of what the speaker is saying, rather than how it is spoken and addressed to the addressee (Cutting, 2002). This system prioritizes the content of one's statement and generally is not adjusted for different receivers in conversations. As long as there is mutual understanding, relevance, and reference between two speakers, their linguistic practice is deemed a success (Cutting, 2002). Honorifics or other excessive formalities are not always necessary, nor are they an explicit part of English pragmatics. Although the English language does possess certain variations in honorifics, such as "sir," "ma'am," or "doctor," these markers are mostly used in specific situations or regions and vary significantly depending on the setting and purpose of a given context (AL-Rawi & Al-Assam, 2014).

The use of honorifics is determined by when it is appropriate to use them, where specific addresses, such as "doctor," are only reserved for individuals with that specific title. Additionally, they do not require grammatical changes based on the social positioning of addressees; they utilize syntactic or lexical strategies to employ these markers rather than morphological changes (i.e., adding the marker "Dr." before an individual's last name). English honorifics act as additional markers rather than necessary and culturally essential language factors, where statements would still be socially acceptable and culturally correct without the use of honorifics. This indicates that honorific markers in the English language are not culturally significant and rather, operate more as a social component of language. These are often shown through pragmatic strategies, with politeness acting as their main use for employing honorifics (AL-Rawi & Al-Assam, 2014).

While the English language utilizes honorifics as a means of achieving politeness in different contexts, this is different from how the fundamental anchor honorifics act in the Korean language. This supports the notion that "in English, intimacy overrules rank or social status," (Hijirida & Sohn, 2009, p. 389), suggesting that formality is ranked lower as a priority within topics of power and communication. While honorifics can still be used in the English language, the purpose and intention with which speakers use these markers are ultimately for connection and empathy, rather than for social order or stratification.

The pragmatic and linguistic differences between Korean and English provide an important context for the many observable translation challenges found in Korean films and their corresponding English subtitle translations. Previous research has noted possible reasons for mistranslations, such as cultural substitution, direct translation, omission, and transliteration (Andrianaki, 2021). Many of these analyses have discussed honorifics in order to assess specific mistranslations. More specifically, Kiaer & Kim (2022) note that a common source of translation inconsistency is the concept of "invisibles," which refers to the omission

of cultural linguistic elements, including address-specific Korean honorifics. Commonly used and heard in everyday conversations in Korean society, this display of social hierarchy and status has no true equivalent in American culture or the English language. Thus, if this construct does exist in the English translations, it is never as explicit or embedded as the honorifics found in Korean. Different dynamics often reflect adjustments in the use of honorifics that English subtitle translations are unable to accurately translate.

I intend to build upon this concept of "invisibles" to assess how the omission of culturally significant linguistic markers proves to be detrimental and problematic in providing accurate subtitle translations. I also explore how these findings continuously and consistently influence our differing perspective on Korean and American society and their own respective ideas on the notion of power. Through an analysis of translation practices, I address how mistranslations may misconstrue or generalize specific cultures due to a lack of nuance in subtitle translations. Though past research studies such as Andrianaki (2021) and Kiaer & Kim (2021) have been conducted, there still remains a sparse and insufficient amount of scholarly attention to subtitle translations within Korean film. Although both Andrianaki (2021) and Kiaer & Kim (2021) explore crucial areas of Korean culture and language in relation to how they are translated into the English language, their implications remain broad. Building upon these findings, my research specifically examines how mistranslations surrounding honorifics and "invisibles" affect power dynamics found in particular relationships and characters.

METHODOLOGY

For my analysis, I selected two scenes from *Parasite* that highlight contrasting power dynamics, resulting in notable changes in linguistic choices: *High Status vs. Low Status* and *Dominant vs. Submissive*. These scenes were chosen based on the presence of distinctive power dynamics pertinent to the film's story, which made notable changes that drove the story forward. I began the analysis process by organizing the original dialogue and Netflix-provided subtitle translations into separate charts. Within these charts, I dissected the scene by individual lines, comparing each original Korean dialogue with its counterpart English translation. This involved a comparative analysis of different suffixes or phrasings depending on the presence of honorifics or non-honorifics in Korean, and a parallel assessment of the corresponding English subtitle translations. Markings, such as highlights, underlines, and italicizations, were used to pinpoint divergences.

The most apparent implications and distinctions were noted in a separate column, emphasizing the use of honorifics in Korean dialogue and the lack of this in the translation. After a loose assessment of the differences, an interlinear glossing was conducted, providing a literal translation for the original lines in the film. The process was composed of three varying lines: the first representing the original dialogue written and spoken in Korean, the second representing a general and broad morpheme-by-morpheme breakdown, and the third presenting an idiomatic, cohesive phrasing of the content of the second line. Examining the structure of the lines allowed for a deeper evaluation of the differences found in the subtitle translations and helped identify where certain mistranslations commonly occurred. Because of its focus on textual and contextual interpretation, the methodology is primarily qualitative rather than a quantitative measurement of differences. As a result, the findings are based on an interpretive analysis that may not be generalizable across the entire film or other translations more broadly. Additionally, the analysis may be influenced by the researcher's interpretation bias, as the identification of mistranslations or power dynamics partially relies on personal interpretation. Consequently, alternative readings or conclusions could be drawn by other researchers.

ANALYSIS

As mentioned previously, stark differences are found between English and Korean pragmatics as well as their general linguistic features. This disparity is further highlighted in the film Parasite, in which three distinct power dynamics are analyzed through the lens of language use: *Man vs. Woman, High Status vs. Low Status,* and *Dominant vs. Submissive.*

Cross-Cultural Communication: Examining Translation Gaps Between Korean and English

Using these examples, my analysis of Parasite underscores the importance of recognizing the "invisibles" omitted from subtitle translations, further affecting cultural understandings of power dynamics and shaping Western perspectives of foreign cultures. In the following scene, the character Ki-taek addresses his employer, Yeon-kyo, and reflects a variation in language use and honorifics.

Scene 1: 1:30:38-1:30:24

i. 제가 며칠전에 건강검진 받으러 병원에 갔다가요…

I-formal-1sg-pres couple days ago health check-up to receive hospital went-formal

'I went there for a health checkup a few days ago.'

ii. 어. 이분이 뒤에 보이더란 말입니다…

Yes-informal. her-1sg-past behind saw formal suffix

'I saw her behind my back.'

iii. 어디 통화하고 있는거네 지금?

Somewhere calling is (she)-informal right now?

'Is she talking on the phone?'

High Status vs. Low Status

The first scene provides a glimpse into the working relationship between Ki-taek, the head of the Kim family, and Yeon-kyo, the wife of the family that employs Ki-taek. During their conversation, Ki-taek adopts a formal tone as he informs Yeon-kyo of a previous interaction he has had with her maid. His language reflects his position, a main indicator of their position in the power dynamic of an employer and employee (1.i.). On the other hand, Yeon-kyo replies to Ki-taek casually, using *banmal* (1.iii.). This detail is crucial to the relationship between the two characters; if they were to converse outside of a work setting, Ki-taek's age would deem him to have a higher status than Yeon-kyo.

However, English subtitle translations fail to convey this distinction, giving the impression that the characters occupy the same social status or rank; the translations make it unclear if their relationship reflects friendship, collegiality, or mere acquaintance. Additionally, in one instance, the translations omit Yeon-kyo's response to Ki-taek (1.ii.), where she responds with "어," usually meaning "Yes" or "Yeah," in an informal tone. This phrase further establishes their relationship, where Yeon-kyo is comfortable speaking casually with Ki-taek as his employer. In this scenario, purposefully using formal language towards the wife reveals Ki-taek's ulterior motive: to establish a respectable and trusted relationship with his employee in order to have his family members hired into his workplace as well. The English subtitle translations fail to clarify the nature of their working relationship. Because there is no distinction between the use of honorifics and *banmal*, the implied dynamic between the two characters is flat and eliminates the layered interpretation of both characters' intentions. Although the two characters appear to share a friendly relationship, the translation misses the varying use of honorifics and *banmal* necessary in showcasing the underlying social customs.

The absence of the contrast between honorifics and *banmal* minimizes the substantial gap in the characters' social statuses, and misinterprets their power dynamics as more balanced or equal than they actually are. Because the exploration of power dynamics is an important topic within the film, overlooking the language difference in the way the two characters speak undermines the overall theme of the film. For example, in another sequence, Moon-gwang and Choong-sook meet in a tense confrontation where Moon-gwang's ongoing deception is revealed. The following dialogue represents their conversation after their unexpected encounter.

Scene 2: 45:09-44:55

i. 그쳐 충석이 언니? 내 이름은 어떻게 알아?

Right, Choong-sook sis? My-informal-1sg-pres name how know-informal

'Right, Choong-sook? How do you know my name?'

Cross-Cultural Communication: Examining Translation Gaps Between Korean and English

ii. 아 예, 사실 막내 다송이 하고는 아직 문자를 하거든요.

Oh, yes-formal actually, youngest Da-Song with still texting (to do)-formal

'Oh, actually, I'm still texting with Da-Song.'

iii. 오늘 식구들 캠핑 가는거 알고서 일부러 집으로 온거에요.

Today family camping going knew purposefully to-house came-forma

'I knew they were going camping today. That's why I came today.'

iv. 언니랑 단 둘이 얘기좀 하고 싶어서.

To sister just two(us) speak (to do) wanted-informal

'I wanted to speak to you alone.'

Dominant vs. Submissive

Scene 2 in *Parasite* utilizes the most prominent blend of formal and informal language, exhibited in Moon-gwang's dialogue. Throughout Scene 2, Moon-gwang attempts to appease Choong-sook to keep her secret using specific language tactics. Moon-gwang begins her dialogue formally, addressing Choong-sook respectfully and aligning with regular social norms (2i.-ii.). However, as the scene progresses, she begins to shift towards a friendlier tone, using *banmal* when referring to herself (2.iii.-iv.) and addressing the recipient as "언니," which the subtitle translates as "sis." Both language tactics act as apparent methods to ameliorate her situation and Choong-sook's attitude towards her, and create an obvious power dynamic between the two characters.

The use of "언니" is particularly overlooked, as the term is generally only reserved for casual and intimate relations, which, in scene 2, the characters do not share. The social hierarchy of Korean society and culture emphasizes the intimacy of this word, where "언니" implies a level of trust and mutual connection that purposefully oversteps social boundaries and hierarchy. The translation's use of "sis," although implying a level of closeness, lacks the same impact because it does not follow the switch between informal and formal speech, and is not necessarily exclusive to hierarchical relationships. The use of casual language also reinforces Moon-gwang's desperation by leveling her status to Choong-sook in an effort to establish security in their relationship. Conversely, Choong-sook's cold demeanor is amplified by her use of *banmal*, where her dominant position allows her access to a casual tone, an assertion of power also relayed to Moon-gwang. Language use is imperative in this scene as it reflects not only the social positioning that drives the film's plot but also adds insight into the characters' positions. These choices are invisible in the subtitle translations, where neither character's language choices are differentiated from the other's (2.i.- ii.). Translations, such as "언니" to "sis," are not adequate substitutes without the inclusion of a switch between honorifics and *banmal* due to the hierarchical implications and significance implied in the Korean.

CONCLUSION

Thematically, *Parasite* shows how these "invisibles" play a crucial role in interpreting power dynamics, and their omission in translations removes important implications brought forth by language. In a film that centers on power dynamics, these scenes demonstrate how the absence of "invisibles" results in a loss of nuance present in the original text and film, including motives, relationships, and cultural standards. Often, the omission of these linguistic choices and invisible honorifics may reduce the complexity and sophistication of Korean film, and potentially reflect a Western perspective or perception of other cultures. This is emphasized by the stark contrast between American and Korean societies' perspectives on power dynamics.

Research has noted that "in English, intimacy overrules rank or social status" (Hijirida & Sohn, 2009, p. 389), which highlights a cultural tendency to prioritize closeness over formal hierarchy in communications. The prioritization of relationships shown in the scenes analyzed above suggests that the subtitle translations prioritize conversational intimacy over formal hierarchy, reflecting linguistic conventions more commonly associated with English communication styles. While the original dialogue in Scene 1 includes a distinction in honorifics and *banmal* between

Cross-Cultural Communication: Examining Translation Gaps Between Korean and English

Ki-taek (employee) and Yeon-kyo (employer), the subtitles do not provide the same markers. In a scenario that includes both cordiality and social constraints, the Korean language prioritizes the latter, while the translations prioritize the former. The lack of "invisibles" in English translations could be explained by the fundamental idea that these pragmatic markers or honorifics may be viewed as an impediment to the characters' intimacy and play a minor role in their power dynamics.

The analysis of these scenes suggests that English subtitle translations may place less emphasis on hierarchical distinctions compared to the original Korean dialogue. Past research notes that English communication often prioritizes individualism and intimacy over collectivism (Hijirida & Sohn, 2009), which may explain the decreased emphasis on interpersonal interactions, leading to a lack of customized linguistic practices seen in the subtitle translations. American society is often associated with more egalitarian social values, emphasizing the idea that every individual should be of equal social status (Hijirida & Sohn, 2009). This attitude may help explain why English subtitle translations tend to adopt broader or more fluid language structures than the original Korean. Translation choices that reflect English-speaking cultural norms, even in films that showcase Korean culture and its related power dynamics, may potentially shape how international audiences interpret these relationships. Ultimately, translations often lack the nuances established by linguistic markers such as honorifics, possibly indicating a reductive view of a language and culture. This assumption stems from the idea that more often than not, English subtitle translations generalize the original dialogue, removing essential and foundational components of Korean language, like honorifics, that illustrate varying power dynamics.

While *Parasite* specifically prompts ongoing questions about Korean society and its hierarchy, the translations' simplification presents an adherence to American customs and personal ideologies of power dynamics. Because honorifics—and their implications for illustrating power dynamics in films—play an important role in the Korean language, their absence in translations may contribute to an assertion of Western cultural influence. Implementing a cross-cultural perspective can help establish a more neutral view of other cultures and raise awareness of the values and standards present in different societies, including Korean culture. Although this research focuses primarily on linguistic nuances and honorific usage within specific scenes from *Parasite*, future research could expand to examine other factors that influence subtitle translation choices, such as subtitle length or readability for audiences. In addition, studies specifically on audience reception could provide insight into how viewers are directly affected or influenced by the omission of honorifics and if these changes affect their understanding of Korean social hierarchy and cultural context. While more exploration is required to fully understand the depth and complexities pertaining to the topic of subtitle translations, this research acts as a starting point to understand the specific implications stemming from linguistic nuances.

ACKNOWLEDGMENTS

I would like to extend my warmest gratitude and appreciation to my faculty mentor, Dr. Emily Graham, without whom this project would not have been possible. Her invaluable guidance has been instrumental in the shaping and completion of this project. I would also like to thank my parents for instilling a deep-rooted love for our cultural identity and heritage that has provided the foundation for this project. They are the cornerstone of everything I am.

REFERENCES

Alisoy, H. (2024). *Stratification of language in society*. https://doi.org/10.5281/zenodo.10507792

AL-Rawi, S.S., & Al-Assam, D.A.A. (2018). A pragmatic study of English honorifics forms. *Journal of the College of Languages*, (38), 1-27.

Andrianaki E. (2021, December 21). *An analysis of the translation of culture-specific concepts in the subtitles of* Parasite *and* Squid Game. (Publication No: 202EGG06) [Thesis, Ewha Womans University].

Brown, L., & Yeon, J. (Eds.). (2015). *The handbook of Korean linguistics*. John Wiley & Sons, Incorporated.

Cho, S., & Whitman, J. (Eds.). (2022). Semantics and pragmatics. In *The Cambridge handbook of Korean linguistics* (pp. 487–656). Cambridge University Press. https://doi.org/10.1017/9781108292351

Cutting, J. (2002). *Pragmatics and Discourse: A resource book for students*. Routledge. http://site.ebrary.com/lib/keris/Doc?id=10016807&page=1

Feng, H. (2009). Different languages, different cultures, different language ideologies, different linguistic models. *Journal of Multicultural Discourses*, 4(2), 151–164. https://doi.org/10.1080/17447140802283191

Hijirida, K., & Sohn, H. (1986). Cross-cultural patterns of honorifics and sociolinguistic sensitivity to honorific variables: Evidence from English, Japanese, and Korean. *Paper in Linguistics*, 19(3), 365–401. https://doi.org/10.1080/08351818609389264

Kiaer, J., & Kim, L. (2021). *Soft power of the Korean wave: Parasite, BTS and drama*. Routledge.

Kiaer, J., & Kim, L. (2022). Understanding Korean film: A cross-cultural perspective. Routledge. https://doi.org/10.4324/9781003089896

Chem-AI: Reframing AI-Assisted Research Through Structured, Retrieval-Based Scientific Literature Analysis

Kora Dey, Department of Statistics
Haofei Zhang, Ph.D.; Department of Chemistry

ABSTRACT

The growing volume of scientific literature presents a significant challenge for researchers to identify relevant methods, compare findings, and build upon existing work. Although advances in artificial intelligence have led to new tools for literature analysis, many of these tools rely on generative language models that frequently produce incorrect or made-up information, citing sources that do not exist or drawing conclusions not supported by any published research. Beyond being unreliable and impossible to verify, these outputs raise serious concerns about reliability and reproducibility in scientific research. This study investigates whether a custom-built model that only pulls results from a verified domain can provide more accurate literature analysis than a standard generative language model such as ChatGPT.

This paper presents Chem-AI, an interactive system built in Python that structures the research process into clear steps, including query interpretation, literature retrieval, experiment classification, and method mapping. The system was evaluated using chemistry-related claims from the SciFact dataset (Wadden et al., 2020), a publicly available benchmark of scientific claims paired with verified research abstracts, as well as papers provided by Dr. Haofei Zhang. A retrieval was marked correct when the top-ranked paper returned matched the verified ground-truth abstract in the SciFact dataset. Within this limited 50-claim sample, Chem-AI correctly retrieved the supporting paper 90% of the time (45 out of 50 claims), compared to 62% for an unmodified ChatGPT baseline on the same claims. Notably, rather than guessing, Chem-AI declined to answer the remaining 10% of claims where no sufficiently supported source could be found, ensuring that every response it did produce was fully backed by published evidence.

These results suggest that a retrieval-constrained system may improve accuracy and traceability relative to a generative baseline, though testing on larger and more diverse datasets is needed before broader conclusions can be drawn. This approach is especially useful for undergraduate researchers as it supports more accurate, reproducible, and methodologically grounded work.

KEYWORDS: literature retrieval, research workflows, method recommendation, scientific AI, semantic search, reproducibility, chemistry informatics.

KORA DEY

Kora Dey is an undergraduate student at the University of California, Riverside studying Statistics with a minor in Computer Science. Her research interests include trustworthy AI, statistical modeling, and data-driven systems for scientific research. She has worked on interdisciplinary projects involving retrieval-based AI systems, machine learning, and movement data analysis.

FACULTY MENTOR - Dr. Haofei Zhang, Department of Chemistry

Dr. Zhang is as Associate Professor in the Chemistry Department at UCR. He received his Ph.D. from the University of North Carolina, Chapel Hill. His research investigate the impacts of atmospheric chemistry on air quality and climate change. He is specifically interested in the multiphase chemistry occurring in the atmosphere that dynamically transforms its organic composition in gas and aerosol particles.

Chem-AI: Reframing AI-Assisted Research Through Structured, Retrieval-Based Scientific Literature Analysis

INTRODUCTION

The rapidly growing volume of scientific literature can be daunting for researchers at every level (Van Noorden, 2014). Researchers now face the challenge of not just finding papers, but determining what is relevant, understanding a variety of methods, and connecting findings across studies to advance knowledge rather than repeat prior work (Fortunato et al., 2018). This environment stresses the need for readily available tools and ways to maintain research rigor and meaning.

This challenge is especially acute in fields such as chemistry, where researchers employ a varied array of experimental techniques, analytical systems, and modeling strategies to address comparable scientific questions. The multiplicity of approaches complicates the synthesis of knowledge, as it calls not only for the comparison of results but also for a careful evaluation of underlying assumptions, data structures, and testing conditions. Consequently, literature reviews in these domains are increasingly time-consuming and cognitively demanding, creating major obstacles to thorough comprehension and research progress (Bornmann & Mutz, 2015). Existing retrieval-based tools such as Semantic Scholar, Elicit, and Consensus have begun to address this problem, but none are designed specifically to support the structured, multi-stage reasoning that chemistry research requires. This study asks whether a retrieval-constrained system built on a curated corpus can deliver more accurate, traceable literature analysis than a standard generative model.

To meet these problems, recent advances in artificial intelligence have led to a set of tools to support literature analysis and research synthesis (Wagner et al., 2022). Large language models, in particular, have exhibited outstanding capabilities in generating summaries and explanations from extensive textual corpora (Bolaños et al., 2024). While these systems excel at producing coherent, seemingly informative responses, they face a substantial limitation in scientific settings: their outputs are generated probabilistically and are often unanchored to specific, verifiable sources (Bender et al., 2021). This lack of traceability and methodological precision undermines their usefulness in domains where repeatability and empirical reasoning are fundamental (Thorp, 2023). Tools that generate unsubstantiated or unstructured responses, devoid of explicit source connections, fundamentally fall short of supporting the demands of sound scientific research (Hutson, 2018). These concerns have been documented across multiple domains, including cases where AI-generated abstracts were indistinguishable from human-written ones (Else, 2023; Stokel-Walker, 2023) and where language models confidently produced incoherent or fabricated content (Marcus & Davis, 2020).

A core issue with many existing tools is that they do not reflect the authentic, stepwise process of scientific research. An effective research tool must integrate fluently into research workflows and facilitate, not complicate, the process (Wilkinson et al., 2016).

This paper presents the design and implementation of Chem-AI, a six-stage retrieval pipeline developed to address these limitations. Rather than reporting experimental findings as the primary contribution, this work focuses on the architectural decisions, technical components, and design principles that make Chem-AI a more reliable and transparent alternative to generative AI systems.

Chem-AI was designed to match how researchers think and operate. Rather than simply delivering answers, Chem-AI breaks down research questions, locates relevant papers, identifies which methods are being used, and maps how those methods lead to various outcomes. Each stage of the system was deliberately designed with a specific technical function, from keyword extraction and vector encoding to rule-based method classification and evidence-thresholded recommendations, forming a complete and reproducible pipeline for chemistry literature analysis.

The application was designed to be interactive, permitting researchers to ask follow-up questions, improve their searches, and examine results in detail. Chem-AI enables this level of engagement while making the process more transparent and less overwhelming. This work argues that AI tools designed around the structured logic of scientific research offer a more reliable alternative to generative models. Rather than prioritizing rapid response generation, the importance of structuring the research process itself is emphasized.

Chem-AI: Reframing AI-Assisted Research Through Structured, Retrieval-Based Scientific Literature Analysis

METHODS

Chem-AI was developed as a retrieval-based research tool built entirely in Python. The system was designed to locate, organize, and return information drawn strictly from a curated corpus of chemistry literature rather than generating responses freely. The overall architecture consists of six pipeline stages, each built and connected programmatically. The goal of each stage was not to produce a conversational response, but to replicate the structured reasoning process a researcher would use when reviewing literature. The overall architecture of the Chem-AI system is illustrated in Figure 1.

Part 1: Query Interpretation and Context Extraction

The first stage of the pipeline was responsible for processing and encoding the user's input query. This was implemented in Python using the SentenceTransformers library, which converted each query into a numerical vector representation. Chemical entities and domain-specific terminology were extracted using a keyword script, isolating relevant compounds, reaction types, and research objectives from the raw input. The keyword extraction script was validated by manually reviewing outputs for 20 sample queries and confirming that extracted terms matched the intended chemical entities. This dual representation, combining extracted keywords with a vector encoding, allowed the system to pass both exact terminology and broader conceptual meaning into the retrieval stage. This step was critical to ensuring that the downstream retrieval was precise and relevant to the specific chemistry domain being queried.

Part 2: Corpus Construction and Data Preparation

The corpus used by Chem-AI was constructed from two sources. The first was the SciFact dataset (Wadden et al., 2020), a publicly available benchmark containing scientific claims paired with verified research abstracts. Chemistry-related entries were filtered from the full dataset and retained for use. Entries were identified as chemistry-related if they contained at least one of the following domain keywords in the title or abstract: reaction, compound, molecule, chemical, synthesis, catalyst, spectroscopy, or analytical. The second source was a collection of chemistry papers provided directly by Dr. Haofei Zhang, covering topics including reaction mechanisms, atmospheric chemistry, and analytical techniques. Each paper was preprocessed using a

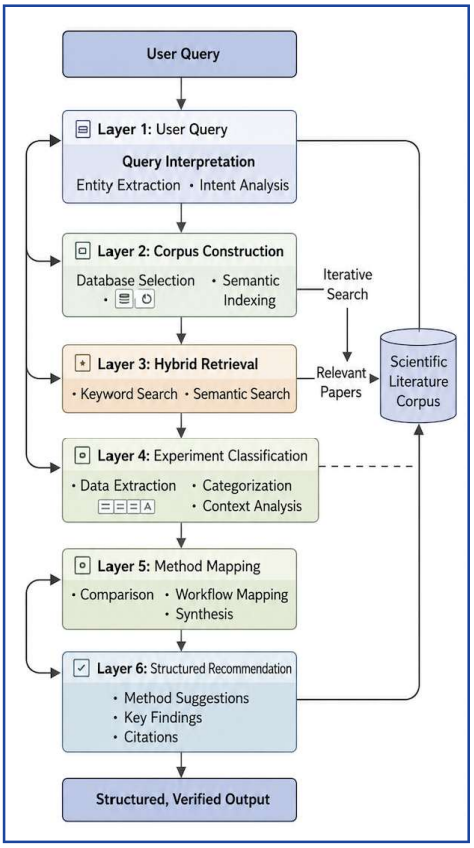

Figure 1: Overview of the Chem-AI system architecture, illustrating the layered workflow from query interpretation to structured recommendation.

Python script that extracted the title, abstract, and keyword fields and stored them in a structured dictionary format. Formatting inconsistencies were resolved during this stage to ensure uniform data structure across the corpus. The final corpus contained 10,000 papers. Because the SciFact dataset is publicly available, the full pipeline can be reproduced by other researchers.

Part 3: Hybrid Retrieval Framework

The retrieval system was built using two separate components that were combined into a single hybrid scoring function. The first component was a keyword-based retrieval system implemented using the Best Match 25 algorithm, which ranked papers by calculating how frequently and distinctively query terms appeared in each document. BM25 was selected for its strong performance on domain-specific

terminology, where exact term matching is critical. The second component was an embedding-based retrieval system implemented using the all-MiniLM-L6-v2 model from the SentenceTransformers library.

This model encoded both the query and each paper in the corpus as high-dimensional vectors, and similarity between them was measured using cosine similarity. This component allowed the system to retrieve papers that were conceptually related to the query, even when the exact wording differed. The final retrieval score for each paper was calculated by combining the BM25 score and the cosine similarity score using a weighted average, with a BM25 weight of 0.4 and a cosine similarity weight of 0.6, selected by testing combinations on a held-out set of 20 claims and choosing the weights that maximized retrieval precision. The top-ranked papers from this combined score were passed to the next stage of the pipeline.

Part 4: Literature Mapping and Structuring

Once Chem-AI retrieves the relevant papers, a structuring script is applied to organize and label all information, underscoring key methods, setups, and findings. The extracted information was stored in a consistent output format grouped by topic and method type, allowing users to directly compare studies without becoming overwhelmed by details. This stage was implemented entirely in Python using dictionary-based data structures and output as formatted text. The goal of this stage was to transform a raw ranked list of papers into an organized summary that reflected the structure of a real literature review.

Part 5: Experiment Classification and Method Identification

A rule-based classification system was developed to identify which experimental techniques and methods appeared in each retrieved paper. A predefined list of chemistry methods defined by SciFact's keyword bank, along with their analytical techniques, was compiled manually and used as a reference dictionary. Each paper was scanned programmatically against this dictionary, and matching methods were tagged and stored as metadata. Papers were then grouped by method type, producing a structured view of which techniques were most commonly used across the retrieved literature. This grouping was performed automatically using Python and required no manual labeling after the initial dictionary was compiled. The output of this stage allowed patterns in methodology to be identified across multiple papers without requiring the user to read each one individually.

Part 6: Structured Recommendation and Research Guidance

Methods that appeared most consistently across the highest-ranked retrieved papers were scored and ranked programmatically. The top-ranked methods were returned as recommendations, each linked directly to the specific papers from which they were derived. If no papers in the corpus scored above the relevance threshold for a given query, the system was programmed to return no recommendation rather than generate an unsupported response.

Part 7: Evaluation

To evaluate the performance of Chem-AI, chemistry-related claims were drawn from the SciFact dataset (Wadden et al., 2020). For each claim, the full retrieval pipeline was run, and the top returned paper was compared against the verified ground truth abstract provided in the dataset. A retrieval was marked correct when the returned paper matched the verified supporting source. An unsupported response was defined as any response that cited or implied a source that could not be traced to a document in the corpus or the verified ground-truth dataset. The same set of claims was passed through ChatGPT as the baseline generative model for comparison. Precision was calculated for both systems as the proportion of correct retrievals out of total claims tested.

Performance was assessed based on four criteria: relevance of retrieved literature, methodological specificity of outputs, clarity and understandability of structured results, and presence of unsupported or generalized claims.

Additionally, user-based evaluation was conducted with 50 graduate-level students. These assessments asked the students to rate system outputs on a scale of 1 to 5 across three criteria: relevance of retrieved papers, clarity of structured output, and confidence in source traceability. To reduce potential bias, participants were not informed which system produced each set of outputs during the rating process. Ratings from all 50 participants were averaged for

Chem-AI: Reframing AI-Assisted Research Through Structured, Retrieval-Based Scientific Literature Analysis

each criterion to produce a mean score out of 5 for each system. No inferential statistical tests were conducted, given the exploratory nature of this evaluation.

RESULTS

For each claim, Chem-AI's top-returned paper was compared against the verified ground-truth abstract. The same 50 claims were submitted to ChatGPT as the baseline. A retrieval was marked correct only when the returned paper matched the verified source.

Chem-AI retrieved the correct paper in 45 out of 50 claims (90%). The baseline generative model retrieved the correct paper in 31 out of 50 claims (62%), a difference of 28 percentage points. For the 5 claims where Chem-AI did not return the correct paper, the system returned no response. Three of those 5 involved highly specialized terminology absent from the corpus; two involved claims that required cross-referencing multiple papers rather than a single source.

Chem-AI returned a source link in 45 out of 50 responses and produced 0 unsupported responses. The baseline model returned a source link in 31 out of 50 responses and produced 19 unsupported responses (38%). A user evaluation was conducted with 50 graduate-level students across multiple University of California campuses. Each participant rated outputs from both systems on a scale of 1 to 5 across three criteria. Participants were not told which system produced each set of outputs.

DISCUSSION

Chem-AI retrieved the correct paper in 90% of claims compared to 62% for ChatGPT, a difference of 28 percentage points. This difference corresponds to how each system is built. ChatGPT generates responses from training data without a mechanism to confirm whether a cited source exists or matches the claim. Chem-AI returns only documents present in its corpus, so each response is tied to a real document. This finding aligns with prior work suggesting that retrieval-augmented approaches reduce hallucination and improve source traceability in AI-generated scientific content (Thorp, 2023; Bender et al., 2021).

The baseline model produced unsupported responses in 38% of cases. Chem-AI produced none. This behavior is a direct result of the relevance threshold in the retrieval pipeline: when no document in the corpus scores above that threshold for a given query, the system returns no response rather than generating one.

User ratings were higher for Chem-AI across all three criteria. The largest gap was in source traceability (4.9 vs 1.9), followed by clarity of structured output (4.6 vs 2.8) and relevance of retrieved papers (4.8 vs 3.1). Participants were graduate students across UC campuses, so these ratings may not generalize to other researcher populations.

ChatGPT was used as a general-purpose baseline without retrieval-specific or citation-constrained prompting, which means the comparison reflects default generative behavior rather than the best possible performance of a prompted generative model. A generative model specifically prompted to cite only verified sources, or one with retrieval capabilities built in, may produce different results. The dataset of 50 claims is also relatively small, and broader conclusions would require testing on larger and more diverse datasets.

Three of the five missed claims involved terminology not present in the corpus. The remaining two pieces of information are required from multiple papers, which the current single-document retrieval framework does not support. The core pipeline, including retrieval, structuring, and the no-response threshold, is not specific to chemistry and could be applied to other domains with a rebuilt method-classification dictionary and a domain-filtered corpus. Planned developments include reference network analysis and multi-document retrieval.

CONCLUSION

Chem-AI is a retrieval-constrained system that structures the research process into six stages: query interpretation and keyword extraction, hybrid retrieval using BM25 and cosine similarity, literature structuring, method classification, and evidence-thresholded recommendations. Each stage produces outputs traceable to a specific source document in its corpus.

Model	Correct Retrievals	Total Claims	Precision
Chem-AI	45	50	90%
Baseline Generative Model	31	50	62%

Table 1: Retrieval precision comparison between Chem-AI and the baseline generative model across 50 SciFact chemistry claims.

Model	Responses With Source Link	Unsupported Responses	Unsupported Rate
Chem-AI	45	0	0%
Baseline Generative Model	31	19	38%

Table 2: Source traceability comparison between Chem-AI and the baseline generative model across 50 claims.

Criteria	Chem-AI Average Score	Baseline Average Score	Difference
Relevance of Retrieved Papers	4.8 / 5	3.1 / 5	+1.7
Clarity of Structured Output	4.6 / 5	2.8 / 5	+1.8
Confidence in Source Traceability	4.9 / 5	1.9 / 5	+3.0

Table 3: Average user ratings (1–5 scale) for Chem-AI and the baseline across three criteria. Ratings were collected under blinded conditions from 50 graduate students across UC campuses.

Chem-AI: Reframing AI-Assisted Research Through Structured, Retrieval-Based Scientific Literature Analysis

Tested against 50 chemistry-related claims from the SciFact dataset, Chem-AI retrieved the correct paper in 90% of cases and produced no unsupported responses. The baseline generative model retrieved the correct paper in 62% of cases and produced unsupported responses in 38% of cases. For the 5 claims where Chem-AI did not return a correct paper, the system returned no response. Three of those cases involved terminology absent from the corpus, and two involved claims requiring cross-referencing multiple papers.

User evaluation with 50 graduate-level students across UC campuses produced average ratings of 4.8, 4.6, and 4.9 out of 5 for Chem-AI across relevance, clarity, and source traceability, respectively, compared to 3.1, 2.8, and 1.9 for the baseline. Ratings were collected under blinded conditions.

The current implementation is limited to chemistry-related queries and a corpus of 10,000 papers. Planned developments include multi-document retrieval and reference network analysis. Future work should test this approach on larger datasets, across more disciplines, and against generative baselines specifically prompted for retrieval tasks.

ACKNOWLEDGMENTS

I extend my sincere gratitude to Professor Haofei Zhang for his guidance, mentorship, and aid throughout this project. I am also grateful to the UC LEADS initiative for providing research opportunities and resources that made this work possible. Further appreciation is extended to the University of California, Riverside, for supporting my scholarly and research development.

REFERENCES

1. Bender, E. M., Gebru, T., McMillan-Major, A., & Shmitchell, S. (2021). On the dangers of stochastic parrots: Can language models be too big? *In Proceedings of the 2021 ACM Conference on Fairness, Accountability, and Transparency* (pp. 610–623). https://doi.org/10.1145/3442188.3445922

2. Bolaños, F., Salatino, A., Osborne, F., & Motta, E. (2024). Artificial intelligence for literature reviews: Opportunities and challenges. *Artificial Intelligence Review, 57*, 209. https://doi.org/10.1007/s10462-024-10902-3

3. Bornmann, L., & Mutz, R. (2015). Growth rates of modern science: A bibliometric analysis based on the number of publications and cited references. *Journal of the Association for Information Science and Technology, 66*(11), 2215–2222. https://doi.org/10.1002/asi.23329

4. Else, H. (2023). Abstracts written by ChatGPT fool scientists. *Nature, 613*(7944), 423. https://doi.org/10.1038/d41586-023-00056-72

5. Fortunato, S., Bergstrom, C. T., Börner, K., Evans, J. A., Helbing, D., Milojević, S., & Barabási, A. L. (2018). Science of science. *Science, 359*(6379), eaao0185. https://doi.org/10.1126/science.aao0185

6. Hutson, M. (2018). Artificial intelligence faces reproducibility crisis. *Science, 359*(6377), 725–726. https://doi.org/10.1126/science.359.6377.725

7. Marcus, G., & Davis, E. (2020). GPT-3, Bloviator: OpenAI's language generator has no idea what it's talking about. *MIT Technology Review.* https://www.technologyreview.com/2020/08/22/1007539/gpt3-openai-language-generator-artificial-intelligence-ai-opinion/

8. Stokel-Walker, C. (2023). Should professors worry that the AI bot ChatGPT writes smart essays? *Nature, 613*(7945), 620–621. https://doi.org/10.1038/d41586-023-00039-8

9. Thorp, H. H. (2023). ChatGPT is fun, but not an author. *Science, 379*(6630), 313. https://doi.org/10.1126/science.adg7879

10. Van Noorden, R. (2014). Global scientific output doubles every nine years. *Nature*. https://doi.org/10.1038/nature.2014.14024

11. Wadden, D., Lin, S., Lo, K., Wang, L. L., van Zuylen, M., Cohan, A., & Hajishirzi, H. (2020). Fact or fiction: Verifying scientific claims. In *Proceedings of the 2020 Conference on Empirical Methods in Natural Language Processing* (pp. 7534–7550). https://doi.org/10.18653/v1/2020.emnlp-main.609

12. Wagner, G., Lukyanenko, R., & Paré, G. (2022). Artificial intelligence and the conduct of literature reviews. *Journal of Information Technology, 37*(2), 209–226. https://doi.org/10.1177/02683962211048201

13. Wilkinson, M. D., Dumontier, M., Aalbersberg, I. J., Appleton, G., Axton, M., Baak, A., & Mons, B. (2016). The FAIR Guiding Principles for scientific data management and stewardship. *Scientific Data, 3*, 160018. https://doi.org/10.1038/sdata.2016.18